Permian diamictites in Northeastern Asia: their significance concerning the bipolarity of the late Paleozoic ice age

John L. Isbell[a,*], Alexander S. Biakov[b,c], Igor L. Vedernikov[b], Vladimir I. Davydov [b,d], Erik L. Gulbranson[a], and Nicholas D. Fedorchuk[a]

[a]Department of Geosciences, University of Wisconsin-Milwaukee, 3209 N. Maryland Ave., Milwaukee, WI , 53211, U.S.A.

[b]North-East Interdisciplinary Scientific Research Institute n. a. N.A. Shilo Far East Branch of the Russian Academy of Sciences, 16 Portovaya, Magadan 685000, Russia

[c]Kazan Federal University, 18 Kremlyovskaya St., Kazan, Republic of Tatarstan 420008, Russia

[d]Department of Geosciences, Boise State University, 1910 University Drive, Boise, Idaho 83725, USA

*Corresponding Author: John L. Isbell

E-mail address: jisbell@uwm.edu

ABSTRACT

Despite a lack of detailed sedimentologic analyses, diamictites in the Middle Permian Atkan Formation were previously interpreted as glaciomarine and glacially-influenced marine deposits. This interpretation allowed this unit to play a prominent role in paleoclimatic and biogeographical reconstructions associated with presumed bipolar glaciation during the late Paleozoic ice age (LPIA). In this sense, the LPIA is considered to be a close analogue to bipolar glaciation and climate change during the Cenozoic. Here, results are presented that challenge the glacigenic interpretation for these strata and negate interpretations of the bipolar nature of the LPIA. The 400 to 1500-m-thick Atkan Formation was deposited in back-arc basins associated with activity of the Okhotsk-Taigonos volcanic arc along the leading edge of Pangea as it drifted across the North Polar Circle. The occurrence of tuffs, volcanic clasts, and glass shards indicate derivation from a nearby arc. Cooling and solidification of some clasts during sedimentation is suggested by the occurrence of clasts with embayments and protrusions that extend into the surrounding matrix, clasts with columnar-like jointing, and alteration of the matrix surrounding some clasts. CA-TIMS dating of tuff zircons indicate a late Capitanian age, which is consistent with fossils within the strata. Bedded diamictites deposited as debrites dominate. These diamictites, which occur as tens of m thick downlapping packages that thicken then thin upward, were deposited as prograding and abandoning sediment gravity-flow fans. Chaotic and folded strata formed as slumps. Graded sandstones and conglomerates were deposited as turbidites, and mudstones were deposited as mudflows, low-density turbidites, and hemipelagic deposits. Striated clasts and outsized clasts piercing bedding were not observed in the study area. Strata above and below the Atkan Formation contain abundant graded beds and deep-water trace fossils indicating deposition as turbidites. The combination of debrites, turbidites, slumps, volcanic grains (clasts, glass, and tuffs), and an absence of glacigenic indicators suggest that Atkan strata were deposited in deep-water basins associated with the development of the volcanic arc rather than due to glacial activity. These findings are significant as they require reconsideration of current views of LPIA glaciation and suggest that ice sheets were limited to Gondwana.

Keywords

late Paleozoic ice age; diamictites; Siberia; Permian; Northeastern Russia; Capitanian;

1. Introduction

The late Paleozoic Ice Age (LPIA) is one of Earth's most important climatic events as it represents the longest, most widespread glacial interval of the Phanerozoic (Crowley and North, 1991; Frakes et al., 1992; Eyles, 1993). This dynamic ice age played an important role in driving linked oscillations in climate, eustasy, and floral and faunal restructuring during the Carboniferous and Permian (e.g., Waterhouse, 1976; Heckel, 1994, 2008; Raymond and Metz, 2004; Cleal and Thomas, 2005; Dimichele et al, 2005; Falcon-Lang and Dimichele, 2010; Horton et al., 2012). However, despite an evolving understanding of the LPIA (Isbell et al., 2003, 2012, 2013; Fielding et al., 2008a, 2008b, 2008c; Montañez and Poulsen, 2013; Frank et al., 2015), the size, distribution, paleogeography, timing, and depositional settings of its glacial events remain unresolved. Although Gondwana glaciation is well established (Crowell and Frakes, 1970; Crowell, 1978, 1983, 1999, Veevers and Powell, 1987; López-Gamundí, 1997;

Visser 1997a, 1997b; Isbell et al., 2003, 2012; Fielding et al., 2008c), reported glaciation in the Northern Hemisphere is less well defined (e.g., Ustritsky and Yavshits, 1971; Epshteyn 1981a, 1981b; Chumakov, 1994; Zharkov and Chumakov, 2001; Chumakov and Zharkov, 2003; Biakov and Shi, 2010; Biakov et al., 2010; Shi and Waterhouse, 2010). Nonetheless, a growing body of literature invokes bipolar glaciation for the LPIA and the development of ice centers in northeastern Asia to explain trends found elsewhere around the globe (e.g., Waterhouse, 1976; Stanley, 1988; Raymond and Metz, 2004; Fielding et al., 2008c; Rygel et al., 2008). Despite the potential significance of strata in northeastern Asia, little attention has been focused on deposits from this region and their potential to provide information that can be tied directly into the LPIA record.

Carboniferous and Permian strata in Northeast Russia (Figs. 1, 2, and 3) figure prominently in paleo-environmental, paleoclimatic, and biogeographical reconstructions for the LPIA in helping to explain changes in late Paleozoic sea level, paleobiogeography, biotic reorganization (diversity and abundance), chemical signatures within strata derived from low paleolatitudes, and climate model results (e.g., Waterhouse, 1976; Stanley, 1988; Davydov et al., 1996; Crowley et al., 1989; Zharkov and Chumakov, 2001; Beauchamp and Baud, 2002; Chumakov and Zharkov, 2003; Stanley and Powell, 2003; Raymond and Metz, 2004; Horton et al., 2007, 2010; Fielding et al., 2008c; Rygel et al., 2008; Birgenheier et al., 2010; González and Díaz Saravia, 2010; Koch and Frank, 2012; Chen et al., 2014; Frank et al., 2015). However, conflicting reports of whether this region was ever glaciated, how extensive glaciation was, or the conditions under which glaciation could occur make LPIA reconstructions in the Northern Hemisphere problematic (cf. Shi and Waterhouse, 2010). Diamictites, and lonestones have been reported from Carboniferous and Permian strata in the Kolyma and adjacent river basins (Fig. 1), and have been interpreted as the result of glaciomarine and/or glacially-influenced marine deposits resulting from sea ice (shore ice), river ice, and iceberg rafting; ice proximal; ice contact/subglacial processes; and sediment gravity flows (Andrianov, 1966; Ustritsky and Yavshits, 1971; Frakes et al., 1975; Epshteyn, 1981a, 1981b; Chumakov, 1994). Current climate models also simulate land-based ice in Northern Pangea during the LPIA, although, in general, simulated ice sheets are small and likely had a negligible impact on global ice volume (Horton et al., 2007, 2010). However, work by Biakov and Vedernikov (1990), and Biakov et al. (2010) suggests, that the diamictites are not of glacial origin, but instead, the result of marine slumping and debris flows associated with the development of the Okhotsk-Taigonos Volcanic Arc.

The diamictite-bearing successions in northeastern Asia are poorly dated and reports appear primarily in obscure summary papers lacking detailed analyses. Only the Middle Permian diamictites have received modest attention (Epshteyn 1981b; Chumakov, 1994; Grinenko et al., 1997; Biakov et al., 2010; Shi and Waterhouse, 2010). Therefore, these strata require further scrutiny to ascertain the occurrence, distribution, and timing of possible bipolar glaciation during the LPIA. Because of the general poor constrains on descriptions and interpretations of Carboniferous and Permian deposits in northeastern Asia and their importance to global reconstructions of the late Paleozoic, systematic analyses of these strata are warranted. A robust near-field data set, from North Polar Pangea, which is currently lacking, is needed to rigorously test models for the LPIA and to constrain processes and environmental conditions responsible for the initiation, maintenance, and demise of the glaciation and to determine the LPIA’s influence on the evolution of Earth’s natural systems.

Herein, we report the results of field work in the Kolyma River region (Fig. 1) of the Magadan Oblast to investigate the occurrence of glacial signatures within the Middle

Permian Atkan Formation (Figs. 2 and 4). Fieldwork was conducted over a three week period during the summer of 2013. These strata were accessed by driving overland up braided river systems using a Kamaz 6x6 expedition truck capable of driving through 2.5 m of water and a tracked vehicle. Steeply dipping strata of the Khuren/Forel, Atkan, and Druzhba/Omchak formations (Fig. 2) along Druzhba Creek (60˚54.056'N; 146˚49.628'E) and the Khuren River ice fields in the northeastern part of the Okhotsk Basin (61˚04.775'N; 147˚21.716'E), and the Nelkoba River in the Ayan-Yuryakh Anticlinorium (61˚19.784'N; 148˚49.532'E; Fig. 1) were studied for their lithofacies content, facies associations, clast contents, occurrence of tuffaceous materials, and fossil content (Figs. 2 and 4). Samples were sectioned and polished to conduct process sedimentology on representative sedimentation units and thin sectioned for petrographic and micromorphologic analysis at the University of Wisconsin-Milwaukee. Chemical analysis of diamictites and tuffs contained within the diamictites were run at the North-East Interdisciplinary Scientific Research Institute and Institute of Tectonics and Geophysics (ICP-MS analysis of rare earth elements in tuffs and matrix of the diamictites) of the Far East Branch of the Russian Academy of Sciences. At Boise State University, tuffaceous materials, volcanic clasts, and the matrix of the diamictites were processed for zircons and analyzed for isotopic dates using the chemical abrasion isotope dilution thermal ionization mass spectrometry (CA-TIMS) method on single zircon grains (Davydov et al., 2015).

2. Diamictites in Northeast Asia

In northeastern Asia (Fig. 1), upper Paleozoic diamictites and/or lonestone-bearing mudrocks are identified from Lower and Middle Pennsylvanian (Fig. 3; Bashkirian-

Moscovian; Ustritskiy and Yavshits, 1971; Epshteyn, 1981a), Lower Permian (Sakmarian; Ustritsky, 1973) and Middle Permian strata (Kungurian--Raymond and Metz, 2004; Kungurian and Early Capitanian--Grinenko et al., 1997; Capitanian--Mikhaylov et al., 1970; Epshteyn, 1981b Chumakov, 1994; Biakov et al., 2010) exposed in the Lena, Kolyma, Khuren and Omolon river watersheds (Fig. 1). The Carboniferous and Middle Permian diamictites are best described from outcrops along the Kolyma, Khuren, and Omolon River systems to the north and northwest of Magadan, while the Lower Permian diamictites are exposed in the Verkhoyansk-Okhotsk region between the Lena and Yana Rivers, and between the Aldan and Kolyma Rivers (Fig. 1; Ustritskiy and Yavshits, 1971; Epshteyn, 1981a, 1981b; Chumakov, 1994; Biakov et al., 2010).

The Carboniferous units, consisting of massive sandstone/siltstone with rare pebbles and cobbles in beds up to 10 m thick, are attributed to deposition due to sea-ice rafting (Epshteyn, 1981a); whereas, Sakmarian diamictites, which occur as 2- to 30-m-thick successions of pebble to boulder-bearing sandstones and mudrocks, are interpreted as products of sea-ice and/or iceberg rafting (Andrianov, 1966; Utritsky, 1973). However, purported Sakmarian diamictites in Northeast Russia are problematic as Epshteyn (1981a) indicates that these deposits may actually be Middle Carboniferous (Bashkirian-Moscovian) in age.

The Middle Permian (Capitanian) diamictites, the subject of this paper, are complex and are contained in brachiopod and bivalve-bearing marine successions in the Okhotsk, Ayan-Yuryakh, Balygychan, Gizhiga, Taigonos, and Omolon basins. The thickest and most widespread diamictite-bearing strata, up 1500 m thick, are found in the Atkan Formation of the Okhotsk and Ayan-Yuryakh basins and to a lesser extent as discontinuous lenses in the Omchak Formation (Ayan-Yuryakh Basin; Frakes et al., 1975; Biakov, 2007; Biakov et al, 2010). Such rocks occur, but are rare in the lower part of the Balygychan Formation of the

Balygychan Basin, and macroscopically similar rocks also occur in the Gizhiga Formation of the south-eastern part of the Omolon basin and in the Aulanzha Formation of the Gizhiga basin (Ganelin, 1984; Kashik et al., 1990).

The best know Middle Permian diamictites occur in the Atkan Formation (Figs. 2, 3, and 4) and are reported to consist of laterally continuous horizons of stratified and massive diamictites, and/or mudstone (gritty to pebbly) with dispersed clasts (Epshteyn, 1981b; Chumakov, 1994). Clasts range from sand to pebble size (2-3 cm). However, rare boulders up to 40 cm in diameter have been described (Epshteyn, 1981b). Although the vast majority of the clast are reported as rounded (Mikhaylov et al., 1970; Epshteyn, 1981b), Chumakov (1994) also reported bladed, faceted, and striated pebbles and boulders, as well as sediment aggregates similar to diamictite pellets (till pellets). Both Epshteyn (1981b) and Chumakov (1994) reported penetration of lonestones into fine-grained deposits, and those authors, as well as Biakov et al. (2010), noted the occurrence of soft-sediment folds within sandstone interbeds. Such features lead Chumakov (1994) to interpret the diamictites in the Atkan Formation as deposits from sea-ice and iceberg rafting, sediment gravity flows (turbidites, debris flows, and slumps), and possible ice-marginal conditions. However, agreement on depositional processes for these strata is not unanimous as some authors favor sea ice or sediment gravity flow processes as the prime mode of deposition rather than glacimarine processes (cf., Frakes et al., 1975; Epshteyn, 1981b; Biakov et al., 2010). Clasts and sand grains in these units are primarily of igneous and volcanic origin (Epshteyn, 1981b). Chumakov (1994) considered these clasts to have been derived from Devonian acidic and intermediate volcanic rocks, which are widespread throughout the present southern portion of the Okhotsk massif. However, the matrix in these diamictites is composed of volcanic glass and grains displaying relic ash structures. Therefore, Biakov et al. (2010)

suggested that these units resulted from sediment gravity flows associated with concurrent development of the Okhotsk-Taigonos Volcanic Arc. It should also be noted, that Grinenko et al., (1997) identified boulders and large limestone blocks (mixtites and olistostromes) contained in, and surrounded by, fine-grained Tumarinian and Lower Dulgalakh (Kungurian and Early Capitanian strata according to recent data) base-of-slope deposits. They interpreted these features to have accumulated as avalanche deposits derived from the collapse of self-edge carbonate reefs along the margin of the North Asian Craton (Siberian Craton).

In northeastern Asia, diamictites and mudrocks with dispersed clasts disappear at the top of the Gizhigina Horizon strata (Mikhaylov et al., 1970; Ustritskiy and Yavshits, 1971; Utritsky, 1973; Epshteyn, 1981b; Chumakov, 1994; Biakov et al., 2010), which are considered here as the Capitanian. Until the last decade, the age of these strata were considered as Late Permian (Kazanian or Early Tatarian) sensu old Russian Stratigraphic Scale.

3. Late Paleozoic paleogeography of NE Asia

Throughout the Carboniferous and Permian, the northern margin of Pangea drifted from ~60˚N in the Middle Mississippian (Viséan) to the North Pole by the end of the Permian (Fig. 5; Scotese, 1997; Torsvik and Cocks, 2004; Blakey, 2008). During this time, the leading edge of the continent was marked by an expansive system of subduction zones and volcanic arcs (the Okhotsk-Taigonos Arc and the Alazeya-Oloi Arc), which extended along the North-Asian Craton across the Eastern Boreal Realm (Kolyma-Omolon Province, the Verkhoyan-Okhotsk Province) to the Western Boreal Realm (west coast of North America). Volcanic rocks of the calc-alkaline Okhotsk-Taigonos Arc (also referred to as the Koni-Taigonos or Uda-Murgal Volcanic Arc) formed along the northern edge of the supercontinent during the Middle to Late Carboniferous and reached their maximum development during the Capitanian (late Middle Permian; Umitbaev, 1963; Ustritsky, 1975; Zaborovskaya, 1978; Nekrasov, 1976; Parfenov, 1984; Biakov, 2003; Biakov et al., 2005, 2007; Shi, 2006).

A complex series of accreted terranes, back-arc basins and marginal seas/passive margins were located between the Okhotsk-Taigonos Arc, the Alazeya-Oloi Arc, and the North-Asian Craton (Shi, 2006). These features formed both shallow- and deep-water marine basins (Biakov et al., 2005, 2010; Ganelin and Biakov, 2006; Klets et al., 2006; Shi, 2006).

Relatively shallow-water basins included: the Verkhoyansk passive margin or marginal-epicontinental sea located along the North-Asian Craton, and the central part of the Okhotsk, Penzhina, and Omolon Basins, which were located adjacent to the Okhotsk-Taigonos Arc (Parfenov et al., 2003; Klets et al., 2006; Biakov et al., 2007). However, terrestrial and shallow marine areas on the Okhotsk Microcontinent were likely part of the arc and contain substantial volumes of volcanic rocks (cf., Umitbayev, 1963; Ustritsky, 1975). These shallow water regions were bordered by deep-water basins, which included the Ayan-Yuryakh, Balygychan, and northeastern parts of the Okhotsk, Taigonos, and Gizhiga basins. It is in these deep water basins, along with limited occurrences in the Verkhoyansk, Omolon and the Penzhina basins, where late Paleozoic diamictites occur.

4. Age of the Atkan Formation

Fossils are rare in strata of the Atkan Formation. However, identified taxa include: brachiopods (*Cancrinelloides* ex gr. *ochotica* (Zavodowsky), *C. obrutshewi* (Licharew), *Cleiothyridina*? sp. indet.), bivalves (*Maitaia bella* Biakov, *Maitaia* aff. *bella* Biakov, *Phestia cumboides* (Lutkevich et Lobanova), *Myonia vel Praeundulomya* sp. indet., *Conocardium* sp.), gastropods (*Mourlonia* sp. no. 4, *Mourlonia* aff. *yabeshigerui* (Kobayashi)), crinoids (*Neocamptocrinus groschini* (Scoropisceva)), foraminifers (*Frondina* sp., *Rectoglandulina* sp. indet.), tabulate corals (*Cladochonus* sp.), and fragments of reticulate bryozoan colonies. These taxa make up the *Cancrinelloides obrutshewi–Maitaia bella* Regional lone in the lower half of the *Maitaia bella* bivalve zone (Fig. 2; Biakov, 2007; Biakov et al., 2010). This zone corresponds to the lower Gizhigian Regional Stage in Northeast Russia (Ganelin and Biakov, 2006; Biakov et al., 2010), which, due to the occurrence of the ammonoid *Timorites* and Gizhigian bivalves in the Transbaikal Region (Kotlyar et al., 2004), correlates with the Capitanian of the International Time Scale (Ganelin and Biakov, 2006, 2007; Biakov et al., 2010).

More recently, Davydov et al. (2015) dated zircons obtained from a tuff bed in the Atkan Formation and from a rhyolite boulder contained within one of the diamictite beds. Using CA-TIMS analysis, they identified the youngest population of zircons in the volcanic ash as 262.45 ± 0.21 Ma, which is late Capitanian in age. Zircons within the boulder identify a latest Roadian crystallization age of 269.80 ± 0.08 Ma (cf. Henderson et al., 2012). The age of the boulder is significant as it indicates that clasts were derived from an adjacent Middle Permian volcanic arc (Davydov et al., 2015) rather than reworking of Devonian volcanic deposits as suggested by Chumakov (1994).

5. Description and interpretation of lithofacies

Strata of the Atkan Formation are composed of 3 main lithofacies associations. These are (1) bedded diamictites; (2) interstratified diamictites, conglomerates, sandstones and mudrocks; and (3) thick, fossil-bearing mudrocks. Characteristics of these lithofacies are given in Table 1 and described below. All of the strata in the study area dip at high angles. The interstratified sandstone, mudstone, and diamictite associations occur at the top of the Khuren Formation and correlative units and into the base of the Atkan Formation, and at the top of the Atkan Formation and into the overlying Druzhba Formation and correlative units. Thick successions of diamictite and fossil-bearing mudstone associations occur throughout the Atkan Formation and are interstratified on an approximately 50m scale. Hummocky cross-stratification and wave ripples where not observed in any of the facies associations. Therefore, the occurrence of marine fossils and an absence of wave reworked strata indicate that these strata were deposited in a marine setting well below wave base.

5.1 Bedded diamictites

5.1.1. Bedded diamictites description

In the Atkan Formation, cm- to m-thick diamictites occur as massive tabular beds (Fig. 6A) with sharp, non-erosive basal and sharp to gradational upper contacts. They also occur as chaotic beds of diamictite, sandstone, and mudstone (Fig. 6B). The diamictites occur in successions up to 50 m thick, which display coarsening- (largest clast within individual units) and thickening-upward beds overlain directly by thinning- and fining-upward diamictite beds (Figs. 6C, 6D, and 6E). In areas of extended lateral exposures, these diamictites display downlapping stratal patterns onto underlying beds (Fig. 7A). Chaotic bodies, up to 10 m thick, of diamictite, sandstone, and mudstone are common and consist of either internally folded (soft sediment folds) bodies, or occur as admixtures of diamictite and mudstone with stringers of sandstone with irregular diffuse and sharp boundaries. Rare tuff beds (cm to dm thick) also occur within bedded diamictites and as admixtures within chaotic diamictites (Figs. 7B and 7C).

The diamictites are matrix supported and occur as both clast-rich (Fig. 8A) and clast-poor deposits (Fig. 8B) as determined using the classification scheme of Hambrey and Glasser (2003) as modified from Moncrieff (1989) for poorly sorted sediments. The coarsening and fining upward successions described above show up-section changes from mudstone, to clast-poor, to clast-rich diamictites returning to class poor diamictites and mudstones at the top of individual successions. The diamictite matrix is silicified, but consist of clay (50-95%), and silt and sand-sized (5-50%) particles. The matrix maybe mud rich, contain higher proportions of sand and silt, or consist of admixtures of the two with separate mud-rich and more sand/silt-rich domains that may display diapir-like structures with highly irregular and diffuse boundaries that cross-cut one another (Fig 8B). Microstructures within the diamictites include: rotational structures (turbate or galaxy-like structures; Fig. 8C), necking of matrix between grains, multiple diamictite domains (Fig. 8D), water escape structures, and an absence of oriented plasma fabric (Table 2; cf. Menzies et al., 2010). No brittle deformational structures (i.e., shear planes, stacked grains) were observed in thin section, and where grain-on-grain contacts occur, no evidence of crushed grains were observed (Fig 8C).

Clasts range in size from granules to boulders. However, boulders up to 70 cm in diameter are rare and the vast majority of clasts fall within the granule to pebble size range. Striated and bullet shaped clasts were not observed. In general, the clasts are randomly dispersed throughout the diamictite and do not display preferred orientations or clast clustering (Fig. 8A). However, rare thin-bedded diamictites may show preferred horizontal orientation of clasts. Using the roundness chart of Powers (1953), clasts range from very angular to rounded (Figs. 4 and 8A) with larger grains tending to be better rounded than smaller grains (Fig. 8C). However, over 71% of the clasts are subangular to very angular (Fig. 4). Irregular shaped clasts with embayments and protrusions are common in the diamictites, while some clasts also show diffuse boundaries with the surrounding matrix (Fig. 9).

Clasts within the diamictites and conglomerates are composed almost exclusively of volcanic clasts. However, intraformational mudstone clasts are also present, but are not abundant. The volcanic clasts are acidic (65%) and intermediate (35%) in composition and consist of dacite (56%), andesite (34%), pumice/altered glass (6%), and rhyolite (4%). Euhedral granule-sized grains of hornblende also occur. Sand and silt grains consist of volcanic rock fragments, euhedral and embayed quartz, feldspar (laths and tablets), carbonate grains, and altered glass shards (Fig. 10). Tectonic setting discrimination plots of chemical compositions of strata in the Atkan Formation are given in (Fig 11).

Although strata in the Atkan Formation display fracture cleavage that cross-cuts both clasts and the surrounding matrix, there are many examples of intra-clast fractures that end at grain boundaries. These intra-clast fractures have a variety of joint-spacings and are typically at near orthogonal to slightly oblique angles to the long-axis of the clasts. As such, when the clasts in a deposit show no preferred orientation, these intra-clast fractures or joints have different orientations from one clast to another, and the joints are not aligned with cleavage planes of the rock unit as a whole. These clasts display a relationship between the length of a clast's long axis and the average spacing of joints within the clasts. This relationship can be expressed by the equation: $spacing\ length = e^{(clast\ length/0.2911 - 4.2284)}$ (Fig. 12).

5.1.2. Bedded diamictites interpretations

Diamictites in the Atkan Formation were originally interpreted to have had, at least in part, a glacigenic origin (e.g., Epshteyn 1981b; Chumakov, 1994) as diamictites are common products of glacial and glacimarine processes (Powell and Domack, 2002; Benn and Evans, 2010). However, Biakov et al. (2010) recently challenged this interpretation as diamictites are also common products of mass transport and sediment gravity flows especially cohesive debris flows (Mulder and Alexander, 2001; Talling et al., 2012). Our results found no glacial indicators within strata in the study area. The absence of bullet-shaped clasts, striated clasts, and a lack of grooved and striated surfaces beneath diamictites precludes interpretation of the diamictites as resulting from subglacial abrasion and deposition, or due to iceberg turbate processes (cf. O'Brien and Christie-Blick, 1992; Woodworth-Lynas and Dowdeswell, 1994; Eyles et al., 2005; Vesely and Assine, 2014). We also found no evidence for deposition in a glacimarine setting. Glacimarine diamictites are produced by ice contact processes (i.e., rock fall, grounding line fans, glacial shove), deposition from a two component system where fines settle out of buoyant meltwater plumes and sand and gravel are released as ice-rafted debris, and by reworking of ice proximal deposits as sediment gravity flows. Glacimarine deposits are characterized by thick massive and stratified diamictites that typically display gradational bases and tops, structures indicating clasts "dropped" through a water column, bullet-shaped and striated clasts, wedge-shaped sandstone bodies, thrust faulted sediment bodies, and grooved surfaces (cf. Thomas and Connell, 1985; Carr, 2001; Powell and Domack, 2002). None of these features were observed in strata from the Atkan Formation. However, a number of macroscopic features suggest that these units are the deposits of subaqueous cohesive debris flows These features include: 1) the stacked bedded (less than 2 m thick beds) nature of the diamictites, 2) sharp non-erosive bases, 3) sharp to gradational tops, 4) an absence of preferred orientation of the clasts, and 5) the occurrence of clasts randomly distributed throughout individual units (cf. Mulder and Alexander, 2001; Haughton et al., 2009; Carto and Eyles, 2012). The non-erosive bases maybe the result of hydroplaning of individual flows which may have resulted in reduced friction and hence reduced erosion along the base of flows (Mohrig et al., 1998; Harbitz et al., 2003; Ilstad et al., 2004; De Blasio et al. 2004, 2006). Gradational upper contacts, where present, suggest that these flows mixed with ambient waters in the basin and that sediment was stripped from the tops of flows possibly forming linked debris and turbulent flows (cf. Amy and Talling, 2006; Haughton et al., 2009). Chaotic diamictites are sediment bodies that are highly deformed with intense internal deformation including folding and mixing of individual sedimentary units. These units are interpreted as slump blocks (cf. Martinsen, 1989).

Structures and associated microstructures contained within the Atkan diamictites indicate that deformation within the depositing fluids was ductile in nature (rotational structures, necking of matrix between grains; cf. Menzies et al., 2010). Such structures are consistent with deposition of the diamictites as cohesive subaqueous debris flows rather than due to glacigenic processes (cf. Menzies and Zaniewski, 2003; Phillips, 2006; Kilfeather et al., 2010; Henry et al., 2012). Microstructures resulting from subglacial deposition are characterized by both ductile and brittle deformational structures. However, they are dominated by structures produced by shearing, brittle deformation, and grain crushing. Microscopically, glacimarine diamictites may contain dropstone trails, brittle deformation structures (thrusting do to glacial shove), grains and clasts showing evidence for glacial abrasion, and dewatering structures (cf. Thomas and Connell, 1985; Carr, 2001; Powell and Domack, 2002; Menzie et al., 2006; Kilfeather et al., 2010). Although diamictites in the Atkan Formation show structures produced by post-depositional water escape processes (i.e., multiple plasma domians, diapirs/flame structures that cross-cut individual domains; cf. Menzies et al., 2010), these features are also common in debrites. Cohesive subaqueous debris flow deposits typically have high pore-water pressures at the time of their emplacement due to a combination of low permeability of the clay-rich matrix, trapping of water beneath the deposits during hydroplaning, and/or trapping of water incorporated into the flow due to mixing with ambient basinal waters (cf. Sohn, 2000; Ilstad et al., 2004; Elverhøi et al., 2005; De Blasio et al., 2006). Escape of water within debris flow deposits results in hydrofractures and water escape-structures (cf. Phillips, 2006).

Strata of the Atkan Formation contains stacked diamictite beds that occur in multiple thickening/coarsening followed by thinning/fining upward successions. These successions along with the downlapping of diamictite beds onto underlying beds within the successions suggest deposition within prograding and abandoning sediment gravity-flow fans (cf. Nemec and Steel, 1984; Carto and Eyles, 2012).

The abundant of clasts with embayments and finger-like protrusions are evidence that little modification to the original grain shape occurred during transport, which is more characteristic of debris flow transport where high energy grain to grain interactions are greatly reduced due to the presence of a matrix rather than the intense grain abrasion and grain crushing that occurs during subglacial transport (cf. Benn and Evans, 2010; Caballero et al., 2012).

Roundness values for the vast majority of clasts (subangular to very angular) also suggest minor shape modification of clasts during transport.

The predominance of volcanic clast, volcaniclastic sand grains, grains containing altered volcanic glass, and an abundance of glass shards in the Atkan diamictites indicate that these strata were derived from a volcanic provenance (Biakov et al., 2010) dominated by dacite and andesite with lesser amounts of pumice and rhyolite. The chemical composition of the diamictites is equivalent to material derived from dacitic-andesitic tuffs, and tectonic setting discrimination plots using chemical compositions indicate that sediment was derived primarily from an oceanic volcanic arc. However, some plots indicate that a continental volcanic arc also supplied some sediment to strata in the Atkan Formation (Bhatia and Crook, 1986). Diffuse boundaries between some clasts and the surrounding matrix raise the possibility that some of the volcanic material may have cooled within the diamictite following deposition. The presence of tuff deposits indicates the occurrence of contemporaneous volcanism (Davydov et al., 2015).

Numerous clast within the Atkan Formation display intra-clast fractures that are oriented nearly perpendicular to the long axis of the clasts. Although rocks in the Atkan Formation display fracture cleavage, these intra-clast fractures are not aligned with regional cleavage as the orientation of fractures within the clasts varies from one particle to another as the orientation of the clasts A axis varies. The relationship between joint spacing and the length of a clast’s long axis suggest that these joints may have formed due to differential cooling, thus they may represent a form of columnar jointing. It is difficult to determine when these clasts cooled. However, a lack of glass coatings on the outer surface of large columnar jointed clasts deposited by subaqueous, volcaniclastic, gravity-flows from the Miocene of New Zealand lead Balance and Gregory (1991) to conclude that cooling of such clasts may have occurred in a subaerial setting prior to transport of particles into deep marine environments. Glass coatings were not observed on the columnar jointed Atkan clasts.

5.2. Interstratified diamictites, conglomerates, sandstones and mudrocks

5.2.1. Interstratified diamictites, conglomerates, sandstones and mudrocks description

Interstratified clast-rich diamictite, conglomerate, sandstone, and/or mudrock occur as coarse- and fine-grained couplets and triplets (diamictite/conglomerate, sandstone, mudstone) in the upper Khuren, Atkan, and lower Druzhba formations (Figs. 2, 4, and 13). However, they make up only a small portion of the strata in the Atkan Formation. Whereas, in the Khuren and Druzhba Formations, much of the succession is composed of graded sandstone beds alternating with thin beds of mudstone. In this facies association, coarse members are mm to m scale in thickness and alternate with approximately equal thicknesses of mudrock, or in some cases, clast-poor diamictite (Fig. 13). In the Atkan Formation, conglomerates and diamictites are typically cm to dm thick. However, mm thick diamictite layers also occur where individual clasts may have diameters larger than the thickness of individual units (Fig. 13C). The diamictites and conglomerates rest on sharp to erosional basal contacts and in turn are bounded above by erosional, sharp, and gradational upper contacts (Fig. 13). Granules and pebbles comprise the clasts in both the conglomerates and diamictites. Neither cobbles, boulders, nor striated clasts were observed in this facies association. The conglomerates display normal grading with pebbles and granules grading upward into coarse- to fine-grained sandstone. However, reverse grading occasionally occurs (Fig. 13A). Diamictites are typically ungraded, but normal and inverse graded units occur, and some units contain clasts sticking out of the tops of beds. The diamictites occur as both matrix and clast supported units with the matrix composed of equal proportions of silt and mud. Rotational structures occur both at a macroscopic and microscopic scales and consist of alignment of sand and silt grains around clasts (Fig. 13C). In outcrops and in thin section, some diamictites also display multiple diamictite domains, flame and diapir structures, and admixtures of sandstone and diamictite (Figs. 13C and 14; Table 1; cf. Menzies et al., 2010). The clast display the same composition and shape as clast in the bedded diamictite facies association, (i.e., volcanic clasts and volcanic sand grains), However, rare diamictite clasts, which are composed of volcanic sand grains floating in a mudstone matrix, also occur. Some pebbles are loaded into underlying mudstone as are small lobes of diamictite (Figs. 13C and, 14A). These loads are associated with small mudstone flame structures (mm to cm scale), which intrude upward into the base of the diamictites. Diamictites also form flame structures that cross cut overlying sandstones (Figs. 13C and 14). Clast clusters and clast penetrating stratification were not observed in these units. The diamictites may also be overlain by graded sandstone or grade upward into mudstone. Sandstones are mm to cm thick (Fig. 13). However, sandstones in the Khuren and Druzhba Formations, are cm to m scale in thickness (Fig. 13B). Sandstones have sharp to erosional bases with some sandstones containing small sole marks (i.e., flute, prod, and bounce marks) and mudstone rip-up clasts. The sandstones are normally graded and may contain horizontal laminations near the tops of units where they grade into mudstone (Figs. 13A and 13C). Some sandstones contain multiple mud/diamictite and sand domains, diamictite and mudstone diapirs, and sandstone pipes. Some sandstones also contain *Nereites missouriensis* and *Zoophycos* trace fossils (Fig. 15). Interstratified mudstones may display internal laminations and may contain scattered sand grains, granules and granule sized diamictite clasts. Soft sediment folds occur within this facies association.

5.2.2. Interstratified diamictites, conglomerates, sandstones and mudrocks interpretations

The absence of wave ripple and hummocky cross-stratification, suggest that this facies was deposited below storm wave base. This is supported by the occurrence of *Nereites missouriensis* and *Zoophycos* trace fossils, which are typically deep-water indicators (Buatois and Mángano, 2011).

The composition of the clasts and matrix in the thinly stratified diamictites are identical to those in the thicker diamictite facies association indicating that diamictites in these two facies association share a common origin. Micromorphology of the diamictites indicates that they were characterized by ductile-like deformation (rotational structures) during emplacement and that dewatering (multiple diamictite domains, and water escape structures) of the deposits occurred after deposition (cf. Menzies et al., 2010). Such structures are consistent with emplacement by debris flows (cf. Lachniet et al., 1999; Menzies and Zaniewski, 2003; Phillips, 2006; Kilfeather et al., 2010; Henry et al., 2012). Different types of grading (non-graded, normal, or inverse) within debrites are the result of changing flow dynamics within the depositing flows, which include: changes in the rheology of the flow (i.e., water content, viscosity); changes in the thickness of the plug do to incorporation or expulsion of water, clay, and silt; thickness and degree of basal shearing; surges within the flow; grain interactions; development of transport lags; reworking of the top of the flow due to flow transformations; and/or conveyor-belt like overturning at the snout of flows as faster moving material in the upper portions out ran slower moving basal portions of the flows (Naylor, 1980; Nemec and Steel, 1984; Suwa et al., 1984; Broster and Hicock, 1985; Hand, 1997; Sohn 2000).

The occurrence of interstratified diamictites, graded conglomerates, graded sandstones with sole marks, and mudstones suggest that these units were deposited from sediment gravity flows as debrites, turbidites, and suspension deposits (cf. Talling et al., 2012). While the diamictites are interpreted as debrites; graded conglomerates, graded sandstones, and mudstones are interpreted as turbidites. Mudstones also likely formed as hemipelagic deposits and as mudflows. The relationship between diamictites, overlying graded sandstones, and mudstones, or diamictites that grade into mudstone suggest that these couples and triplets may have been linked at the time of deposition as composite/co-genetic debris flows and turbidity currents (Hampton, 1972; Sohn, 2000; Haughton, 2000; Haughton et al., 2003, 2009; Amy and Talling, 2006). Low density turbidity currents are produced by flow transformation as sediment is stripped from the head and body of subaqueous debris flows (cf. Fisher, 1983). Such flows may be deposited as debrite-turbidite couplets, or, if the faster moving turbidity current outruns the slower moving debris flow, debrites maybe sandwiched between turbidites as the turbidite generating debris flow moves out over sediment left behind by the faster flowing portions of the turbidity current (Sohn, 2000; Haughton et al., 2003; Talling et al., 2004; Amy and Talling, 2006). Typically, deposits from co-genetic sediment gravity flows are dm to m scale or more in thickness. However, mm to cm-scale debrites and turbidites may be the result of material shed laterally away from the margins of thicker flows, derived from the head of slow moving flows, or reworked from debris flows that have stopped moving (Nemec and Steel, 1984; Postma, 1984; Carto and Eyles, 2012). Soft sediment folding resulted from slumping associated with instability of deep-marine slope deposits. Such slumping could have been initiated by a number of factors, which included: 1) over steepening of the slope due to rapid sedimentation, 2) cyclic wave loading, 3) seismic events, and 4) over pressurization and fluid expulsion of rapidly deposited sediment (Posamentier and Martinsen, 2011; Pickering and Hiscott, 2016).

These interstratified deposits show evidence of high pore-water pressures following deposition as indicated by the occurrence of multiple sandstone and diamictite domains, dewatering pipes, flame/diapir structures, and load structures. Such structures suggest rapid deposition of both coarse clastic and mudstone members within this facies association, and that overlying layers were deposited as either linked co-genetic flows or that sediment compaction had not occurred prior to deposition of the overlying layers.

Ice rafting by either icebergs or sea ice was originally hypothesized as an important depositional process (Frakes et al., 1975; Epshteyn, 1981b; Chumakov, 1994). For example, in his paper, Chumakov (1994) included a description of “till” (diamictite) pellets and outsized clasts including a drawing of a pebble with “splash structures” (ruck structures of Thomas and Connell, 1985) that he interpreted as dropstones. Although rare diamictite “pellets” and outsized clasts (clast larger than surrounding sediment particles) occur within Atkan strata in the study area, deposition of these clast are better explained by processes other than ice rafting. Rare diamictite pellets within the studied strata appear to have formed due to loading at the base of debrites, detachment of the load structures, and the formation of pellets as the diamictite sank into underlying water-saturated mudstones (cf. Phillips, 2006). Outsized clasts easily mistaken for “dropstones” with ruck structures within thin diamictites and mudstone laminae include: 1) clasts at the base of diamictites loaded into underlying mudstones, which deform but do not pierce stratification; 2) clasts protruding from the tops of debrites that were carried in suspension due to the viscosity/yield strength of the flow (Talling et al., 2012); and 3) clast within thin debrites that are larger than the surrounding diamictite lamina, which resulted when clast were stranded on a soft substrate by thinning debris flows that continued on down slope (cf. Carto and Eyles, 2012), and 4) sand and granule clast in mudstone that were deposited by mudflows. Some of the outsized clast are core stones within rotational structures indicating that they were transported and deposited by ductile viscous flows (cf. Phillips, 2006) rather than having been "dropped" into the succession. Pumice sand grains and clasts are also common. Due to their density, such particles can be "floated in" and deposited as dropstones when they become water-logged and settle through the water column following volcanic eruptions (cf. Manville et al., 1998, 2002; Bryan et al., 2004). Chumakov (1994) also showed photos of a striated and faceted pebble and a cobble from the Atkan Formation in the Kolyma River drainage basin that he interpreted as glacially abraded clasts. No striated or faceted clasts were observed during the course of this study. However, it should be noted that numerous processes can striate clasts including: 1) abrasion during glacial transport, 2) abrasion by sea and lake ice, 3) tectonic deformation, 4) abrasion by high-velocity water flow, 5) wind abrasion, 6) mass movement (i.e., slides, slumps, debris flows, rock fall) and 7) volcanic activity including volcanic blasts and pyroclastic flows (Judson and Bark, 1961; Zamoruev, 1974; Dionne, 1985; Atkins, 2003). Although ice rafting of some particles cannot be completely ruled out, the absence of exotic far-traveled clasts, an absence of glacially abraded clast (bullet-shaped and striated clasts), and an absence of structures produced by "dropped" particles other than pumice clasts indicates that iceberg rafting of particles was not an important process during Atkan deposition in the study area (cf. Thomas and Connell, 1985; Gilbert, 1990; Eyles, 1993; Benn and Evans, 2010; Menzies et al., 2010).

5.3. Fossil-bearing mudrocks

5.3.1. Fossil-bearing mudrocks description

Mudrocks in the Atkan Formation vary in thickness from cm to several tens of m in scale (Figs. 2, 4, and 13). Thicker successions are typically highly cleaved and poorly exposed. Thin mudrocks are interstratified with graded sandstone, graded conglomerate, and diamictites. Thicker mudrocks are interstratified with thick diamictites successions. The mudrocks occur both as massive units and as laminated and thinly bedded deposits. These mudrocks are classified as mudstones/sandy mudstones and mudstones/sandy mudstones with dispersed clasts (<1% granule and larger sized particles) using the classification scheme of Hambrey and Glasser (2003) as modified from Moncrieff (1989) for poorly sorted sediments. These strata form a continuum with the diamictites described above in that the diamictites have a higher percentage of clasts. Sand grains and granules found in the mudstones are identical to those found in the diamictites. Laminated and thin bedded mudstones/sandy mudstones with dispersed clasts (Sand grains and granules) occur directly beneath and overlying the thick diamictite successions. Carbonate grains are common in the mudstone, but many of these grains appear to be the result of alteration and replacement of original detrital grains. Fossils contained in these mudrocks include brachiopods (*Cancrinelloides* ex gr. *ochotica* (Zavodowsky), *Cleiothyridina*? sp. indet.), bivalves (*Maitaia bella* Biakov), gastropods (*Mourlonia* sp. no. 4), and crinoids (*Neocamptocrinus groschini* (Scoropisceva)).

5.3.1. Fossil-bearing mudrocks interpretation

The presence of marine fossils in the mudrock facies association and an absence of deposits and structures produced by wave activity indicate this lithofacies association was deposited in marine waters below wave base. The thick mudrocks are interpreted as hemipelagic deposits. However, the thin-bedded and laminated mudstones/sandy mudstones containing rare dispersed clasts, which are interstratified or grade upward into diamictites, and which have a similar clast composition as those in the diamictites, are likely deposited by mud-rich, clast poor debris flows (mudflows; Talling et al., 2012). Because these units tend to occur near the base and at the top of thick diamictite successions, they likely represent the distal deposits of the prograding/abandoning debrite fans described above.

6. Discussion

Detailed sedimentology presented here confirms conclusions by Biakov et al. (2010) that strata in the upper Khuren, Atkan and lower Druzhba formations along Druzhba Creek, the Khuren River, and the Nelkoba River were deposited in a deep-water basin by sediment gravity flows and hemipelagic sedimentation during the Capitanian. The presence of marine fossils, deep-water trace fossils and an absence of wave indicators within these strata indicate deposition within a marine basin well below storm wave base. Thick diamictites were deposited by debris flows within prograding and abandoning debrite fan complexes. Features that substantiate these interpretations include: 1) stacked diamictites beds with sharp lower and sharp to gradational upper contacts indicating that the strata were deposited by fluid flow events; 2) clast randomly distributed throughout individual beds and an absence of preferred clast orientations indicating that the fluid did not segregate or orient sedimentary particles during transport or deposition; 3) macro and microstructures that indicate that the depositing flows behaved in a ductile viscous manner; 4) thickening/coarsening upward and thinning/fining upward diamictite successions along with downlapping stratal patterns within the diamictite successions indicating progradation and abandonment of the sediment systems through time; and 5) the occurrence of interstratified turbidites and debrites indicating that the depositional system was dominated by sediment gravity flows (cf. Mulder and Alexander, 2001; Haughton et al., 2009; Menzies et al., 2010; Carto and Eyles, 2012). Interstratified debrite and turbidite couplets suggest that sediment was stripped off of debris flows by the process of flow transformation producing linked co-genetic debris flows and turbidity currents (cf. Sohn, 2000; Haughton et al., 2003; Talling et al., 2004; Amy and Talling, 2006).

The preponderance of volcanic particles (clast, sand grains, and glass shards) contained within the Atkan diamictites indicate that these strata were derived from a volcanic provenance, primarily from volcanic island arcs with lesser amounts of detritus coming from an arc situated on continental crust (cf. Bhatia, 1983; Bhatia and Crook, 1986; Biakov et al., 2010). Although previous reports suggested that the clast were derived from Devonian volcanic rocks (Chumakov, 1994), zircon ages obtained from an Atkan tuff and a clast contained in a diamictite indicate that the source of the detritus was that of an active Middle Permian volcanic arc (Davydov et al., 2015). This explains the occurrence of clasts with embayments and finger-like protrusions, grains containing altered volcanic glass, and an abundance of glass shards, all of which would be unlikely to survive reworking due to their low chemical or physical stability during weathering and abrasion. The presence of possible incandescent clasts within the debris flows suggest that these flows resulted from contemporaneous eruptions. Therefore, these debrites represent subaqueous volcanic debris flows or lahars (Fisher, 1984) in a back-arc basin associated with development and continued activity of the Okhotsk-Taigonos Volcanic Arc (Figs. 5 and 16). The chemical composition indicates that most of the material was derived from an island arc system, but some material derived from a continental arc is consistent with small continental fragments being imbedded in the arc like that of the Okhotsk Microcontinent (Figs. 1 and 5; cf., Umitbayev, 1963; Ustritsky, 1975).

In regards to depositional processes and plate tectonic setting, the Grenada back-arc basin located behind the Lesser Antilles volcanic arc in the Caribbean Sea provides a modern analogue to late Paleozoic deposition of the Atkan Formation within a deep-water basin located behind the Okhotsk-Taigonos Volcanic Arc. The Grenada basin has an average depth of 2,900 m and contains up to 12,000 m of sediment (Picard et al., 2006). Based on shallow cores within the Grenada Basin, recent volcanogenic sediment consist of 99% pyroclastic debris flow and ash-turbidite deposits while less than 1% is composed of air-fall tephra layers (Sigurdsson et al, 1980). Sediment gravity flows within this basin are initiated by pyroclastic flows and debris avalanches that occur during contemporaneous eruptions and large-scale flank collapses of active volcanoes within the arc (Picard et al., 2006). One of the better studied debris flow deposits in this system is the Roseau subaqueous pyroclastic debris flow. This deposit is 1-3 m thick 250 km away from its source on the island of Dominica (Sigurdsson et al, 1980, Carey and Sigurdsson, 1980), which indicates that volcanic debris flows can extend long distances into back arc basins.

Atkan diamictites were previously reported as the products of glacimarine, glacially influenced marine, sea ice, subglacial and mass transport processes (Andrianov, 1966; Ustritsky and Yavshits, 1971; Frakes et al., 1975; Epshteyn, 1981b; Chumakov, 1994). However, within the study area, an absence of glacigenic features (i.e., striated and bullet-shaped clasts, grooved and striated surfaces, microstructures within the diamictite indicating subglacial conditions) contained in strata of the upper Khuren, Atkan and lower Druzhba formations exposed along Druzhba Creek, the Khuren River, and the Nelkoba River precludes a subglacial origin for deposits in the study area, or an origin as iceberg-turbate features (cf. O'Brien and Christie-Blick, 1992; Woodworth-Lynas and Dowdeswell, 1994; Eyles et al., 2005; Vesely and Assine, 2014). Ice rafting by either icebergs or sea ice was also hypothesized as an important depositional process as indicated by the occurrence of diamictite pellets and dropstones (Frakes et al., 1975; Epshteyn, 1981b; Chumakov, 1994). Although we cannot rule out the presence of ice rafted debris within the Atkan strata, ice rafting either by icebergs or sea ice was not an important process for the strata in this study owing to a paucity of features indicating the occurrence of dropstones or clast clusters contained in strata from the study area (cf. Thomas and Connell, 1985; Gilbert, 1990; Isbell et al., 2013), and diamictite pellets are also a product of subaqueous debris flow activity (Phillips, 2006). However, Chumakov (1994) reported lonestones piercing stratification and the occurrence of striated clasts elsewhere in the Kolyma River region, which suggest that perhaps ice rafting either by sea ice or icebergs may have played a local depositional role in Northeast Russia. Although evidence for glaciation is lacking within our study area, we calculated what maximum changes in eustasy would have resulted if glaciers occurred on the Okhotsk-Taigonos Arc, which was the source of the Atkan detritus. We assumed complete waxing and waning of these hypothetical glaciers and that the ice completely covered all of the land surface within the arc. Because the total land surface of the arc is unknown, we took the exposed area of modern volcanic island arcs to provide a range of values. Eustatic changes were calculated using equations for determining ice volume and sea level equivalence (Crowley and Baum, 1991; Paterson, 1994; Isbell et al., 2003). Results (table 3) indicate that between 0.00012 and 0.118 m of sea level change could have been produced by compete waxing and waning of a single glacier covering the combined area of a single modern arc systems. Although these calculations are a gross over estimate as the calculations assume that the land area is a single land mass that would produce a single glacier rather than individual ice masses located over each individual island. To provide a more realistic calculation, we split the exposed land area equally between all of the islands in the given modern arcs and calculated the size of glaciers that could form on each island, which gives values for glacioeustatic change of between 0.000069 and 0.095 m. Included in these calculations is the Aleutian Islands-Alaskan Peninsula arc. This system may be more in line with the Okhotsk-Taigonos Arc, which appears to have had small micro-continental fragments imbedded in the arc. From these calculations, it is apparent that island arc glaciers would have had little impact on global systems including eustasy. Regardless, we found no evidence for glacial activity within the late Paleozoic strata in the study area.

The question of bipolar glaciation during the late Paleozoic is based primarily on interpretations of strata in the Atkan Formation being glacigenic in origin and then extending that explanation to other poorly documented strata in Northeast Russia. Our results do not support the presumption that Pangea experienced bipolar glaciation during the Middle or Late Permian. Certainly there is no evidence from our study area for the occurrence of ice sheets in north polar Pangea during the Capitanian. In fact, a number of recent developments suggest that the deposition of the Atkan Formation occurred during a global warm interval. These include: 1) the late Sakmarian (2012 time scale; Gradstein et al., 2012; Henderson et al., 2012) end of glaciation in South Polar Gondwana and the end of widespread glaciation across most of Gondwana (Isbell et al., 2008, 2012, 2013; Henderson et al., 2012); 2) new age constraints on mid-latitude glaciation in eastern Australia, which places the P3 and P4 glaciations of Fielding et al. (2008a, 2008b) as Roadian-Wordian and Wuchiapingian respectively and that much of the Capitanian was a non-glacial interval (Frank et al., 2015; Metcalfe et al. 2015); 3) a warming interval during the Capitanian suggested by Waterhouse and Shi's (2011, 2013) estimated brachiopod and bivalve species diversity chart; 4) the occurrence in the Transantarctic Mountains (located within a few degrees of the South Pole) of thick coal seams, fossil forest, and structurally preserved fossil wood that shows no evidence of frost damaged cells during the Middle and Late Permian, which suggest temperate climatic conditions and an absence of ice sheets in Polar Gondwana (Antarctica; Taylor et al., 1992; Isbell and Cuneo, 1996; Isbell et al., 1997, 2008, 2012; Isbell, 2010; Gulbranson et al., 2012; 2014; Miller et al., 2015); 5) increased diversification and the migration of fusulinids and corals (including massive colonial rugose corals) into temperate North American shelves from the early to late Capitanian (Davydov , 2014; Kossovaya and Kropacheva, 2013); and 6) isotopic data from low, middle and high latitudes that suggest a warming trend during the Capitanian (Korte et al., 2008; Chen et al., 2013).

7. Conclusions

The late Paleozoic ice age is one of the most significant and important climatic events of the Phanerozoic. It had profound influences on Earth systems. Although many researchers consider it to have had a bipolar distribution and that Northern Hemisphere glaciation influenced much of the Middle and Late Permian, results presented here concerning diamictites in the Atkan Formation challenges this assumption and suggest that ice sheets only occurred in Gondwana. Therefore, our findings constrain boundary conditions such that future climate modeling can better determine factors that allowed Gondwana glaciation to occur while inhibiting the development of land-based ice in Northeastern Asia.

Sedimentology of the Capitanian Atkan Formation indicates that the strata were deposited by sediment gravity flows associated with volcanic activity in the Okhotsk-Taigonos Volcanic Arc and that the strata were not deposited by glacigenic activity as previously reported. These strata, which consist primarily of diamictites, were deposited in deep-water, back-arc basins by debris flows, mudflows, turbidity currents, slumps, and settling from suspension. Due to an absence of glacial indicators within the strata, the occurrence of bipolar glaciation during the LPIA cannot be confirmed for northern Pangea.

The fossil record of fusulinids and corals along with isotopic data derived from biogenic apatite of conodonts agrees with results presented here. The combination of these data coupled with the non-glacial record in Antarctica and the record from eastern Australia suggest that the Capitanian was a global, non-glacial interval with climate warming occurring from the early-middle Guadalupian to the end of the Capitanian.

Evidence in the literature for the mid Carboniferous and Early Permian (which may have also been mid Carboniferous) glaciations in Northeast Russia are even sparser than the previously reported evidence for a glacigenic Atkan Formation. The few reports that are available for these units suggest that diamictites and other pebbly deposits were most likely the result of deposition from sea ice (Utritsky, 1973; Epshteyn, 1981a). Although sea ice requires cold winter conditions, the presence of sea ice should not be construed as an indicator of glacial conditions. Today, sea ice forms in many areas of the Arctic and mid- to high latitudes without the occurrence of glaciers.

Despite the findings presented here, northeastern Russia is an immense area and it contains thick successions of strata deposited during the Carboniferous and Permian. Our work is only one small piece of the story and further work needs to be conducted on strata in this region to better understand the environments, the biota, and the processes that occurred in the North Polar regions of Pangea during the late Paleozoic.

Acknowledgements

The University of Wisconsin-Milwaukee's Research Grant Initiative (RGI) program, the Russian Foundation for basic Research (grants N 14-05-00217 and 15-55-10007), and grants (1444181 and 0943935) from the National Science Foundation funded this work. The research was also funded, in part, by the subsidy of the Russian Government to support the Program of Competitive Growth of Kazan Federal University among the World Leading Academic Centers. Their support is greatly appreciated. Logistic support in Russia was provided by the North-East Interdisciplinary Scientific Research Institute of the Far East Branch of the Russian Academy of Sciences. We also thank Mark Schmidts of Boise State University for access to his geochronology lab. We are forever grateful to Y.Y. Ivanov, E.V. Kolesov, and S. Kuznetsov (tracked vehicle driver) for their help in the field. Luis Buatois aided in identifying trace fossils from Northeast Russia, and Lindsay McHenry and Barry Cameron provided advice in dealing with volcanic clasts within the Atkan Formation. We also thank Daniel Horton and an anonymous reviewer for their comments on an earlier draft of this manuscript.

Figure Captions

Fig. 1. A and B). Distribution of Carboniferous and Permian strata in Northeast Russia (modified after Epshteyn, 1981b). C) Generalized tectonic map of North East Russia (modified from Shpikerman, 1998; Biakov, 2006; Davydov et al., 2015).

Fig. 2. Permian stratigraphic successions and biostratigraphic subdivisions in the Okhotsk Massif and the Ayan-Yuryakh Anticlinorium study area (modified from Biakov, 2007). See Figure 1 for the location of the measured sections.

Fig. 3. Summary diagram showing previous (Mikhaylov et al., 1970; Ustritskiy and Yavshits, 1971; Utritsky, 1973, Epshteyn, 1981a, 1981b; Chumakov, 1994; Raymond and Metz, 2004) and emerging (Biakov et al., 2010; Davydov et al., 2015; This Paper) views of the distribution of diamictites and their interpreted origins in North East Russia (Siberia). This is in comparison with emerging views for Gondwana glaciation from three different selected sites of crustal blocks located in eastern Australia (deposited at mid to high southern latitudes; Fielding et al.,2008a, 2008b; Frank et al., 2015; Metcalfe et al. 2015), Tasmania (high to polar southern latitudes; Truswell, 1978; Clarke & Forsyth, 1989; Price, 1997; Briggs, 1998; Mantle et al., 2010; Isbell et al., 2013), and Antarctica (located over the South Pole during much of the Pennsylvanian and Permian; Isbell et al., 2008).

Fig. 4. Stratigraphic section of Middle Permian strata of the Khuren and Atkan formations exposed along Druzhba Creek (60˚54.056'N; 146˚49.628'E) and a plot of clasts roundness based on Power’s (1953) classification scheme.

Fig. 5. Paleogeographic maps of northern Pangea during the Late Permian (modified from Lawver et al., 2008; Davydov et al., 2015) and North East Asia during the Capitanian (modified from Biakov et al., 2005, 2010, Biakov and Shi, 2010).

Fig. 6. Bedded diamictites in the Atkan Formation. A) Massive diamictite bed exposed along Druzhba Creek. B) Chaotic diamictites represented by soft-sediment folds exposed along the Khuren River. C-E) Thickening and thinning upward diamictite successions exposed along Druzhba Creek.

Fig. 7. A) Diamictite succession exposed along Druzhba Creek displaying downlapping stratal patterns. B) Bentonite bed exposed along Druzhba Creek. C). Chaotic admixture of tuff and diamictite exposed along Druzhba Creek.

Fig. 8. Features and structures contained within Atkan Diamictites. A) Cut and polished bed of clast-rich diamictite from Druzhba Creek showing the lack of internal stratification (massive), random clast orientations, angularity of clasts, and the distribution of clast throughout the bed. All clast are igneous clasts. B) Clast-poor diamictite exposed along Druzhba Creek showing sand-rich and mud-rich domains and the cross cutting diapiric nature of the mud-rich domains. C) Diamictite photomicrograph showing alignment of small grains around a large core stone (rotational structure). Sample is from a diamictite exposed along Druzhba Creek. D) Photomicrograph of cross-cutting sand rich and mud-rich domians from a diamictite exposed along Druzhba Creek.

Fig. 9. Irregular-shaped volcanic clasts displaying embayments and protrusions. Clast are from diamictites exposed along Druzhba Creek. Note that clast in photos 9D and 9E have diffuse boundaries between the volcanic clasts and the surrounding matrix.

Fig. 10. Volcanic grains (granule, sand and silt) contained within the matrix of diamictites exposed along Druzhba Creek include: A) quartz grain displaying euhedral shape and embayment, B) ignimbrite clasts showing flow banding, C) andesite grain, D) altered glass shards, E) dacite grain, and F) Pumice grain.

Fig. 11. Tectonic setting discrimination plots showing Th-La-Sc, Th-Zr/10-Co, Th-Zr/10-Sc and La-Th plots. The data points are for diamictite matrix, tuff beds and clasts contained within the Atkan Formation exposed along Druzhba Creek, NE Russia. The fields for various tectonic settings are from Bhatia (1983) and Bhatia and Crook (1986) and include fields for material derived from (A) oceanic island arc, (B) continental island arcs, (C) active continental margins, and (D) passive continental margins.

Fig. 12. A) Volcanic clasts (arrows) in Atkan diamictites that display intra-clast fractures not aligned with regional cleavage and where the fractures end at grain boundaries. B) Plot of the spacing of intra-clast fractures or joints relative to the long axis of clasts.

Fig. 13. Interstratified clast-rich diamictite, conglomerate, sandstone, and mudrock facies in the Atkan and Druzhba Formation. A) Interstratified beds and laminations of diamictite, conglomerate, sandstone, and mudstone exposed along the Khuren River. Note that the

conglomerates and sandstones display graded beds. Note that one part of the lower conglomerate displays reverse grading. B) Thickening upward succession of graded sandstone beds with thin mudrock interbeds exposed along Druzhba Creek. C) Cut and polished section of interstratification of thinly stratified diamictite, sandstone, and mudstone collected from Atkan strata exposed along the Khuren River. Note the occurrence of load structures, flame structures, outsized clast as part of a rotational structure (core stone), outsized clasts within the mm-scale thick diamictites, and the graded sandstone unit.

Fig. 14. A) Diamictite load and mudstone flame structure in Atkan strata exposed along the Khuren River. B) Cross-cutting admixture of sandstone and diamictite in the Atkan Formation exposed along the Khuren River.

Fig. 15. Trace fossils from the transition zone between the Khuren and Atkan Formations along Druzhba Creek. A) *Zoophycus* trace fossil on the top of a sandstone bed in the Atkan Formation. B and C) *Nereites missouriensis* on the upper surface of a sandstone bed at the top of the Khuren Formation/Base of the Atkan Formation.

Fig. 16. Model for the deposition of Middle and Upper Permian strata of the Khuren, Atkan, and Druzhba formations as deep-water debrites, slumps, and turbidites within a back-arc basin associated with the Okhotsk-Taigonos volcanic arc (modified from a model for volcanic sediment gravity flows deposited in the Grenada back-arc basin off of the Lesser Antilles volcanic arc; Sigurdsson et al., 1980).

References

Amy, L.A. and Talling, P.J., 2006. Anatomy of turbidites and linked debrites based on long distance (120X30 km) bed correlation, Marnoso Arenacea Formation, Northern Apennines, Italy. Sedimentology, 53(1): 161-212.

Andrianov, V.N. (Editor), 1966. Verkhnepaleozoiskie otlozheniya Zapadnogo Verkhoyan'ya (Upper Paleozoic Sediments of the Western Verkhoyansk Region). Trudy soveshchaniya po stratigrafii Severo-Vostoka SSSR (Transactions of a Conference on the Stratigraphy of Northeastern USSR). Nauka, Moscow, 153-156 pp (in Russian).

Atkins, C.B., 2003. Characteristics of striae and clasts in glacial and non-glacial environments. Doctoral Thesis, Victoria University of Wellington, Wellington, New Zealand, 321 pp.

Ballance, P.F. and Gregory, M.R., 1991. Parnell Grits-large subaqueous volcaniclastic gravity flows with multiple particle-support mechanisms. In: R.V. Fisher and G.A. Smith (Editors), Sedimentation in volcanic settings. Society of Sedimentary Geology Special Publication 45, Tulsa, pp. 190-200.

Beauchamp, B. and Baud, A., 2002. Growth and demise of Permian biogenic chert along northwest Pangea: Evidence for end-Permian collapse of thermohaline circulation. Palaeogeography, Palaeoclimatology, Palaeoecology, 184(1-2): 37-63.

Benn, D.I. and Evans, D.J.A., 2010. Glaciers and Glaciation. Arnold, London, U.K., 802 pp.

Bhatia, M.R., 1983. Plate tectonics and geochemical composition of sandstones. Journal of Geology, 91(6): 611-627.

Bhatia, M.R. and Crook, K.A.W., 1986. Trace element characteristics of graywackes and tectonic setting discrimination of sedimentary basins. Contributions to Mineralogy and Petrology, 92(2): 181-193.

Biakov, A.S., 2003. On Permian geodynamics and paleogeography of Northeast Asia (from sedimentologic and biogeographic data). In: V.I. Goncharov (Editor), Geodynamics, Magmatism and Minerageny of Continental Margins in North Pacific. Severo-Vostochnyi Kompleksnyi Nauchno-issledovatel'skii Insitut Dal'nevostochnogo Otdeleniya Rossiiskoi Akademii nauk, Magadan, pp. 131-134 (in Russian).

Biakov, A.S., 2006. Permian bivalve mollusks of Northeast Asia. Journal of Asian Earth Sciences, 26: 235-242.

Biakov, A.S., 2007. Permian Biostratigraphy of the Northern Okhotsk Region (Northeast Asia). Stratigraphy and Geological Correlation, 15(2): 161-184.

Biakov, A.S., Prokopiev, A.V., Kutygin, R.V., Vedernikov, I.L. and Budnikov, I.V., 2007. Geodynamic environments of Permian sedimentary basins in the Verkhoyansk–Kolyma folded region. In: A.I. Khanchuk and A.I. Khanchuk (Editors), Tectonics and Metallogeny of the Circum-North Pacific and Eastern Asia: Proc. of the Leonid Parfenov Memorial Conference, June 11-16. Khabarovsk. Institute of Tectonics and Geophysics. Far East Branch of the Russian Academy of Sciences, Khabarovsk, pp. 79-81 (in Russian).

Biakov, A.S., Prokopiev, A.V., Kutygin, R.V., Vedernikov, I.V. and Budnikov, I.V., 2005. Geodynamic formation environments of Permian sedimentary basins in Verkhoyansk-Kolyma folded area. Otechestvennaya geologiya, 5: 81-85 (in Russian).

Biakov, A.S. and Shi, G.R., 2010. Palaeobiogeography and palaeogeographical implications of Permian marine bivalve faunas in Northeast Asia (Kolyma-Omolon and Verkhoyansk-Okhotsk regions, northeastern Russia). Palaeogeography, Palaeoclimatology, Palaeoecology, 298(1-2): 42-53.

Biakov, A.S. and Vedernikov, I.L., 1990. Stratigraphy of Permian deposits of northeast framework of Okhotsk Massif, central and southeast parts of Ayan-Yuryakh antiklinorium. . North-East Interdisciplinary Scientific Research Institute. Far East Branch of the Russian Academy of Sciences,, Magadan, Russia, pp. 1-69 (in Russian).

Biakov, A.S., Vedernikov, I.L. and Akinin, V.V., 2010. ПЕРМСКИЕ ДИАМИКТИТЫ СЕВЕРО-ВОСТОКА АЗИИ И ИХ ВЕРОЯТНОЕ ПРОИСХОЖДЕНИЕ (Permian Diamictites in Northeast Asia and their Possible Origins). ВЕСТНИК СВНЦ ДВО РАН (Vestnik SVNC DVO RAN), 1 14-24 (in Russian).

Birgenheier, L.P., Frank, T.D., Fielding, C.R. and Rygel, M.C., 2010. Coupled carbon isotopic and sedimentological records from the Permian system of eastern Australia reveal the response of atmospheric carbon dioxide to glacial growth and decay during the late Palaeozoic Ice Age. Palaeogeography, Palaeoclimatology, Palaeoecology, 286: 178-193.

Blakey, R.C., 2008. Gondwana paleogeography from assembly to breakup--A 500 m.y. odyssey. In: C.R. Fielding, T.D. Frank and J.L. Isbell (Editors), Resolving the Late Paleozoic Ice Age in Time and Space. Geological Society of America Special Publication. Boulder, CO, pp. 1-28.

Briggs, D.J.C., 1998. Permian Productidina and Strophalosiidina from the Sydney-Bowen Basin and New England Orogen; systematics and biostratigraphic significance. Memoir of the Association of Australasian Palaeontologists, 19: 258.

Broster, B.E. and Hicock, S.R., 1985. Multiple flow and support mechanisms and the development of inverse grading in a subaquatic glacigenic debris flow. Sedimentology, 32(5): 645-657.

Bryan, S.E., Cook, A., Evans, J.P., Colls, P.W., Wells, M.G., Lawrence, M.G., Jell, J.S., Greig, A. and Leslie, R., 2004. Pumice rafting and faunal dispersion during 2001-2002 in the Southwest Pacific; record of a dacitic submarine explosive eruption from Tonga. Earth and Planetary Science Letters, 227(1-2): 135-154.

Buatois, L.A. and Mángano, M.G., 2011. Ichnology: Organism-Substrate Interactions in Space and Time. Cambridge University Press, Cambridge, 366 pp.

Caballero, L., Sarocchi, D., Borselli, L. and Cardenas, A.I., 2012. Particle interaction inside debris flows; evidence through experimental data and quantitative clast shape analysis. Journal of Volcanology and Geothermal Research, 231-232: 12-23.

Carey, S.N. and Sigurdsson, H., 1980. The Roseau ash; deep-sea tephra deposits from a major eruption on Dominica, Lesser Antilles arc. Journal of Volcanology and Geothermal Research, 7(1-2): 67-86.

Carr, S., 2001. Micromorphological criteria for discriminating subglacial and glacimarine sediments: Evidence from a contemporary tidewater glacier, Spitsbergen. Quaternary International, 86: 71-79.

Carto, S.L. and Eyles, N., 2012. Sedimentology of the Neoproterozoic (c. 580 Ma) Squantum ‘Tillite’, Boston Basin, USA: Mass flow deposition in a deep-water arc basin lacking direct glacial influence. Sedimentary Geology, 269–270(0): 1-14.

Chen, B., Joachimski, M.M., Shen, S., Lambert, L.L., Lai, X., Wang, X., Chen, J. and Yuan, D., 2013. Permian ice volume and palaeoclimate history; oxygen isotope proxies revisited. Gondwana Research, 24(1): 77-89.

Chumakov, N.M., 1994. Evidence of Late Permian glaciation in the Kolyma River Basin: a repercussion of the Gondwana glaciations in northeast Asia? Stratigraphy and Geological Correlation, 2(5): 426-444.

Chumakov, N.M. and Zharkov, M.A., 2003. Climate during the Permian-Triassic biosphere reorganizations. Article 2. Climate of the Late Permian and Early Triassic: General Inferences. Stratigraphy and Geological Correlation, 11(4): 361-375.

Clarke, M.J., Forsyth, S.M., Bacon, C.A., Banks, M.R., Calver, C.R. and Everard, J.L., 1989. Late Carboniferous-Triassic. In: C.F.M. Burrett, E L (Editor), Geology and mineral resources of Tasmania; Geological Society of Australia Special Publication, pp. 293-338.

Cleal, C.J. and Thomas, B.A., 2005. Palaeozoic tropical rainforests and their effect on global climates: is the past the key to the present? Geobiology, 3: 13-31.

Crowell, J.C., 1983. Ice ages recorded on Gondwanan continents. Geological Society of South Africa Transactions, 86: 238-261.

Crowell, J.C., 1999. Pre-Mesozoic ice ages: their bearing on understanding the climate system. Geological Society of America Memoir, 192: 1-106.

Crowell, J.C. and Frakes, L.A., 1970. Ancient Gondwana glaciations. In: S.H. Haughton (Editor), Proceedings and Papers of the Second Gondwana Symposium, South Africa. CSIR, Pretoria, pp. 469-476.

Crowley, T.J. and Baum, S.K., 1991. Estimating Carboniferous sea-level fluctuations from Gondwana ice extent. Geology, 19: 975-977.

Crowley, T.J., Hyde, W.T. and Short, D.A., 1989. Seasonal cycle variations on the supercontinent of Pangaea. Geology, 17: 457-460.

Crowley, T.J. and North, G.R., 1991. Paleoclimatology. Oxford University Press, New York.

Davydov, V., 2014. Warm water benthic Foraminifera document the Pennsylvanian-Permian warming and cooling events; the record from the Western Pangea tropical shelves. Palaeogeography, Palaeoclimatology, Palaeoecology, 414: 284-295.

Davydov, V.I., Belasky, P. and Karavayeva, N.I., 1996. Permian fusulinids from the Koryak Terrane, northeastern Russia, and their paleobiogeographic affinity. Journal of Foraminiferal Research, 26(3): 213-243.

Davydov, V.I., Biakov, A.S., Isbell, J.L., Crowley, J., Schmitz, M.D. and Vedernikov, I., 2015. Middle Permian U–Pb zircon ages of the “glacial” deposits of the Atkan Formation, Ayan-Yuryakh anticlinorium, Magadan province, NE Russia: Their significance for global climatic interpretations. Gondwana Research, http://dx.doi.org/10.1016/j.gr.2015.10.014

De Blasio, F., Engvik, L., Harbitz, C.B. and Elverhoi, A., 2004. Hydroplaning and submarine debris flows. Journal of Geophysical Research, C, Oceans, 109: no.1, 1-15.

De Blasio, F.V., Engvik, L.E. and Elverhoi, A., 2006. Sliding of outrunner blocks from submarine landslides. Geophysical Research Letters, 33(6).

DiMichele, W.A., Gastaldo, R.A., Pfefferkorn, H.W. and Jablonski, N.G., 2005. Plant biodiversity partitioning in the Late Carboniferous and Early Permian and its implications for ecosystem assembly. Proceedings of the California Academy of Sciences (1907), 56, Suppl. 1: 32-49.

Dionne, J.-C., 1985. Drift-ice abrasion marks along rocky shores. Journal of Glaciology, 31(109): 237-241.

Elverhøi, A., Issler, D., Blasio, F.V., Ilstad, T., Harbitz, C.B. and Gauer, P., 2005. Emerging insights into the dynamics of submarine debris flows. Natural Hazards and Earth System Sciences (NHESS), 5(5): 633-648.

Epshteyn, O.G., 1981a. Middle Carboniferous ice-marine deposits of northeastern USSR. In: M.J. Hambrey and W.B. Harland (Editors), Earth's pre-Pleistocene glacial record. Cambridge University Press, Cambridge, pp. 268-269.

Epshteyn, O.G., 1981b. Late Permian ice-marine deposits of the Atkan Formation in the Kolyma River headwaters regions, U.S.S.R. In: M.J. Hambrey and W.B. Harland (Editors), Earth's pre-Pleistocene glacial record. Cambridge University Press, Cambridge, pp. 270-273.

Eyles, N., 1993. Earth's glacial record and its tectonic setting. Earth-Science Reviews, 35: 1-248.

Eyles, N., Eyles, C.H., Woodworth-Lynas, C. and Randall, T.A., 2005. The sedimentary record of drifting ice (early Wisconsin Sunnybrook deposit) in an ancestral ice-dammed Lake Ontario, Canada. Quaternary Research, 63: 171-181.

Falcon-Lang, H.J. and DiMichele, W.A., 2010. What happened to the coal forest during Pennsylvanian glacial phases? PALAIOS, 25: 611-617.

Fielding, C.R., Frank, T.D., Birgenheier, L.P., Rygel, M.C., Jones, A.T. and Roberts, J., 2008a. Stratigraphic imprint of the late Palaeozoic ice age in eastern Australia: a record of alternating glacial and nonglacial climate regime. Journal of the Geological Society, London, 165: 129-140.

Fielding, C.R., Frank, T.D., Birgenheier, L.P., Rygel, M.C., Jones, A.T. and Roberts, J., 2008b. Stratigraphic record and facies associations of the late Paleozoic ice age in eastern Australia (New South Wales and Queensland). In: C.R. Fielding, T. Frank and J.L. Isbell (Editors), Resolving the Late Paleozoic Ice Age in Time and Space. Geological Society of America Special Paper 441, Boulder, pp. 41-57.

Fielding, C.R., Frank, T.D. and Isbell, J.L., 2008c. The late Paleozoic ice age--A review of current understanding and synthesis of global climate patterns. In: C.R. Fielding, T.D. Frank and J.L. Isbell (Editors), Resolving the Late Paleozoic Ice Age in Time and Space. Geological Society of America Special Publication, Boulder, CO, pp. 343-354.

Fisher, R.V., 1983. Flow transformations in sediment gravity flows. Geology (Boulder), 11(5): 273-274.

Fisher, R.V., 1984. Submarine volcaniclastic rocks. Geological Society, London, Special Publications, 16: 5-27.

Frakes, L.A., Kemp, E.M. and Crowell, J.C., 1975. Late Paleozoic glaciation: Part VI, Asia. Geological Society of America Bulletin, 86(4): 454-464.

Frank, T.D., Shultis, A.I. and Fielding, C.R., 2015. Acme and demise of the late Palaeozoic ice age: A view from the southeastern margin of Gondwana. Palaeogeography Palaeoclimatology Palaeoecology, 418: 176-192.

Ganelin, V.G., 1984. Taimyr-Kolyma Subrealm. In: G.V. Kotljar and D.L. Stepanov (Editors), Osnovnye cherty stratigrafii permskoi sistemy SSSR (Main Features of Stratigraphy of the Permian System in the USSR). Nedra, Leningrad, pp. 111-142 (in Russian).

Ganelin, V.G. and Biakov, A.S., 2006. The Permian biostratigraphy of the Kolyma-Omolon region, Northeast Asia. Journal of Asian Earth Sciences, 26(3-4): 225-234.

Gilbert, R., 1990. Rafting in glacimarine environments. In: J.A. Dowdeswell and J.D. Scourse (Editors), Glacimarine environments: processes and sediments. Geological Society Special Publications, pp. 105-120.

González, C.R. and Díaz Saravia, P., 2010. Bimodal character of the Late Paleozoic glaciations in Argentina and bipolarity of climatic changes. Palaeogeography, Palaeoclimatology, Palaeoecology, 298(1-2): 101-111.

Gradstein, F.M., Ogg, J.G., Schmitz, M.D. and Ogg, G.M., 2012. The geologic time scale 2012. The geologic time scale 2012. Elsevier, Oxford, 1144 pp.

Grinenko, V.S., Budnikov, I.V. and Klets, A.G., 1997. Olistostromes in Permian section of central part of Verkhoyansk fold belt. Otechestvennaya Geologiya, 1997(2): 36-43 (in Russian).

Gulbranson, E.L., Isbell, J.L., Taylor, E.L., Ryberg, P.E., Taylor, T.N. and Flaig, P.P., 2012. Permian polar forests: deciduousness and environmental variation. Geobiology, 10(6): 479-495.

Gulbranson, E.L., Ryberg, P.E., Decombeix, A.-L., Taylor, E.L., Taylor, T.N. and Isbell, J.L., 2014. Leaf habit of Late Permian Glossopteris trees from high-palaeolatitude forests. Journal of the Geological Society of London, 171(4): 493-507.

Hambrey, M.J. and Glasser, N.F., 2012. Discriminating glacier thermal and dynamic regimes in the sedimentary record. Sedimentary Geology, 251-252: 1-33.

Hampton, M.A., 1972. The role of subaqueous debris flow in generating turbidity currents. Journal of Sedimentary Petrology, 42(4): 775-793.

Hand, B.M., 1997. Inverse grading resulting from coarse-sediment transport lag. Journal of Sedimentary Research, 67(1): 124-129.

Harbitz, C.B., Parker, G., Elverhoi, A., Marr, J.G., Mohrig, D. and Harff, P.A., 2003. Hydroplaning of subaqueous debris flows and glide blocks; analytical solutions and discussion. Journal of Geophysical Research, B, Solid Earth and Planets, 108: no.7, 18.

Haughton, P.D., 2000. Debrites and turbidites; strange bedfellows. Irish Journal of Earth Sciences, 18: 134-134.

Haughton, P.D., Barker, S.P. and McCaffrey, W.D., 2003. 'Linked' debrites in sand-rich turbidite systems - origin and significance. Sedimentology, 50(3): 459-482.

Haughton, P.D., Davis, C., McCaffrey, W. and Barker, S., 2009. Hybrid sediment gravity flow deposits – Classification, origin and significance. Marine and Petroleum Geology, 26(10): 1900-1918.

Heckel, P.H., 1994. Evaluation of evidence for glacio-eustatic control over marine Pennsylvanian cyclothems in North America and consideration of possible tectonic effects. In: J.M. Dennison and F.R. Ettensohn (Editors), Tectonic and eustatic controls on sedimentary cycles. SEPM (Society of Sedimentary Geology), Tulsa, pp. 65-87.

Heckel, P.H., 2008. Pennsylvanian cyclothems in Midcontinent North America as far-field effects of waxing and waning of Gondwana ice sheets. Special Paper - Geological Society of America, 441: 275-289.

Henderson, C.M., Davydov, V.I. and Wardlaw, B.R., 2012. The Permian Period. In: F.M. Gradstein, J.G. Ogg, M. Schmitz and G. Ogg (Editors), The geologic time scale 2012. Elsevier, Amsterdam, pp. 652-670.

Henry, L.C., Isbell, J.L., Fielding, C.R., Domack, E.W., Frank, T.D. and Fraiser, M.L., 2012. Proglacial deposition and deformation in the Upper Carboniferous to Lower Permian

Wynyard Formation, Tasmania: A process analysis. Palaeogeography, Palaeoclimatology, Palaeoecology, 315-316: 142-157.

Horton, D.E., Poulsen, C.J., Montañez, I.P. and DiMichele, W.A., 2012. Eccentricity-paced late Paleozoic climate change. Palaeogeography, Palaeoclimatology, Palaeoecology, 331-332: 150-161.

Horton, D.E., Poulsen, C.J. and Pollard, D., 2007. Orbital and CO2 forcing of late Paleozoic continental ice sheets. Geophysical Research Letters, 34: 1-6.

Horton, D.E., Poulsen, C.J. and Pollard, D., 2010. Influence of high-latitude vegetation feedbacks on late Paleozoic glacial cycles. Nature Geoscience, 3: 572-577.

Judson, S. and Barks, R.E., 1961. Microstructures on polished pebbles. American Journal of Science, 259: 371-381.

Ilstad, T., Elverhoi, A., Issler, D. and Marr, J.G., 2004. Subaqueous debris flow behaviour and its dependence on the sand/clay ratio; a laboratory study using particle tracking. Marine Geology, 213(1-4): 415-438.

Isbell, J.L., 2010. Environmental and paleogeographic implications of glaciotectonic deformation of glaciomarine deposits within Permian strata of the Metschel Tillite, southern Victoria Land, Antarctica. In: O.R. López-Gamundí and L.A. Buatois (Editors), Late Paleozoic Glacial Events and Postglacial Transgressions in Gondwana. Geological Society of America Special Publication 468, Boulder, CO, pp. 81-100.

Isbell, J.L. and Cuneo, N.R., 1996. Depositional framework of Permian coal-bearing strata, southern Victoria Land, Antarctica. Palaeogeography Palaeoclimatology Palaeoecology, 125(1-4): 217-238.

Isbell, J.L., Henry, L.C., Gulbranson, E.L., Limarino, C.O., Fraiser, M.L., Koch, Z.J., Ciccioli, P.L. and Dineen, A.A., 2012. Glacial paradoxes during the late Paleozoic ice age: Evaluating the equilibrium line altitude as a control on glaciation. Gondwana Research, 22(1): 1-19.

Isbell, J.L., Henry, L.C., Reid, C.M. and Fraiser, M.L., 2013. Sedimentology and palaeoecology of lonestone-bearing mixed clastic rocks and cold-water carbonates of the Lower Permian Basal Beds at Fossil Cliffs, Maria Island, Tasmania (Australia): Insight into the initial decline of the late Palaeozoic ice age. In: A. Gąsiewicz and M. Slowakiewicz (Editors), Late Palaeozoic Climate Cycles: Their Evolutionary, Sedimentological and Economic Impact. Geological Society Special Publication, London, pp. 307-341.

Isbell, J.L., Koch, Z.J., Szablewski, G.M. and Lenaker, P.A., 2008. Permian glacigenic deposits in the Transantarctic Mountains, Antarctica. In: C.R. Fielding, T.D. Frank and J.L. Isbell (Editors), Resolving the Late Paleozoic Ice Age in Time and Space. Geological Society of America Special Publication, Boulder, CO, pp. 59-70.

Isbell, J.L., Miller, M.F., Wolfe, K.L. and Lenaker, P.A., 2003. Timing of late Paleozoic glaciation in Gondwana: was glaciation responsible for the development of northern hemisphere cyclothems? In: M.A. Chan and A.W. Archer (Editors), Extreme depositional environments: mega end members in geologic time. Geological Society of America Special Paper, Boulder, Colorado, pp. 5-24.

Isbell, J.L., Seegers, G.M. and Gelhar, G.A., 1997. Upper Paleozoic glacial and postglacial deposits, central Transantarctic Mountains, Antarctica. In: I.P. Martini (Editor), late glacial and postglacial environmental changes: Quaternary, Carboniferous-Permian, and Proterozoic. Oxford University Press, Oxford, U.K., pp. 230-242.

Kashik, D.S., Ganelin, V.G., Karavaeva, N.I. and Biakov, A.S. (Editors), 1990. Opornyi razres permi Omolonskogo massiva (Permian key section of the Omolon Massif). Nauka, Leningrad, 1-200 (in Russian) pp.

Kilfeather, A., Ó Cofaigh, C., Dowdeswell, J., van der Meer, J. and Evans, D., 2010. Micromorphological characteristics of glacimarine sediments: implications for distinguishing genetic processes of massive diamicts. Geo-Marine Letters, 30(2): 77-97.

Klets, A.G., Budnikov, I.V., Kutygin, R.V., Biakov, A.S., Grinenko, V.S., Shi, G.R., Campi, M.J. and Shen, S., 2006. The Permian of the Verkhoyansk-Okhotsk region, NE Russia. Journal of Asian Earth Sciences, 26(3-4): 258-268.

Koch, J.T. and Frank, T.D., 2012. Imprint of the Late Palaeozoic Ice Age on stratigraphic and carbon isotopic patterns in marine carbonates of the Orogrande Basin, New Mexico, USA. Sedimentology, 59(1): 291-318.

Korte, C., Jones, P.J., Brand, U., Mertmann, D. and Veizer, J., 2008. Oxygen isotope values from high-latitudes; clues for Permian sea-surface temperature gradients and late Palaeozoic deglaciation. Palaeogeography, Palaeoclimatology, Palaeoecology, 269(1-2): 1-16.

Kossovaya, O.L. and Kropatcheva, G.S., 2013. Extinction of Guadalupian rugose corals: an example of biotic response to the Kamura event (southern Primorye, Russia). In: A. Gąsiewicz and M. Slowakiewicz (Editors), Palaeozoic Climate Cycles: Their evolutionary and sedimentological impact. Geological Society, London, Special Publications, London, pp. 407-430.

Kotlyar, G.V., Kossovaya, O.L. and Zhuravlev, A.V., 2004. Interregional Correlation of Main Permian Event Boundaries. Tikhookeanskaya Geologiya, 23(4): 25-42 (In Russian).

Lachniet, M.S., Larson, G.J., Strasser, J.C., Lawson, D.E., Evenson, E.B. and Alley, R.B., 1999. Microstructures of glacigenic sediment-flow deposits, Matanuska Glacier, Alaska. Special Paper - Geological Society of America, 337: 45-57.

Lawver, L.A., Dalziel, I.W.D., Norton, I.O. and Gahagan, L.M., 2008. The Plates 2007 Atlas of Plate Reconstructions (750 Ma to Present Day), Plates Progress Report No. 310-0308.

López-Gamundí, O.R., 1997. Glacial-postglacial transition in the Late Paleozoic basins of southern South America. In: I.P. Martini (Editor), Late glacial and postglacial environmental changes: Quaternary, Carboniferous-Permian, and Proterozoic. Oxford University Press, Oxford, U.K., pp. 147-168.

Mantle, D.J., Kelman, A.P., Nicoll, R.S. & Laurie, J.R., 2010. Australian Biozonation Chart. Geoscience Australia Canberra.

Manville, V., Segschneider, B. and White, J.D.L., 2002. Hydrodynamic behaviour of Taupo 1800a pumice: implications for the sedimentology of remobilized pyroclasts. Sedimentology, 49: 955-976.

Manville, V., White, J.D.L., Houghton, B.F. and Wilson, C.J.N., 1998. The saturation behaviour of pumice and some sedimentological implications. Sedimentary Geology, 119(1-2): 5-16.

Martinsen, O.J., 1989. Styles of soft-sediment deformation on a Namurian (Carboniferous) delta slope, Western Irish Namurian Basin, Ireland. Geological Society, London, Special Publications, 41: 167-177.

Menzies, J., van der Meer, J.J.M., Domack, E. and Wellner, J.S., 2010. Micromorphology: as a tool in the detection, analyses and interpretation of (glacial) sediments and man-made materials. Proceedings of the Geologists' Association, 121(3): 281-292.

Menzies, J., van der Meer, J.J.M. and Rose, J., 2006. Till; as a glacial "tectomict", its internal architecture, and the development of a "typing" method for till differentiation. In: P.J. Fleisher, L.K. Knuepfer and D.R. Butler (Editors), Geomorphology, pp. 172-200.

Menzies, J. and Zaniewski, K., 2003. Microstructures within a modern debris flow deposit derived from Quaternary glacial diamicton; a comparative micromorphological study. Sedimentary Geology, 157(1-2): 31-48.

Metcalfe, I., Crowley, J.L., Nicoll, R.S. and Schmitz, M., 2015. High-precision U-Pb CA-TIMS calibration of Middle Permian to Lower Triassic sequences, mass extinction and extreme climate-change in eastern Australian Gondwana. Gondwana Research, 28: 61-81.

Mikhaylov, Y.A., Ustritskiy, V.I., Chernyak, G.Y. and Yavshits, G.P., 1970. Upper Permian glaciomarine sediments of the northeastern USSR. Doklady. Earth Science Sections, 190(1-6): 100-102 (in Russian).

Miller, M.F., Knepprath, N.E., Cantrill, D.J., Francis, J.E. and Isbell, J.L., 2015. Highly productive polar forests from the Permian of Antarctica. Palaeogeography, Palaeoclimatology, Palaeoecology.

Mohrig, D., Whipple, K.X., Hondzo, M., Ellis, C. and Parker, G., 1998. Hydroplaning of subaqueous debris flows. Geological Society of America Bulletin, 110(3): 387-394.

Moncrieff, A.C.M., 1989. Classification of poorly-sorted sedimentary rocks. Sedimentary Geology, 65(1-2): 191-194.

Montañez, I.P. and Poulsen, C.J., 2013. The late Paleozoic ice age: an evolving paradigm. Annual Review of Earth & Planetary Sciences, 41(24): 1-28.

Mulder, T. and Alexander, J., 2001. The physical character of subaqueous sedimentary density flows and their deposits. Sedimentology, 48(2): 269-299.

Naylor, M.A., 1980. The origin of inverse grading in muddy debris flow deposits; a review. Journal of Sedimentary Petrology, 50(4): 1111-1116.

Nekrasov, G.E., 1976. Tectonics and magmatism and Taigonos North-West Kamchatka. Nauka, Moscow.

Nemec, W. and Steel, R.J., 1984. Alluvial and coastal conglomerates; their significant features and some comments on gravelly mass-flow deposits. Memoir - Canadian Society of Petroleum Geologists, 10: 1-31.

O'Brien, P.E. and Christie-Blick, N., 1992. Glacially grooved surfaces in the Grant Group, Grant Range, Canning Basin and the extent of late Palaeozoic Pilbara ice sheets. BMR Journal of Australian Geology and Geophysics, 13(2): 87-92.

Parfenov, L.M., 1984. Continental Margins and Island Arcs of Mesozoides in Northeast Asia. Nauka, Novosibirsk (in Russian).

Parfenov, L.M., Berzin, N.A., Khanchuk, A.I., Badarch, G., Belichenko, V.G., Bulgatov, A.N., Dril', S.I., Kirillova, G.L., Kuz'min, M.I., Noklerberg, W., Prokopiev, A.V., Timofeev, V.F., Tomurtagoo, O. and Yan, K., 2003. A model for the formation of orogenic belts in Central and Northeast Asia. Tikhookeanskaya Geologiya 6, 6: 7-42 (in Russian).

Paterson, W.S.B., 1994. The physics of glaciers. Pergamon, Oxford, 480 pp.

Phillips, E., 2006. Micromorphology of a debris flow deposit; evidence of basal shearing, hydrofracturing, liquefaction and rotational deformation during emplacement. Quaternary Science Reviews, 25(7-8): 720-738.

Picard, M., Schneider, J.-L. and Boudon, G., 2006. Contrasting sedimentary processes along a convergent margin; the Lesser Antilles arc system. Geo-Marine Letters, 26(6): 397-410.

Pickering, K. and Hiscott, R., 2015. Deep marine systems: Processes, deposits, environments, tectonics and sedimentation. American Geophysical Union, 672pp.

Posamentier, H.W. and Martinsen, O.J., 2011. The character and genesis of submarine mass-transport deposits; insights from outcrop and 3D seismic data. Special Publication - Society for Sedimentary Geology, 96: 7-38.

Postma, G., 1984. Mass-flow conglomerates in a submarine canyon; Abrioja fan-delta, Pliocene, Southeast Spain. Memoir - Canadian Society of Petroleum Geologists, 10: 237-258.

Powell, R. and Domack, E., 2002. Modern glaciomarine environments. In: J. Menzies (Editor), Modern and past glacial environments. Butterworth-Heinemann Ltd., Oxford, pp. 361-389.

Powers, M.C., 1953. A new roundness scale for sedimentary particles. Journal of Sedimentary Petrology, 23(2): 117-119.

Price, P.L., 1997. Permian to Jurassic palynostratigraphic nomenclature of the Bowen and Surat Basins. Queensland Minerals and Energy Review Series, 1997(1039-5555, 1039-5555): 137-178.

Raymond, A. and Metz, C., 2004. Ice and Its Consequences: Glaciation in the Late Ordovician, Late Devonian, Pennsylvanian-Permian, and Cenozoic Compared. Journal of Geology, 112: 655-670.

Rygel, M.C., Fielding, C.R., Frank, T.D. and Birgenheier, L.P., 2008. The magnitude of late Paleozoic glacioeustatic fluctuations: a synthesis. Journal of Sedimentary Research, 78: 500-511.

Scotese, C.R., 1997. The PALEOMAP Project: paleogeographic atlas and plate tectonic software, The PALEOMAP Project: paleogeographic atlas and plate tectonic software. Department of Geology, University of Texas, TX.

Shi, G.R., 2006. The marine Permian of East and Northeast Asia; an overview of biostratigraphy, palaeobiogeography and palaeogeographical implications. Journal of Asian Earth Sciences, 26(3-4): 175-206.

Shi, G.R. and Waterhouse, J.B., 2010. Late Palaeozoic global changes affecting high-latitude environments and biotas: An introduction. Palaeogeography, Palaeoclimatology, Palaeoecology, 298(1-2): 1-16.

Shpikerman, V.I., 1998. Domelovaya minerageniya Severo-Vostoka Azii (Pre-Cretaceous metallogeny of Northeast Asia). Severo-Vostochnyi Kompleksnyi Nauchno-issledovatel’skii Insitut Dal’nevostochnogo Otdeleniya Rossiiskoi Akademii Nauk (in Russian).

Sigurdsson, H., Sparks, R.S.J., Carey, S.N. and Huang, T.C., 1980. Volcanogenic sedimentation on the Lesser Antilles Arc. Journal of Geology, 88(5): 523-540.

Sohn, Y.K., 2000. Depositional processes of submarine debris flows in the Miocene fan deltas, Pohang Basin, SE Korea with special reference to flow transformation. Journal of Sedimentary Research, 70(3): 491-503.

Stanley, S.M., 1988. Paleozoic mass extinctions; shared patterns suggest global cooling as a common cause. American Journal of Science, 288(4): 334-352.

Stanley, S.M. and Powell, M.G., 2003. Depressed rates of origination and extinction during the late Paleozoic ice age; a new state for the global marine ecosystem. Geology, 31(10): 877-880.

Suwa, H., Okuda, S. and Ogawa, K., 1984. Size segregation of solid particles in debris flows; Part 1, Accumulation of large boulders at the flow front and inverse grading by the kinetic sieving effect. Kyoto Daigaku Bosai Kenkyujo Nenpo = Disaster Prevention Research Institute Annuals, 27B-1: 409-423.

Talling, P.J., Amy, L.A., Wynn, R.B., Peakall, J. and Robinson, M., 2004. Beds comprising debrite sandwiched within co-genetic turbidite: origin and widespread occurrence in distal depositional environments. Sedimentology, 51(1): 163-194.

Talling, P.J., Masson, D.G., Sumner, E.J. and Malgesini, G., 2012. Subaqueous sediment density flows: Depositional processes and deposit types. Sedimentology, 59(7): 1937-2003.

Taylor, E.L., Taylor, T.N. and Cúneo, N.R., 1992. The present is not the key to the past: a polar forest from the Permian of Antarctica. Science, 257: 1675-1677.

Thomas, G.S.P. and Connell, R.J., 1985. Iceberg drop, dump, and grounding structures from Pleistocene glacio-lacustrine sediments, Scotland. Journal of Sedimentary Petrology, 55(2): 243-249.

Torsvik, T.H. and Cocks, R.M., 2004. Earth geography from 400 to 250 Ma: a palaeomagnetic, faunal and facies review. Journal of the Geological Society, 161: 555-572.

Truswell, E.W., 1978. Palynology of the Permo-Carboniferous in Tasmania: an interim report. Bulletin of the Geological Survey of Tasmania, 56(1-37).

Umitbaev, R.B., 1963. , 1963. Stratigraphy of Upper Paleozoic rocks in the central part of the Okhotsk median massif. Nauchnye Zapiski NIIGA. Series Paleontology and Biostratigraphy, 2: 5-15 (in Russian).

Ustritsky, V.I., 1973. Permian climate. In: L. A. and L.V. Hill (Editors), The Permian and Triassic systems and their mutual boundary. Canadian Society of Petroleum Geologists Memoir 2, Calgary, pp. 733-744.

Ustritsky, V.I., 1975. The history of the Northeast of the USSR in the Upper Paleozoic. In: V.I. Ustritsky (Editor), Verchnii paleozoi Severo-Vostoka SSSR (The Upper Paleozoic of the Northeast of the USSR). Nauka, Leningrad, pp. 54-75 (in Russian).

Ustritsky, V.I. and Yavshits, G.P., 1971. Middle Carboniferous glaciomarine sediments of the northeastern USSR. Lithology and Mineral Resources: 159-161.

Veevers, J.J. and Powell, C.M., 1987. Late Paleozoic glacial episodes in Gondwanaland reflected in transgressive-regressive depositional sequences in Euramerica. Geological Society of America Bulletin, 98: 475-487.

Vesely, F. and Assine, M.L., 2014. Ice-keel scour marks in the geologic record: evidence from Carboniferous soft-sediment striated surfaces in the Parana´ Basin, southern Brazil. Journal of Sedimentary Research, 84: 26-39.

Visser, J.N.J., 1997a. A review of the Permo-Carboniferous glaciation in Africa. In: I.P. Martini (Editor), Late glacial and postglacial environmental changes: Quaternary, Carboniferous-Permian, and Proterozoic. Oxford University Press, Oxford, U.K., pp. 169-191.

Visser, J.N.J., 1997b. Deglaciation sequences in the Permo-Carboniferous Karoo and Kalahari basins of southern Africa: a tool in the analysis of cyclic glaciomarine basin fills. Sedimentology, 44: 507-521.

Waterhouse, J.B., 1976. World correlations for Permian marine faunas. Papers - Department of Geology, University of Queensland, 7(2): 232.

Woodworth-Lynas, C.M.T. and Dowdeswell, J.A., 1994. Soft-sediment striated surfaces and massive diamicton facies produced by floating ice. In: M. Deynoux, J.M.G. Miller, E.W. Domack, N. Eyles, I.J. Fairchild and G.M. Young (Editors), Earth's Glacial Record. Cambridge University Press, Cambridge, U.K., pp. 241-259.

Zaborovskaya, N.B., 1978. The inner zone of the Okhotsk-Chukchi-Skogen Taigonos belt. Nauka, Moscow (in Russian)

Zamoruev, V.V., 1974. Striations on pebbles and boulders. Lithology and Mineral Resources, 9(4): 475-479.

Zharkov, M.A. and Chumakov, N.M., 2001. Paleogeography and sedimentation settings during Permian-Triassic reorganizations in biosphere. Stratigraphy and Geological Correlation, 9(4): 340-363.

Figure

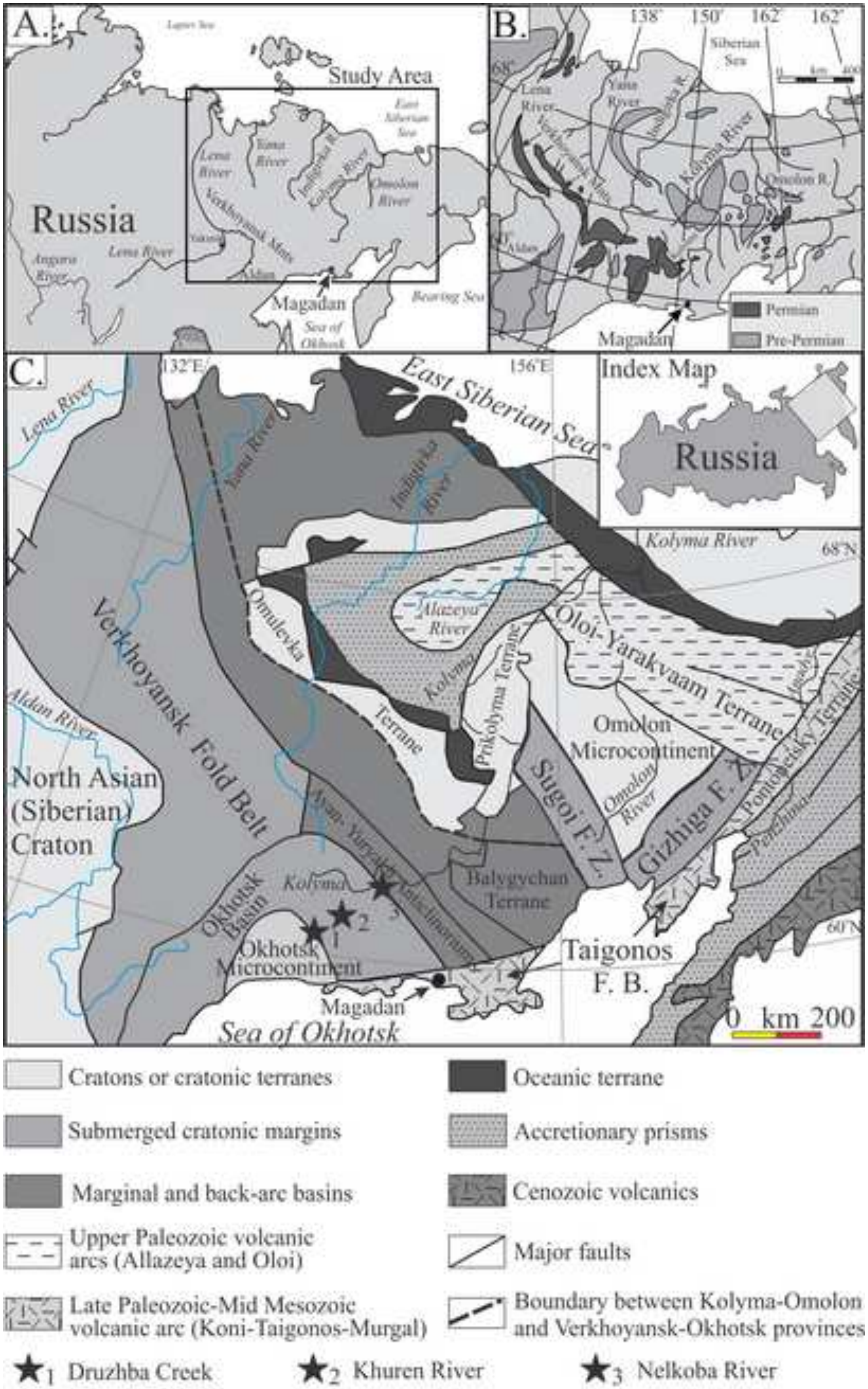

Figure 1. Isbell et al.
1.5 Column Image

Figure

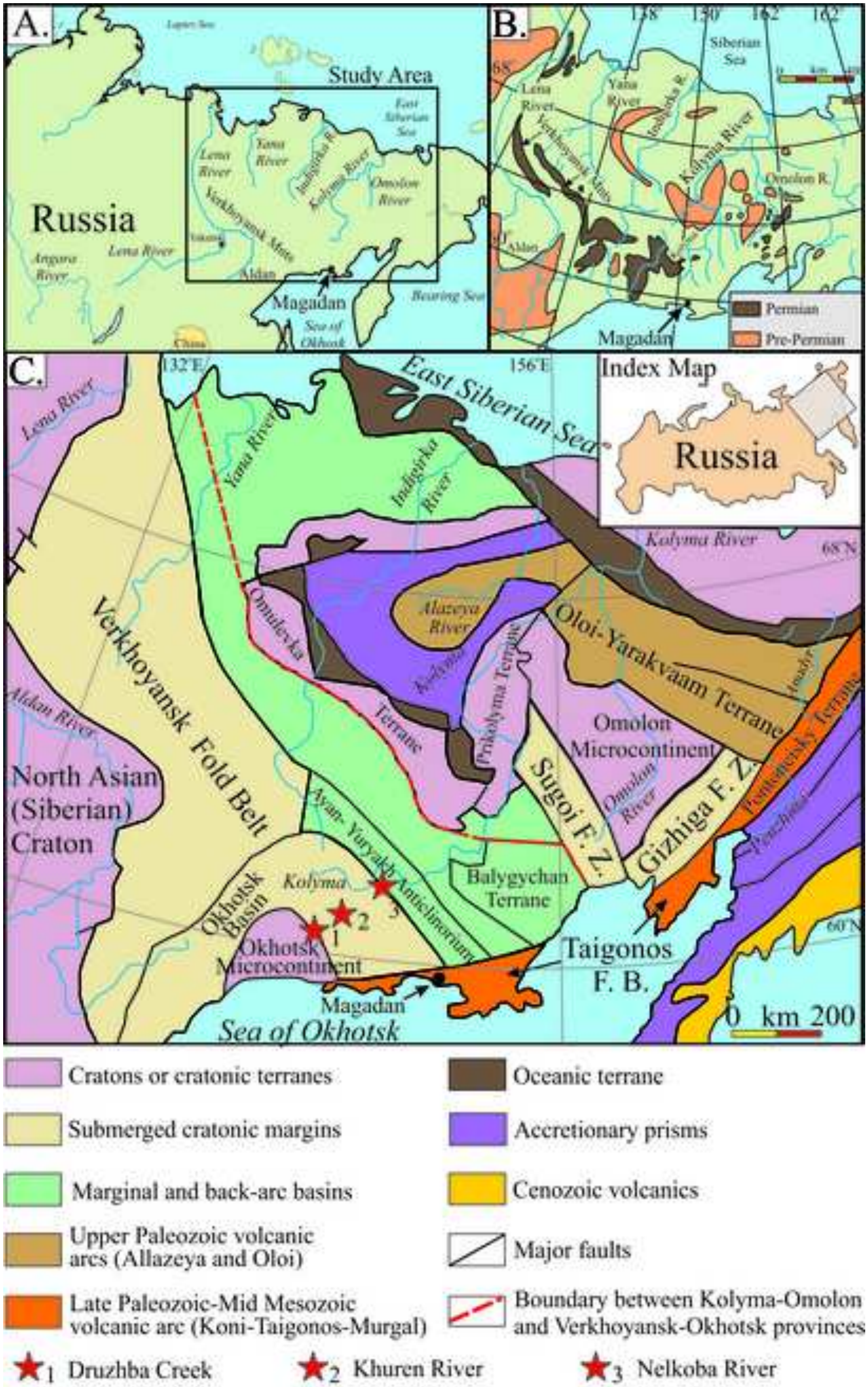

Figure 1. Isbell et al.
1.5 Column Image

Figure

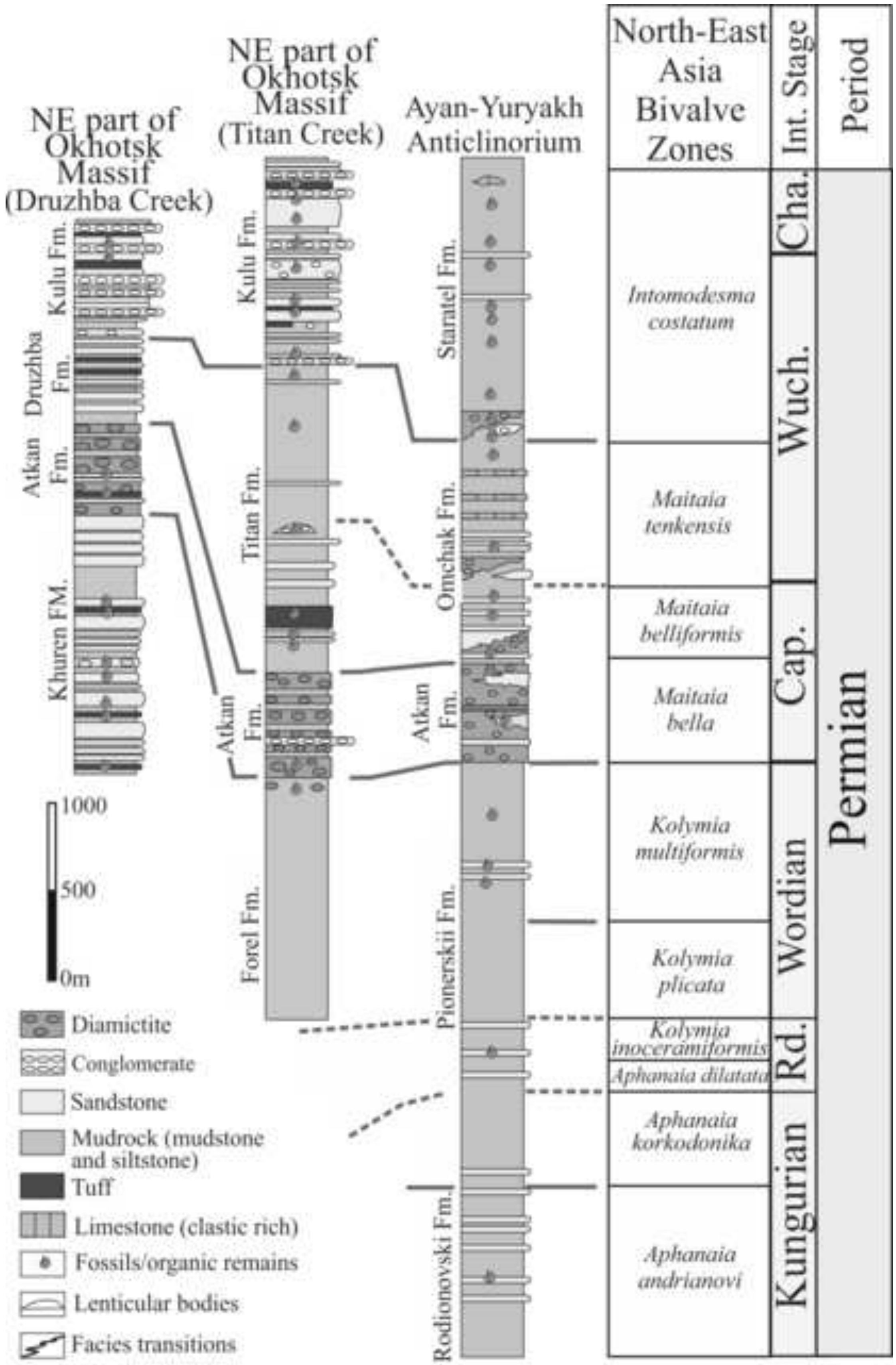

Figure 2. Isbell et al.

1.5 Column Image

Figure

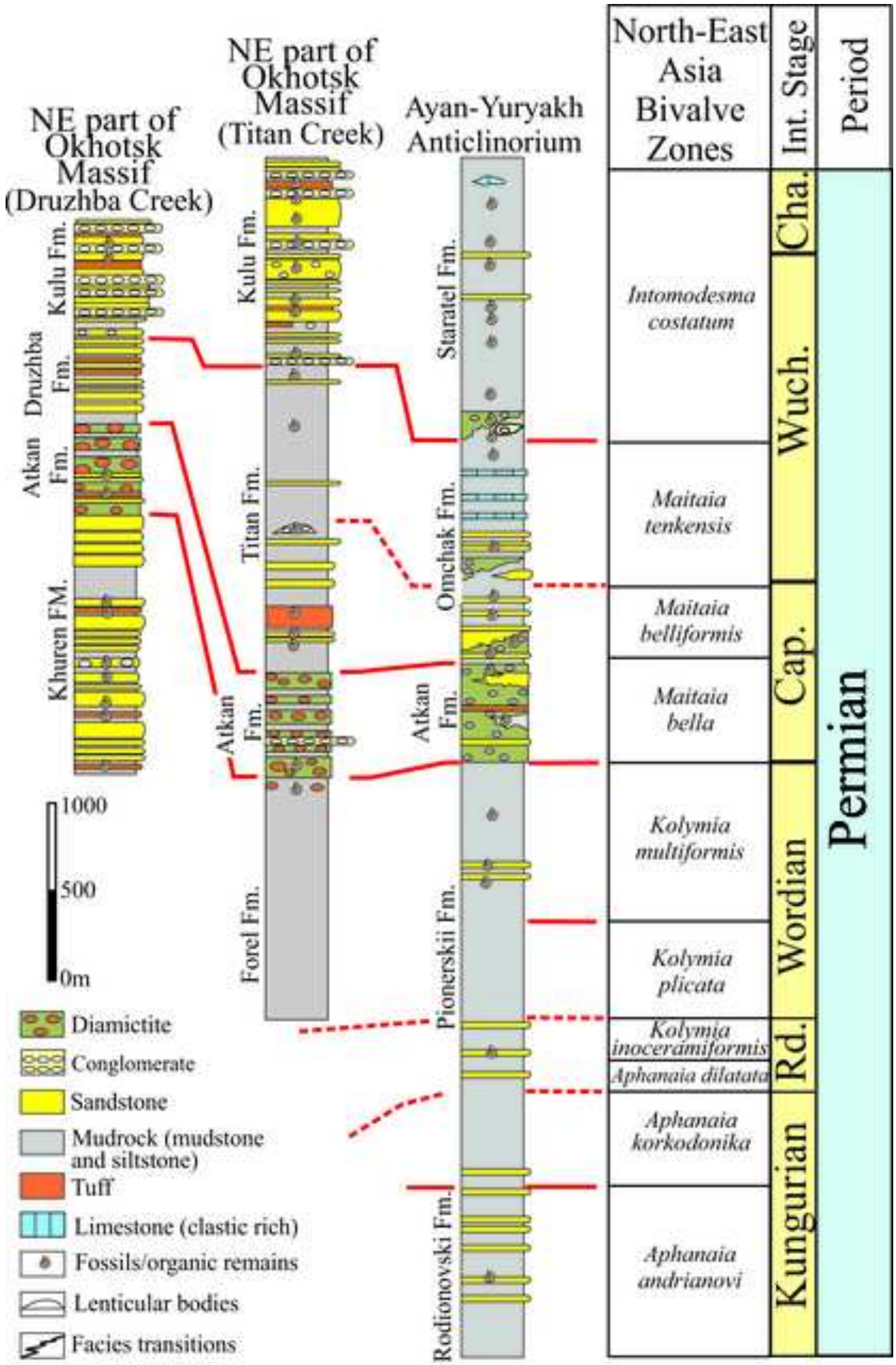

Figure 2. Isbell et al.
1.5 Column Image

Figure

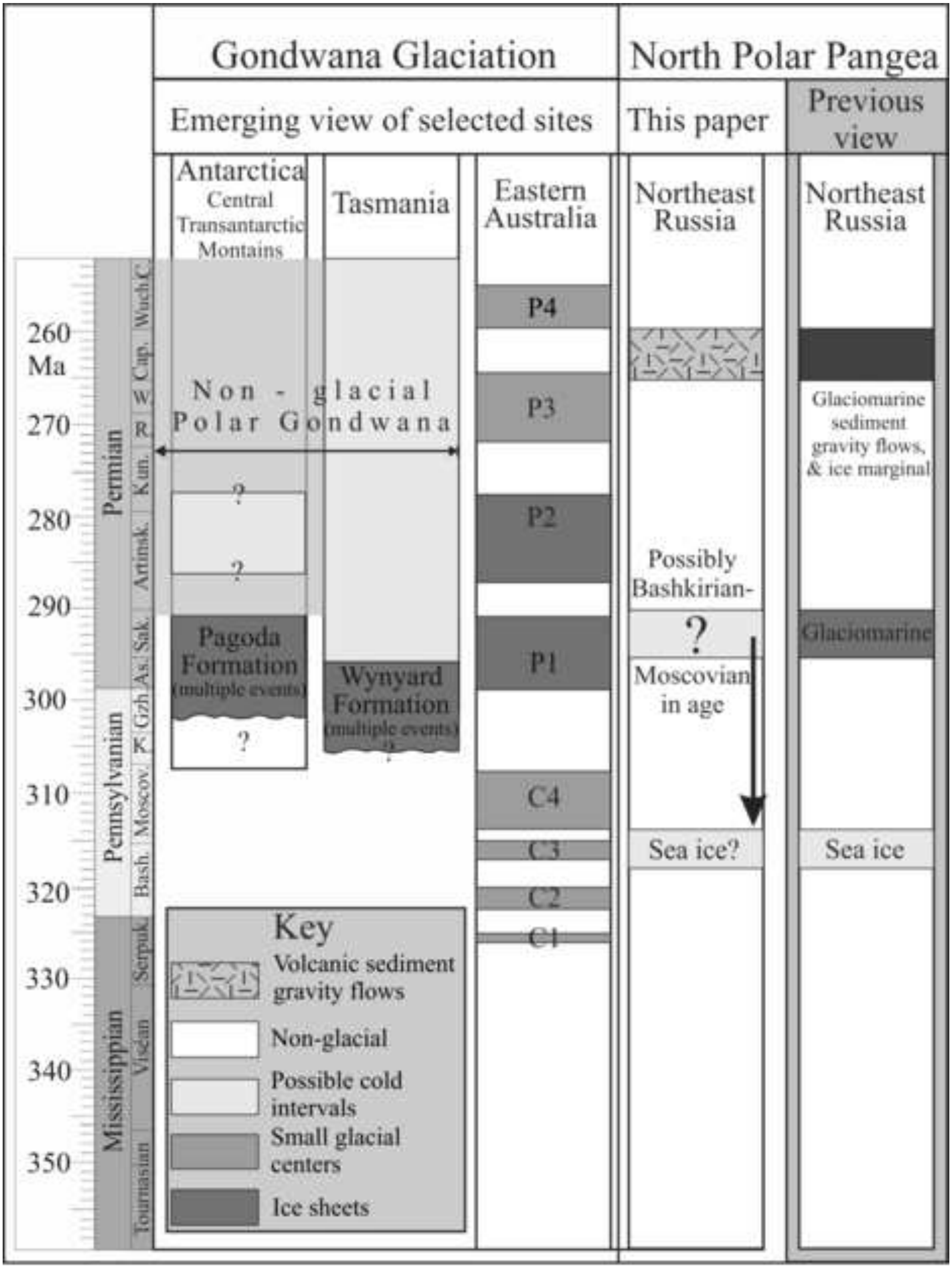

Figure 3. Isbell et al.
1.5 Column Image

Figure

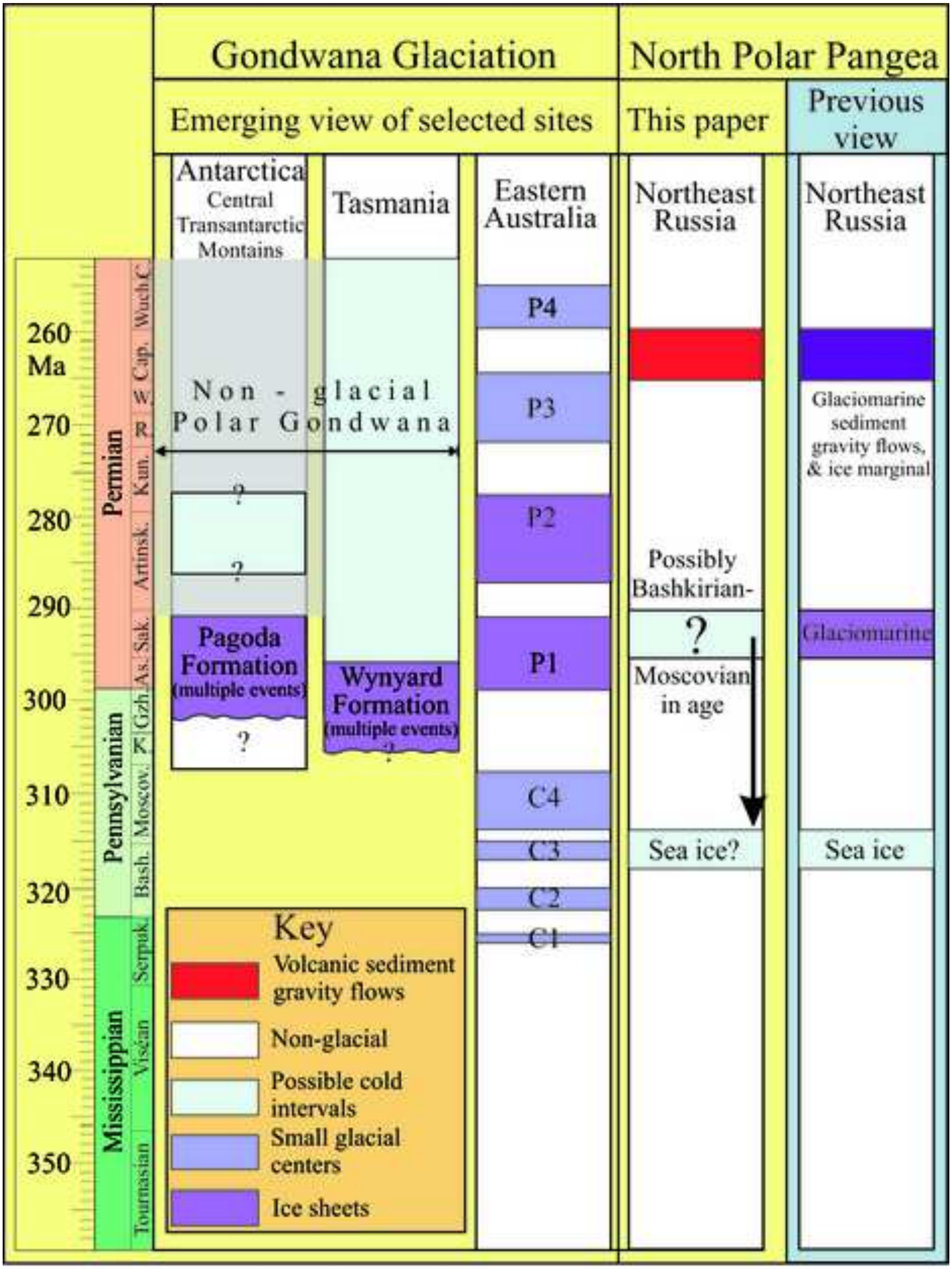

Figure 3. Isbell et al.
1.5 Column Image

Figure

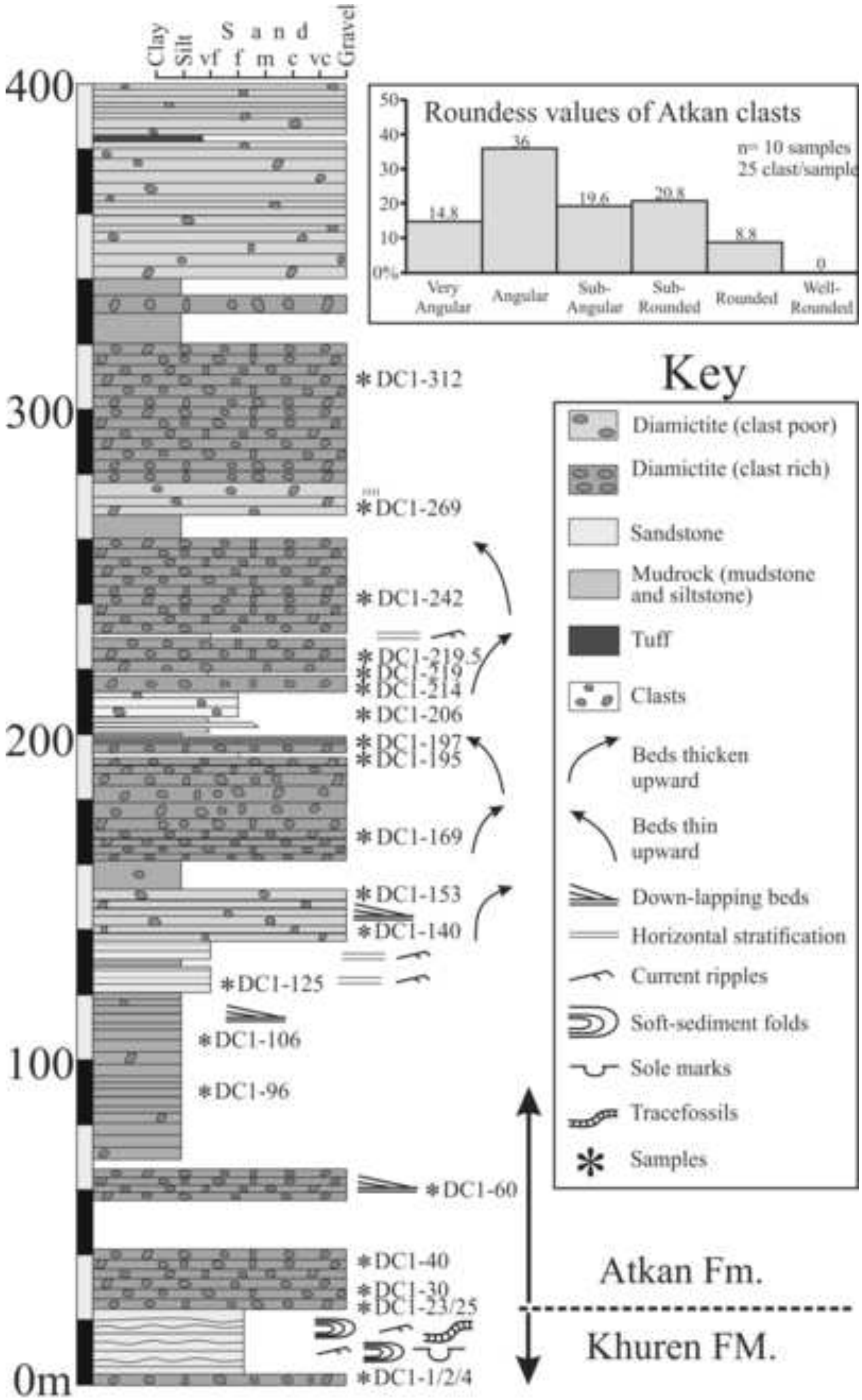

Figure 4. Isbell et al.
1.5 Column Image

Figure

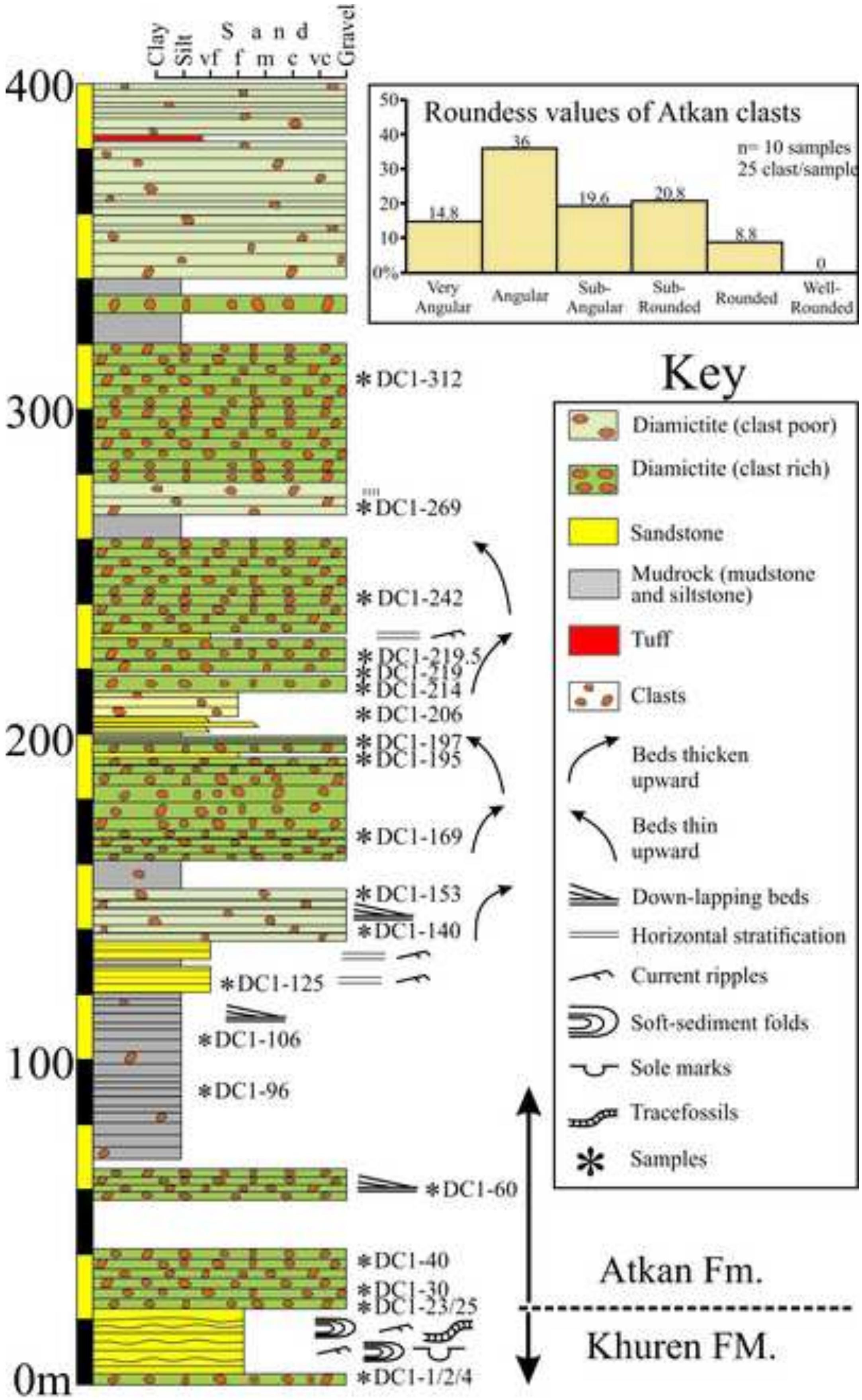

Figure 4. Isbell et al.
1.5 Column Image

Figure

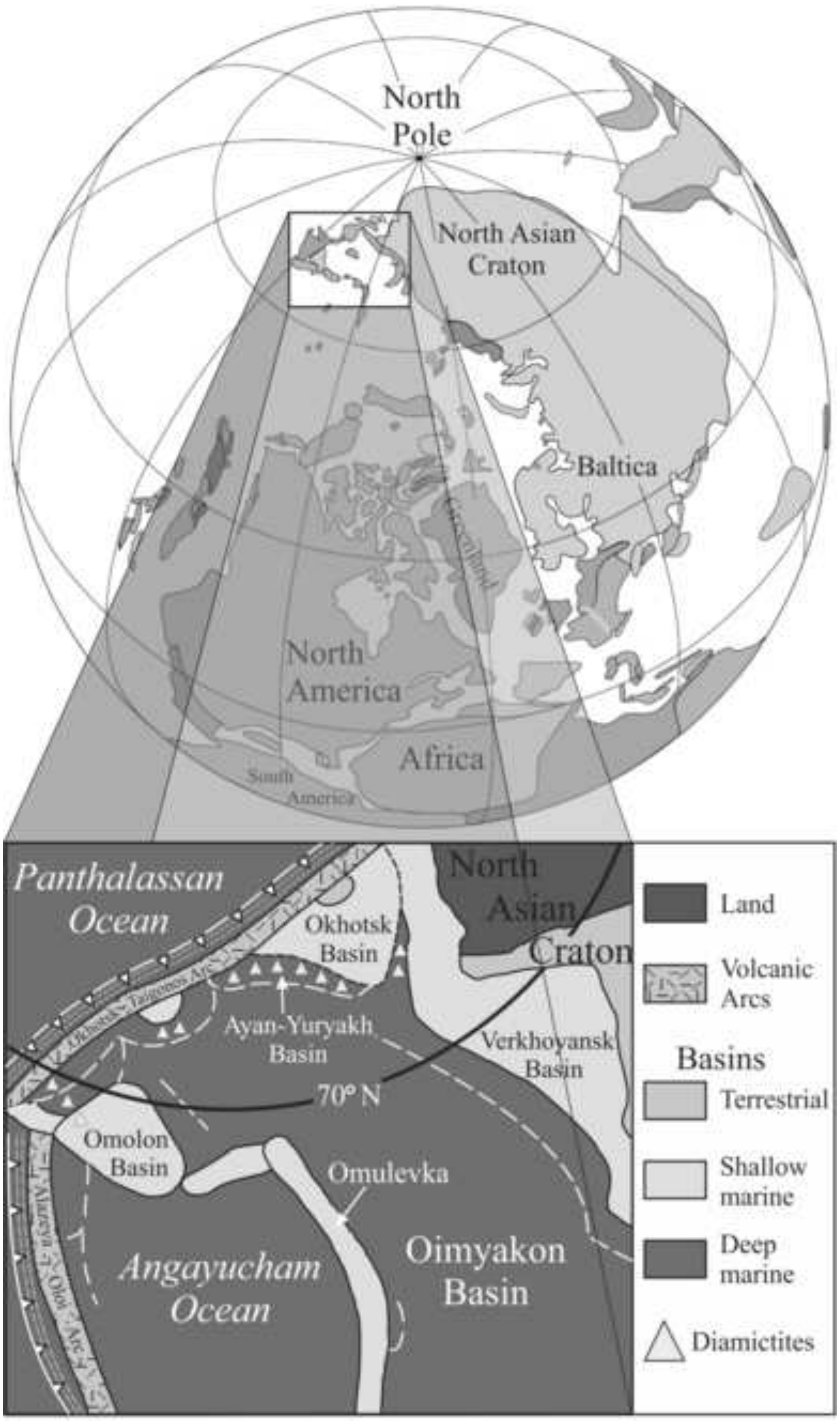

Figure 5. Isbell et al.
1.5 Column Image

Figure

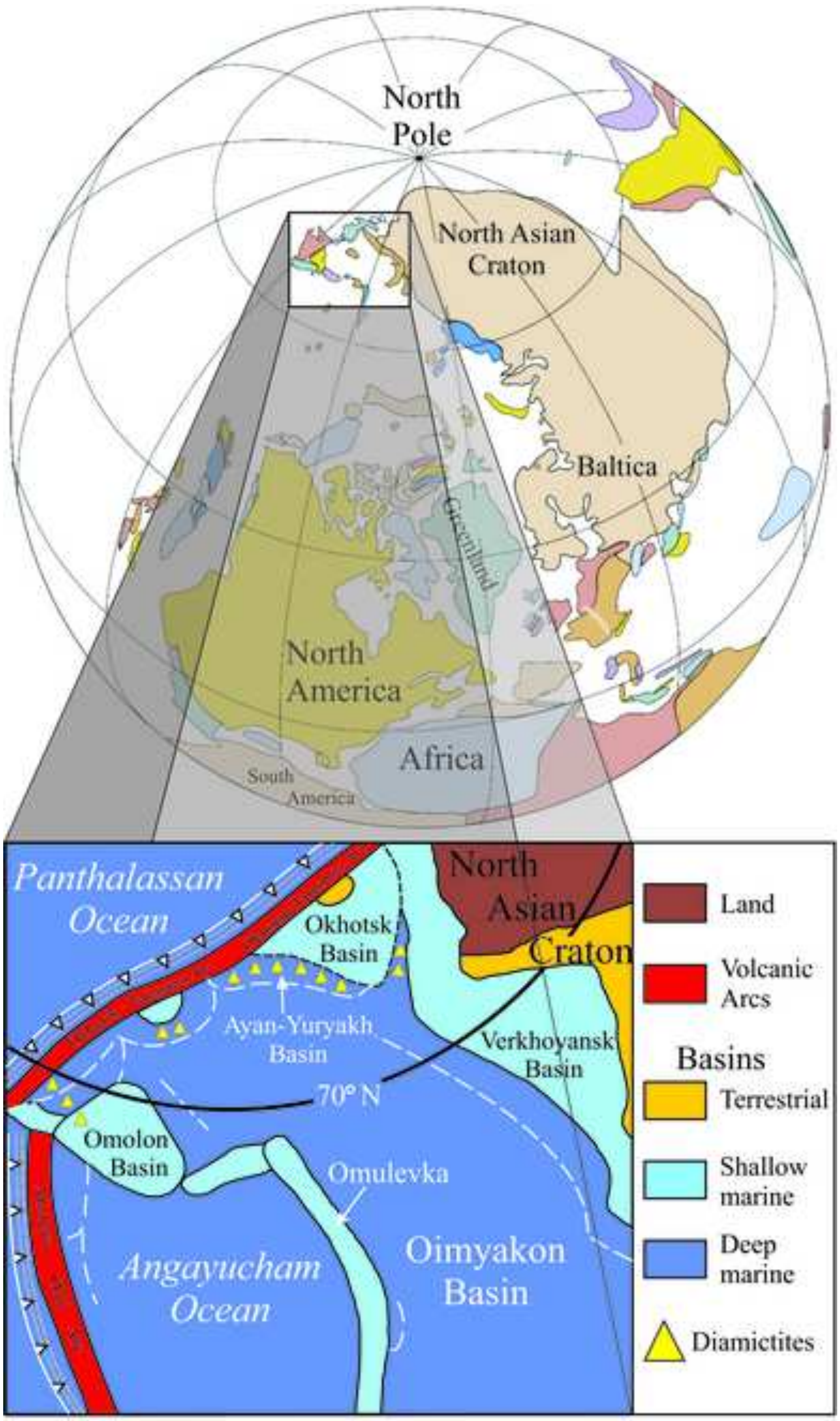

Figure 5. Isbell et al.
1.5 Column Image

Figure

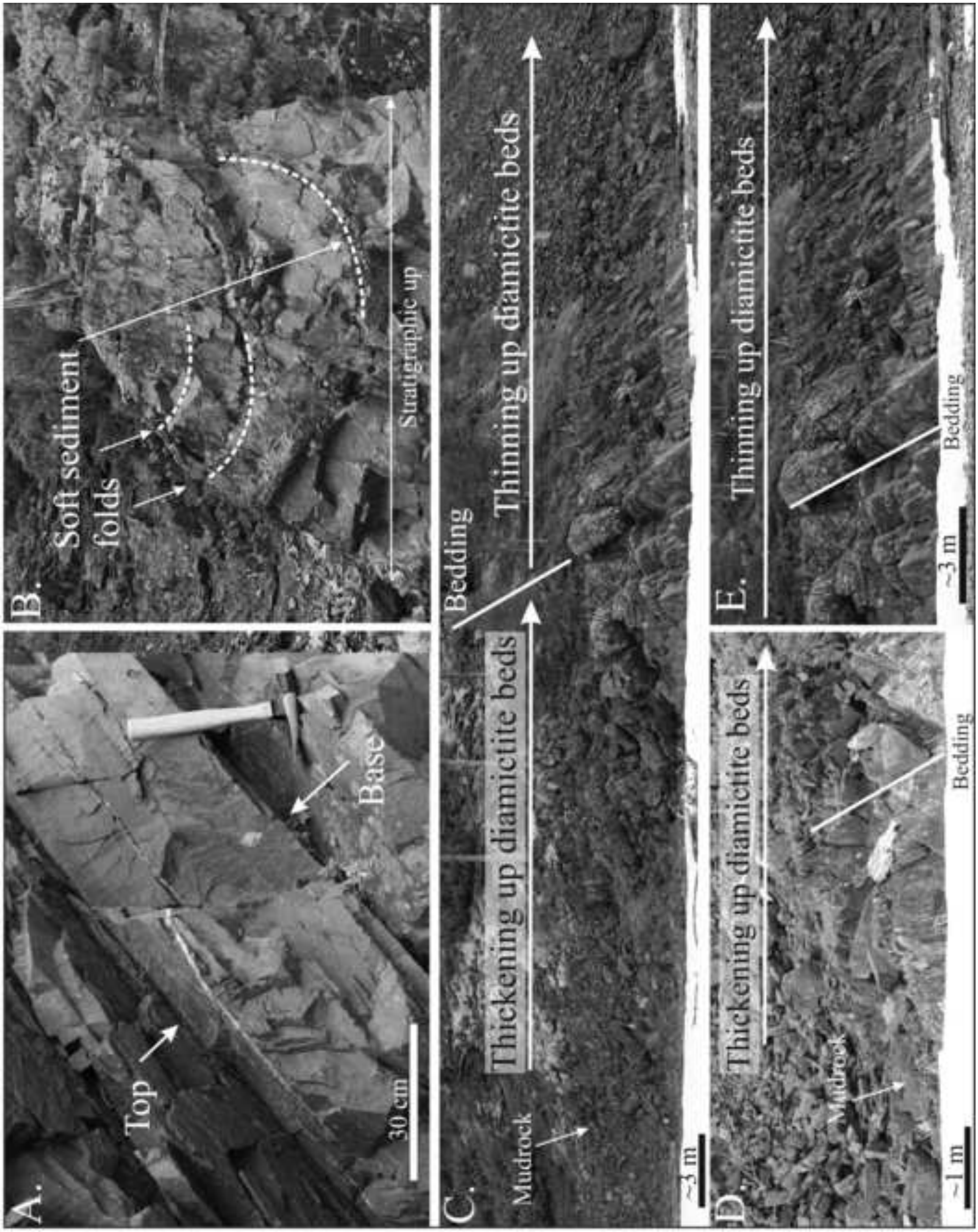

Figure 6. Isbell et al.
2 Column Image

Figure

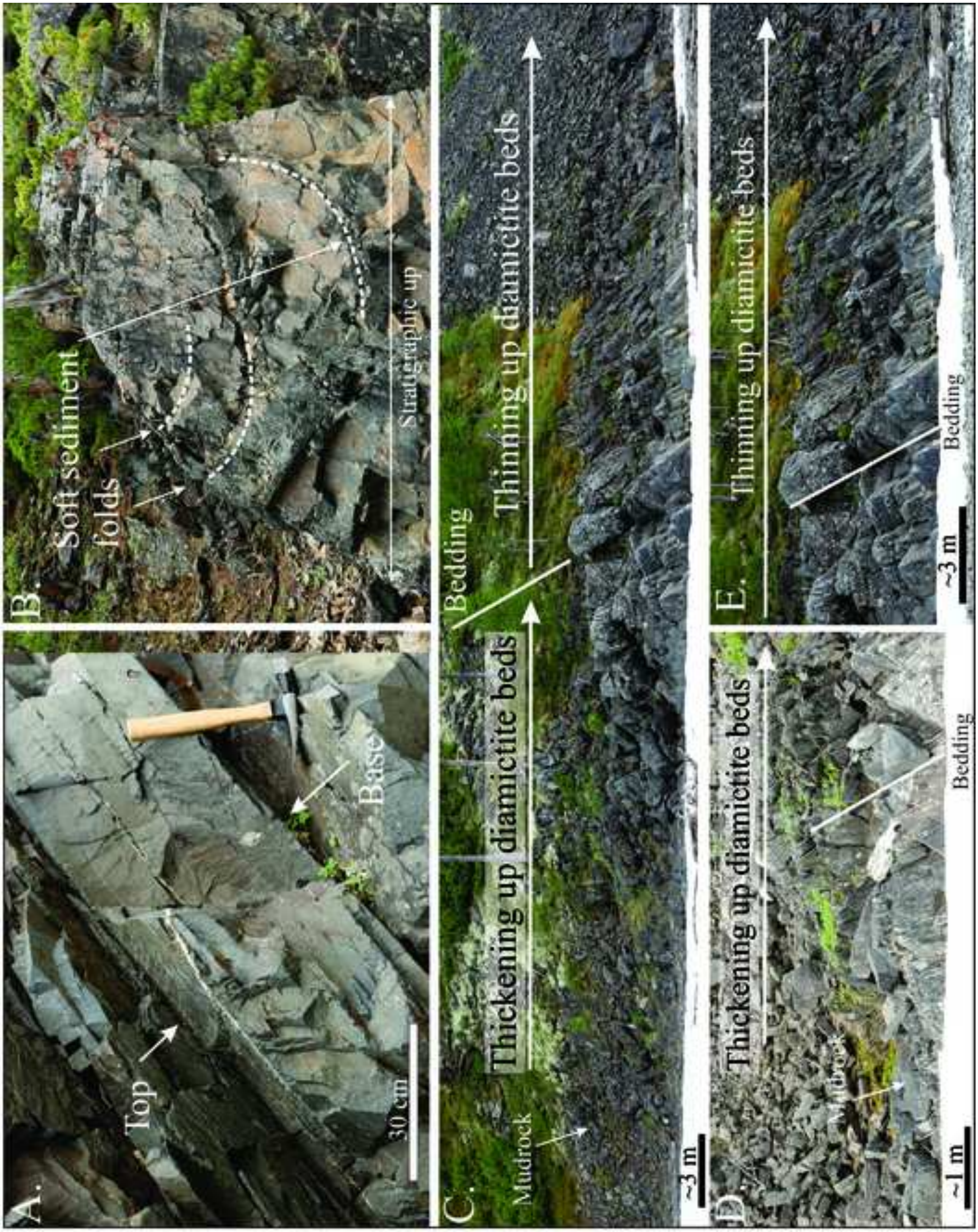

Figure 6. Isbell et al.
2 Column Image

Figure

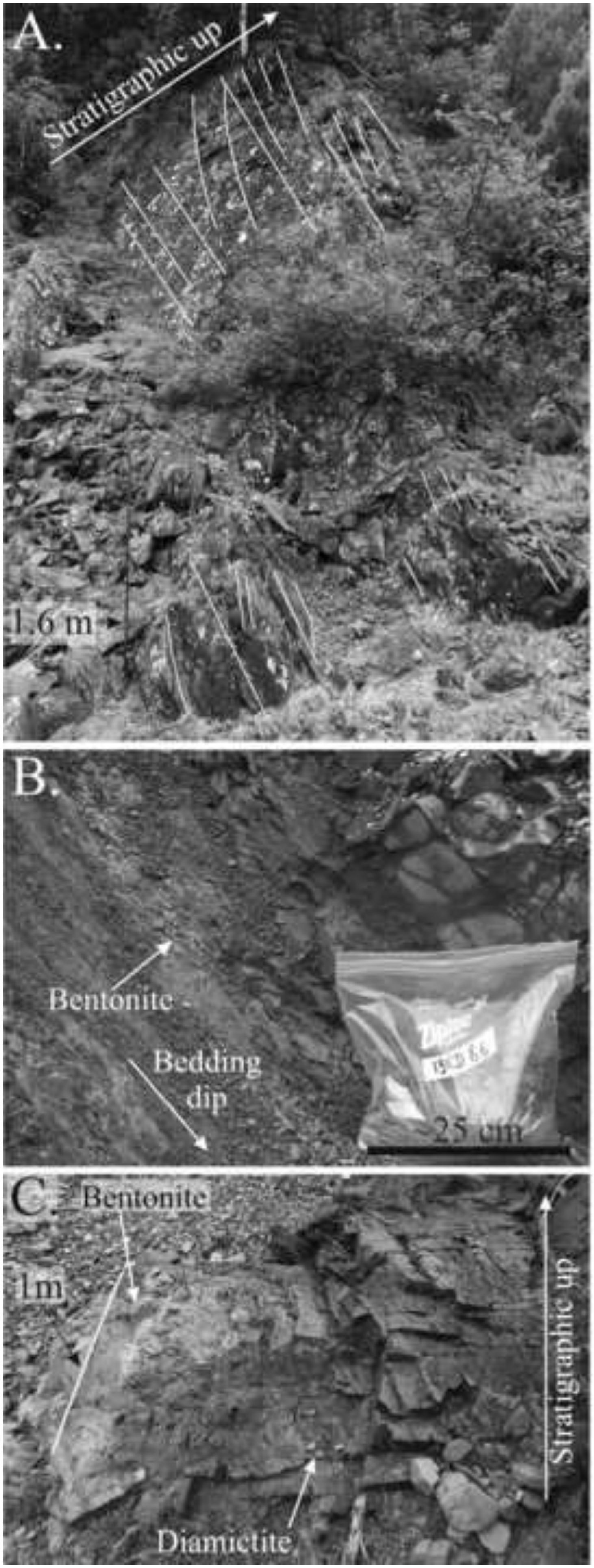

Figure 7. Isbell et al.
1 Column Image

Figure

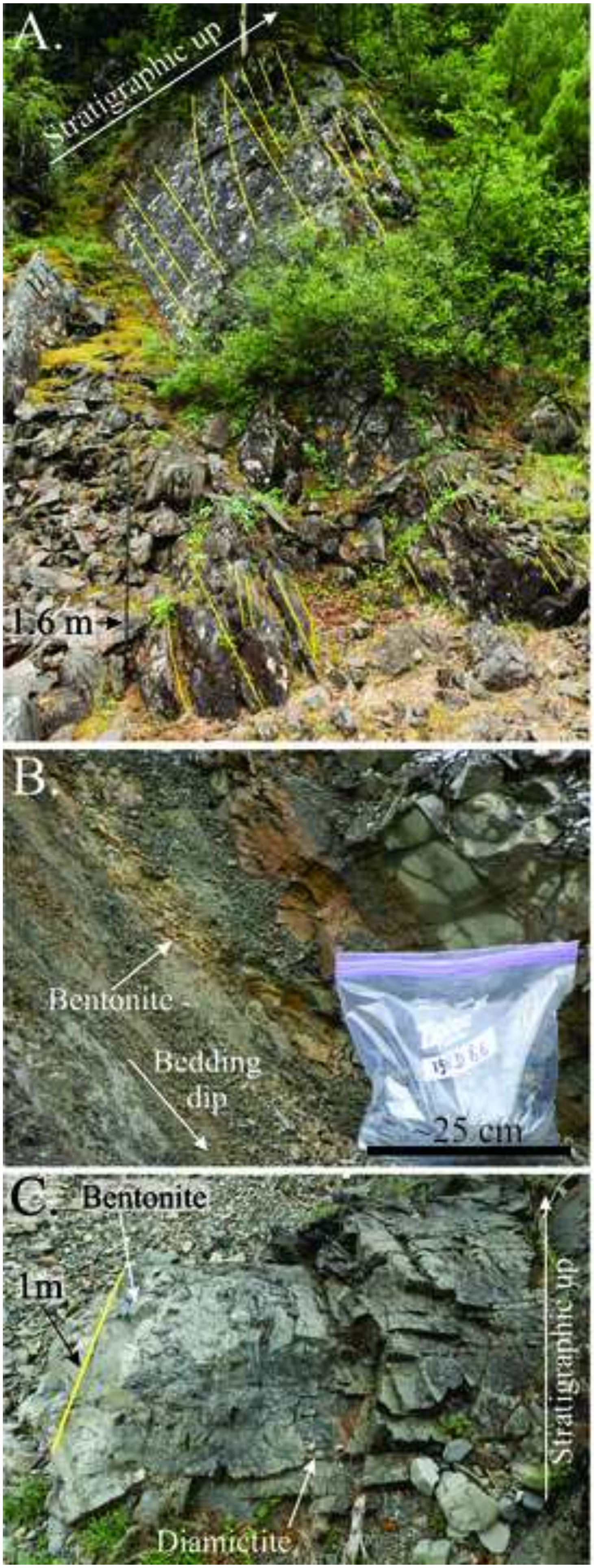

Figure 7. Isbell et al.
1 Column Image

Figure

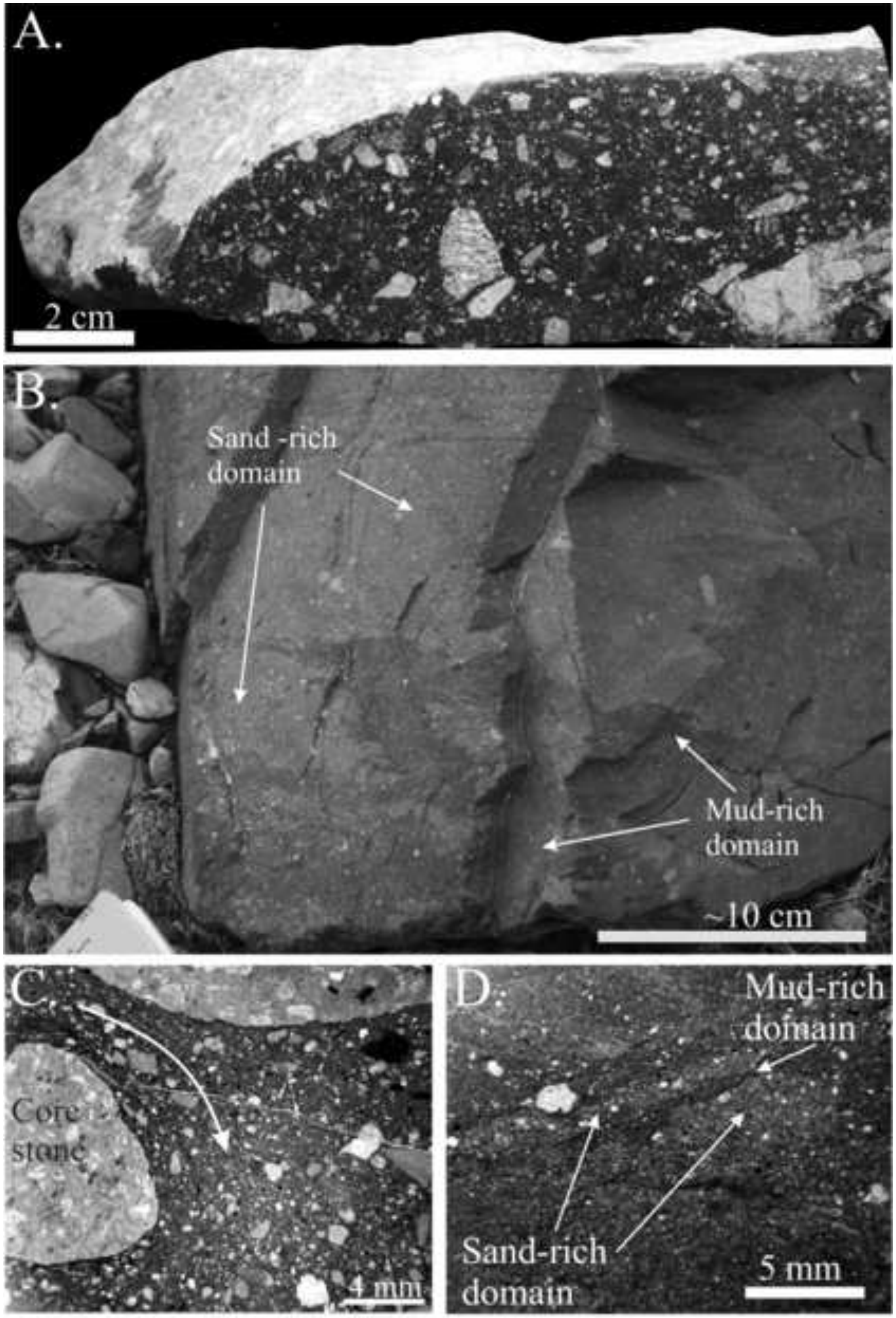

Figure 8. Isbell et al.
1.5 Column Image

Figure

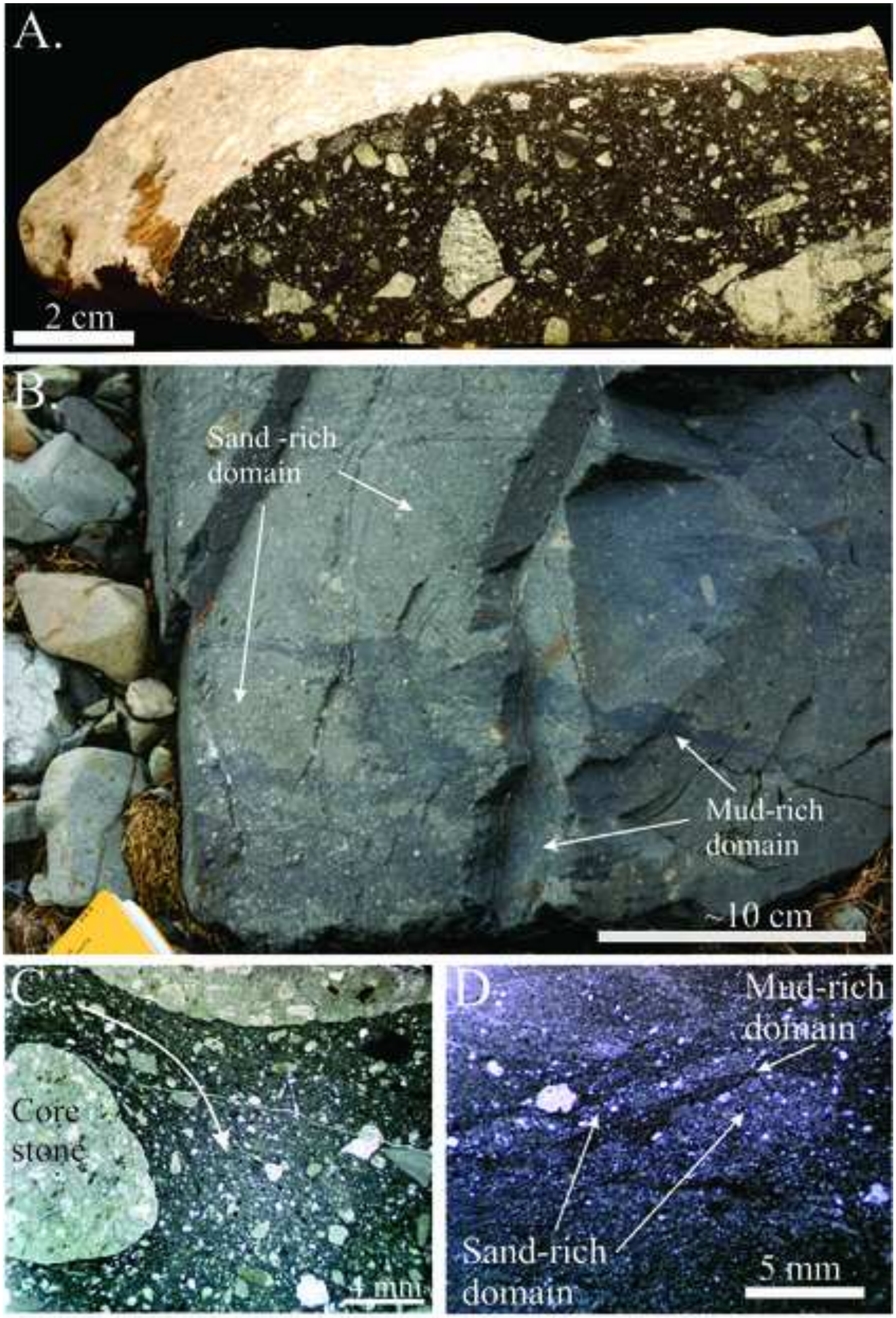

Figure 8. Isbell et al.
1.5 Column Image

Figure

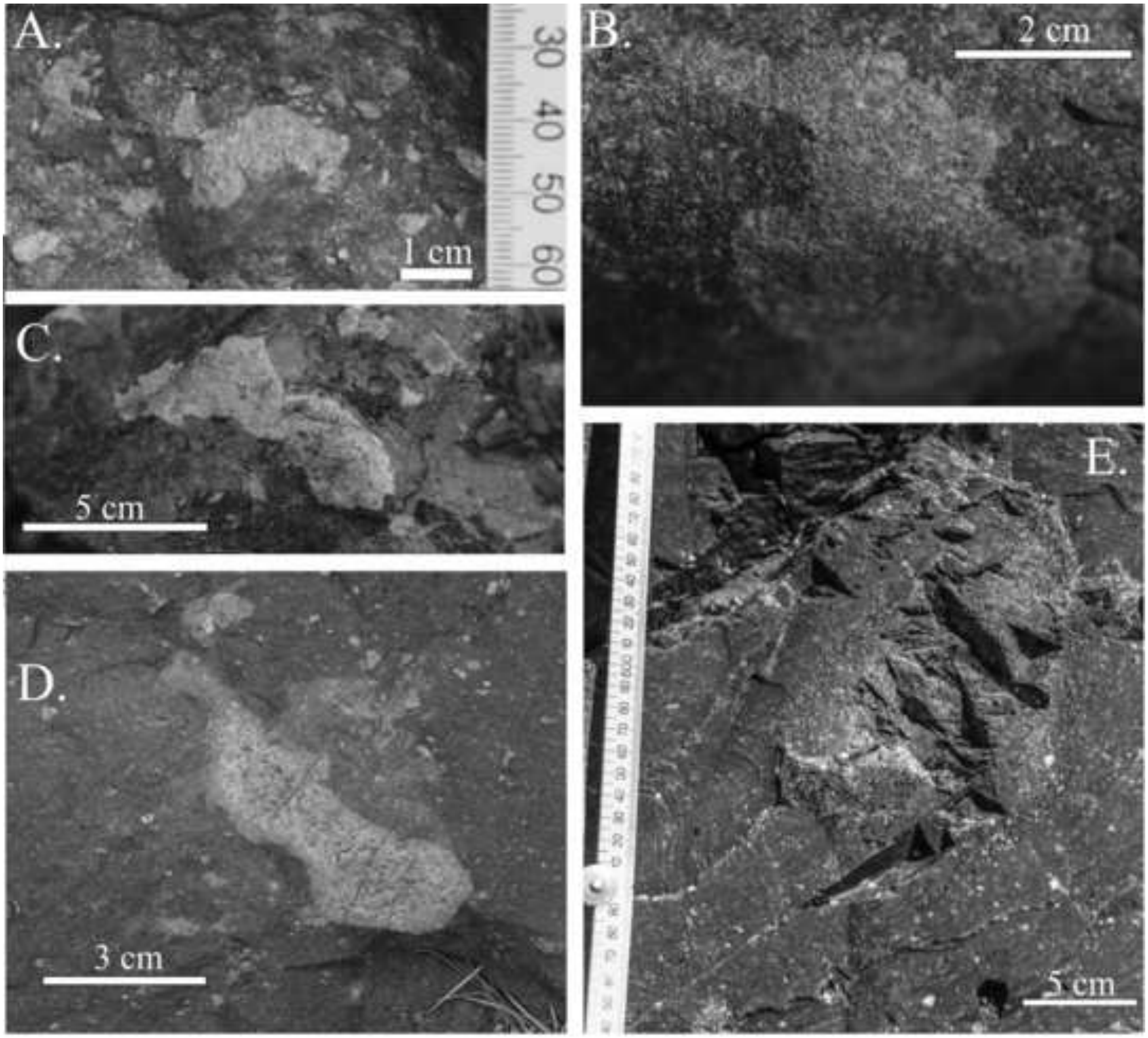

Figure 9. Isbell et al.
1.5 Column Image

Figure

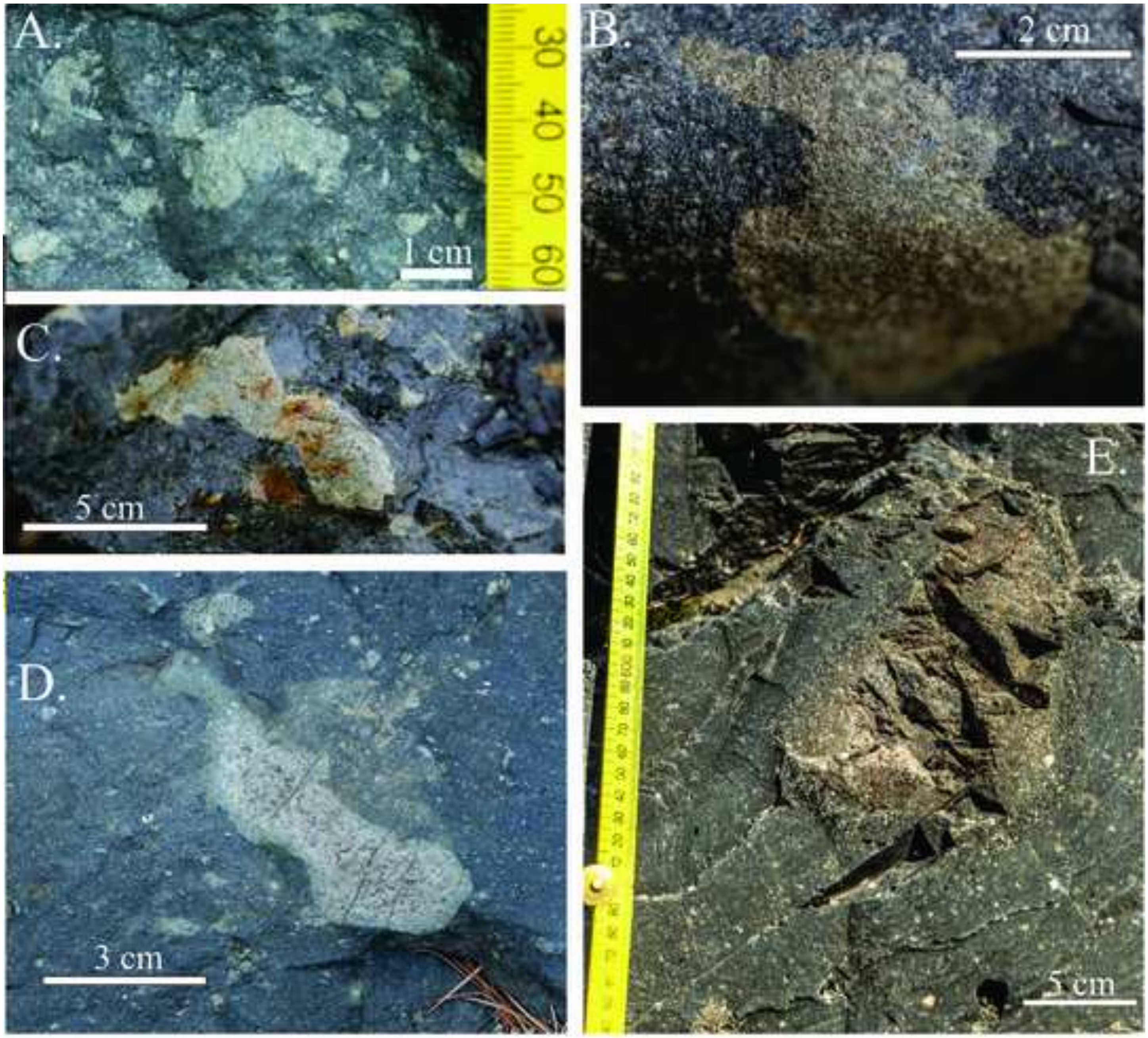

Figure 9. Isbell et al.
1.5 Column Image

Figure

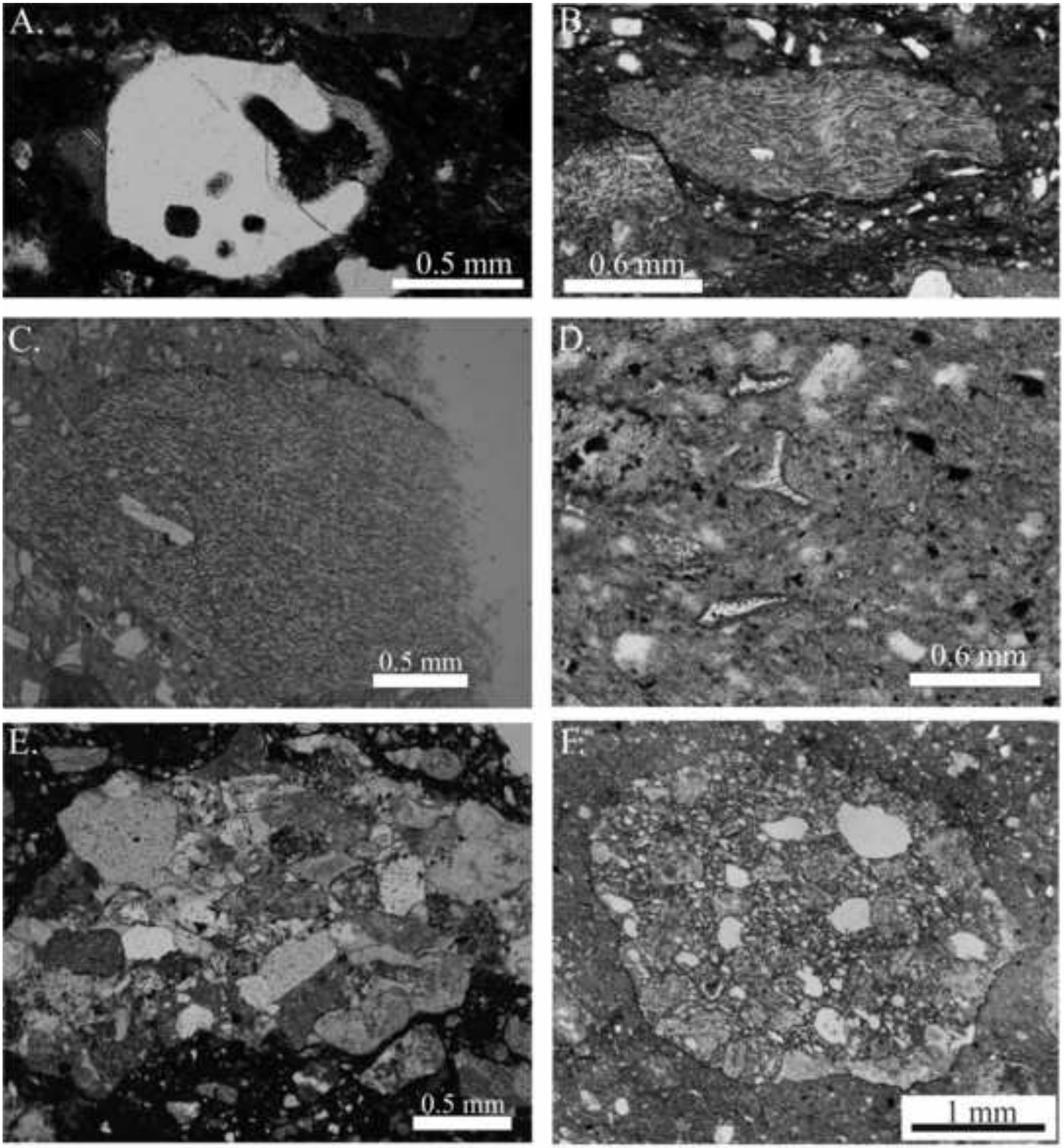

Figure 10. Isbell et al.
2 Column Image

Figure

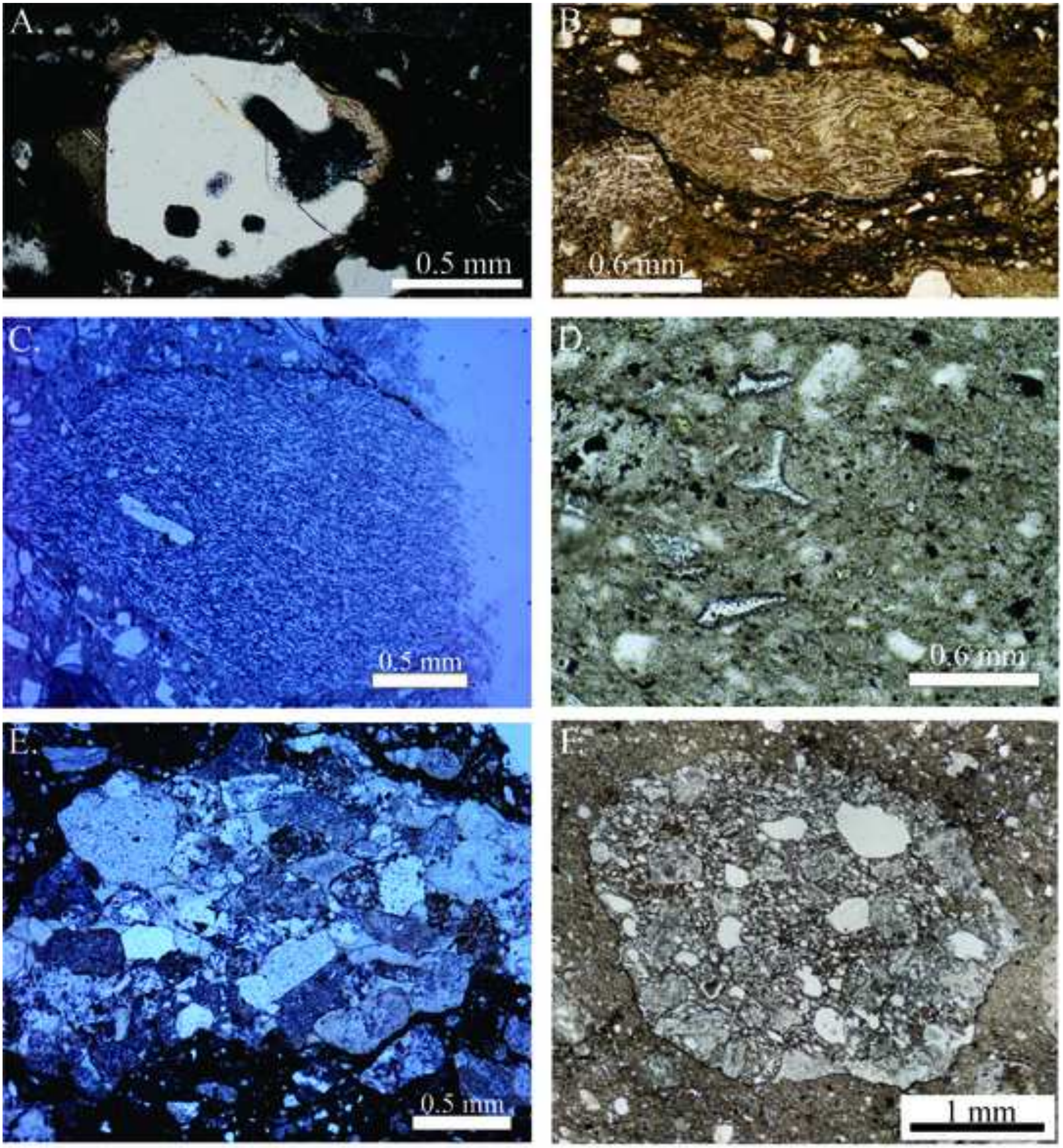

Figure 10. Isbell et al.
2 Column Image

Figure

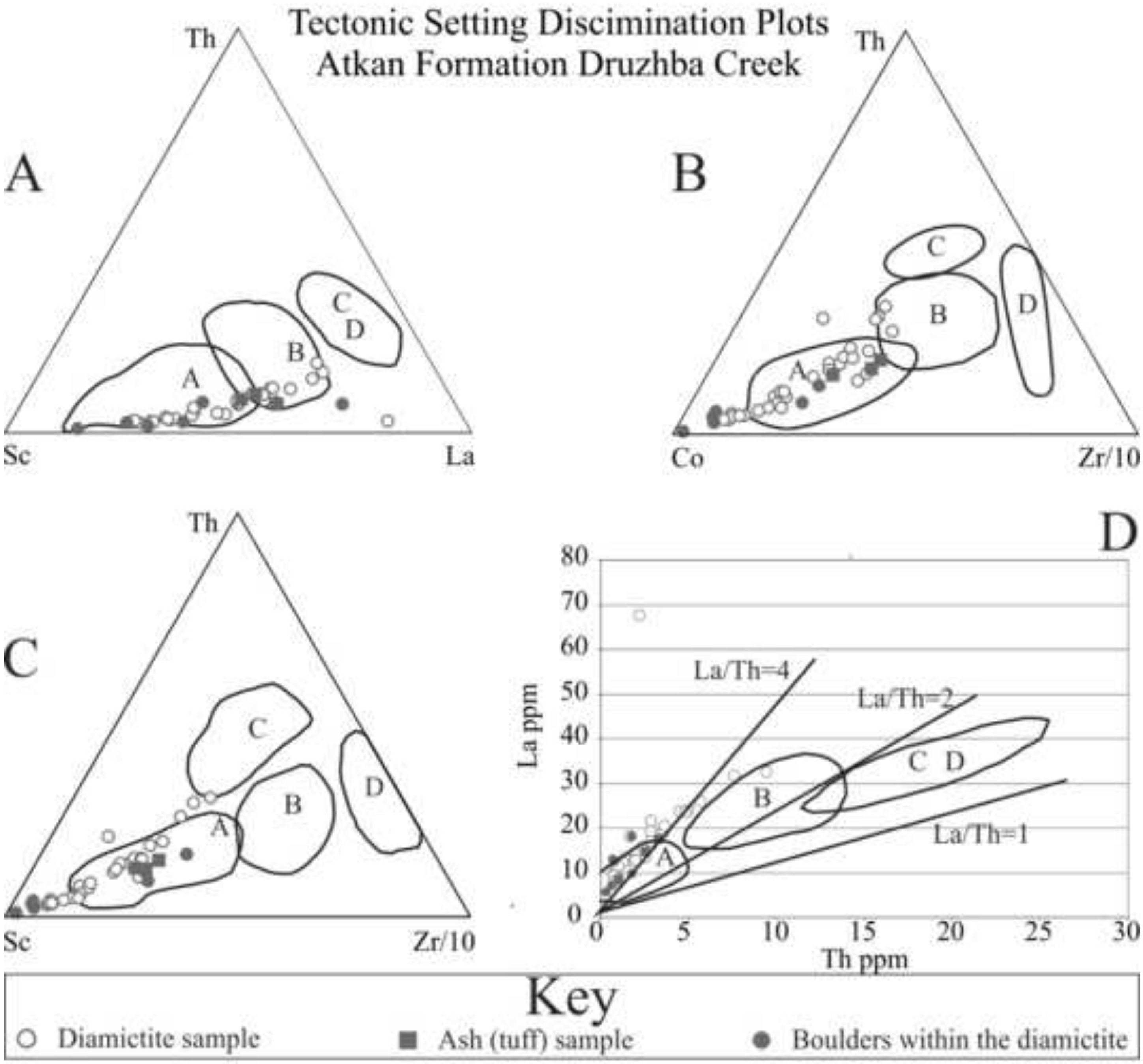

Figure 11. Isbell et al.
1.5 Column Image

Figure

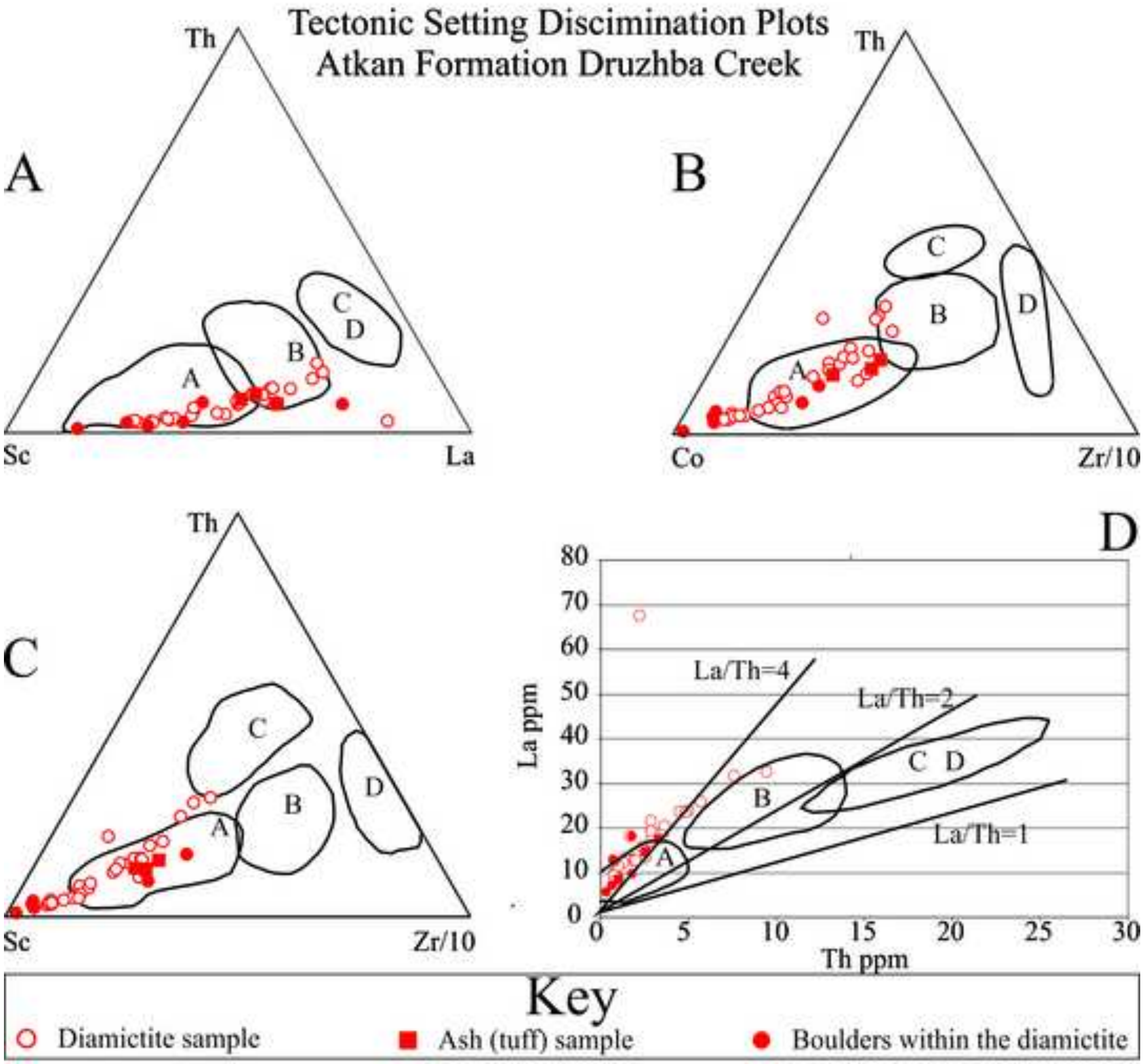

Figure 11. Isbell et al.
1.5 Column Image

Figure

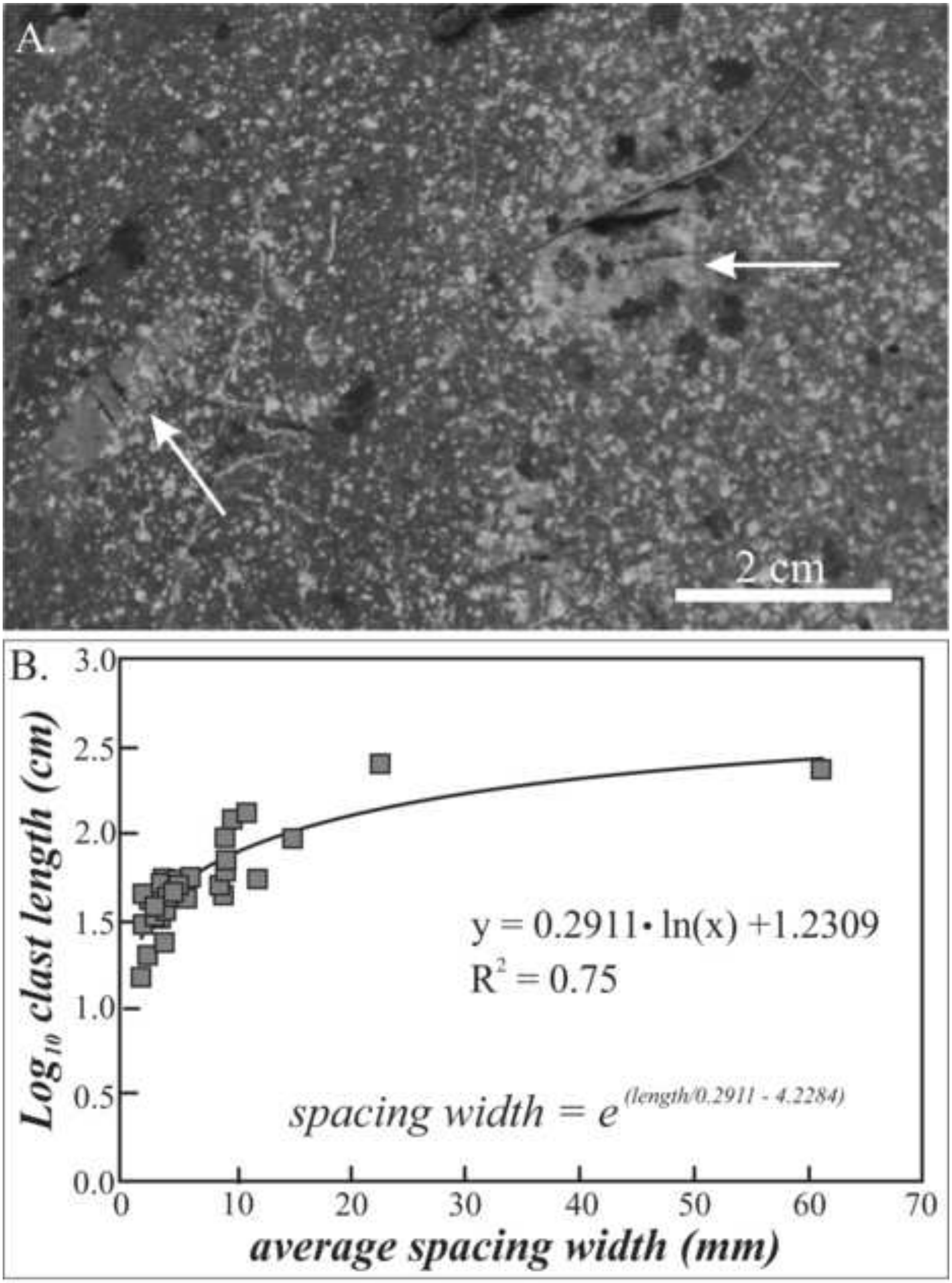

Figure 12. Isbell et al.
1.5 Column Image

Figure

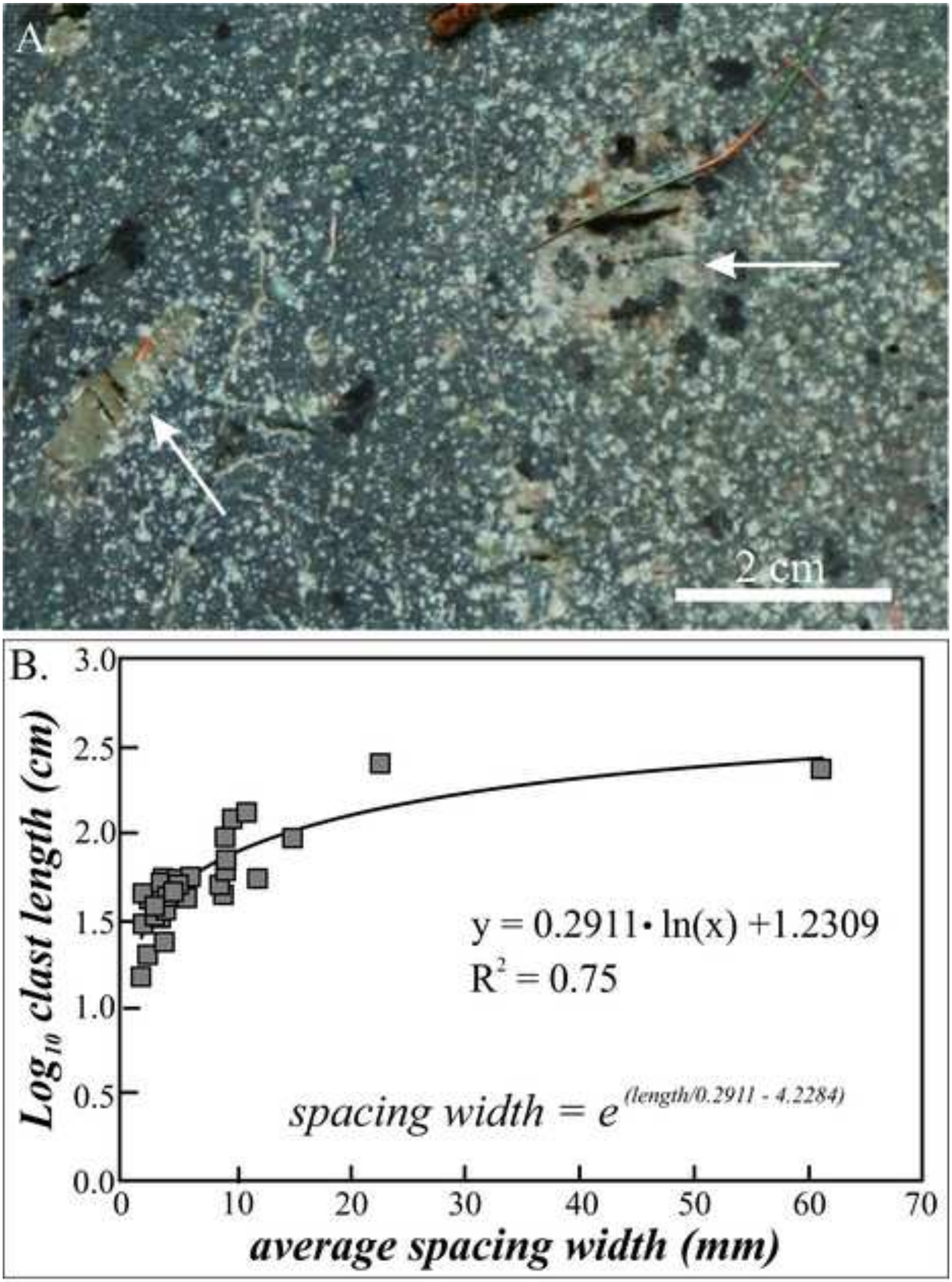

Figure 12. Isbell et al.
1.5 Column Image

Figure

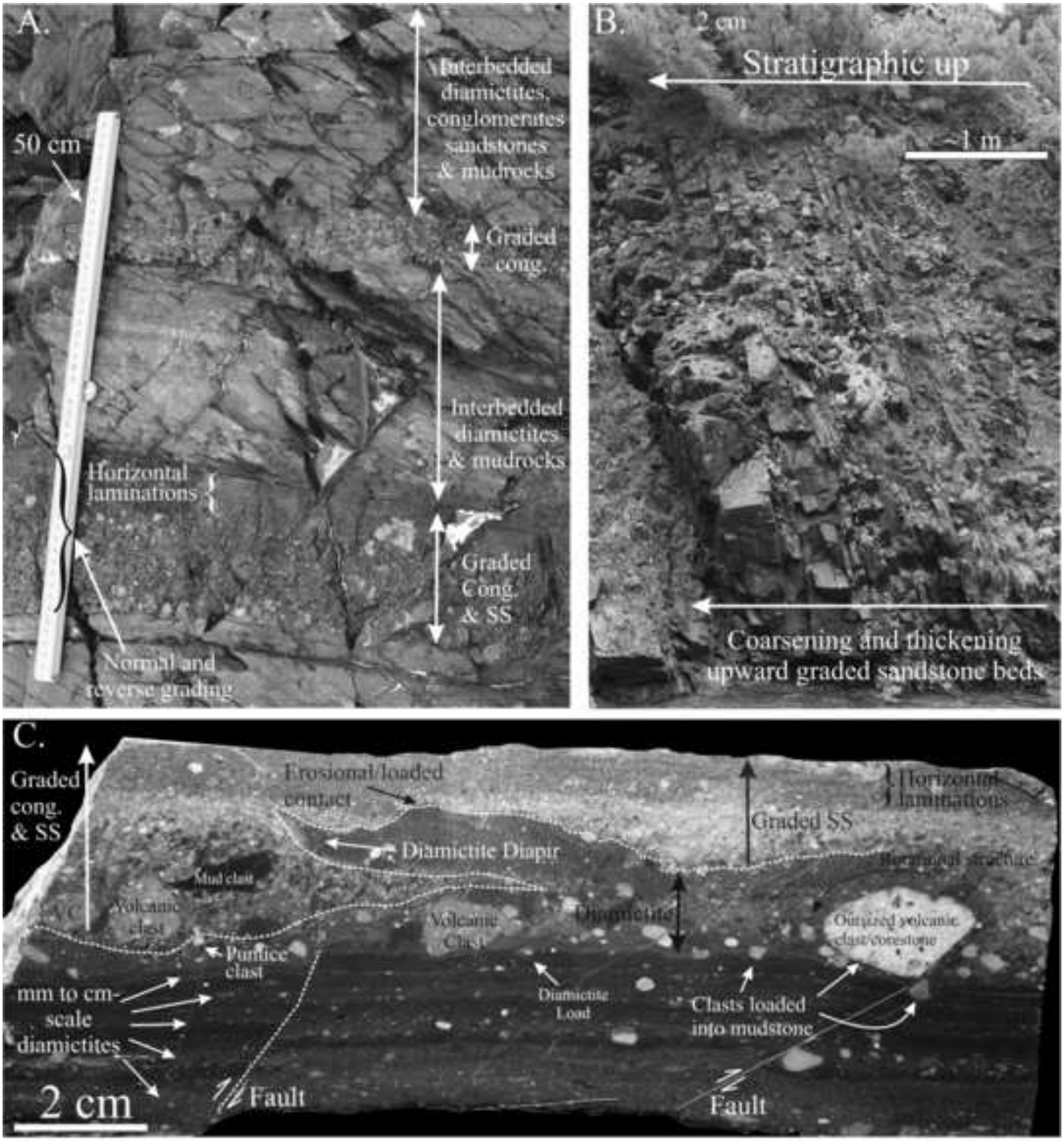

Figure 13. Isbell et al.
2 Column Image

Figure

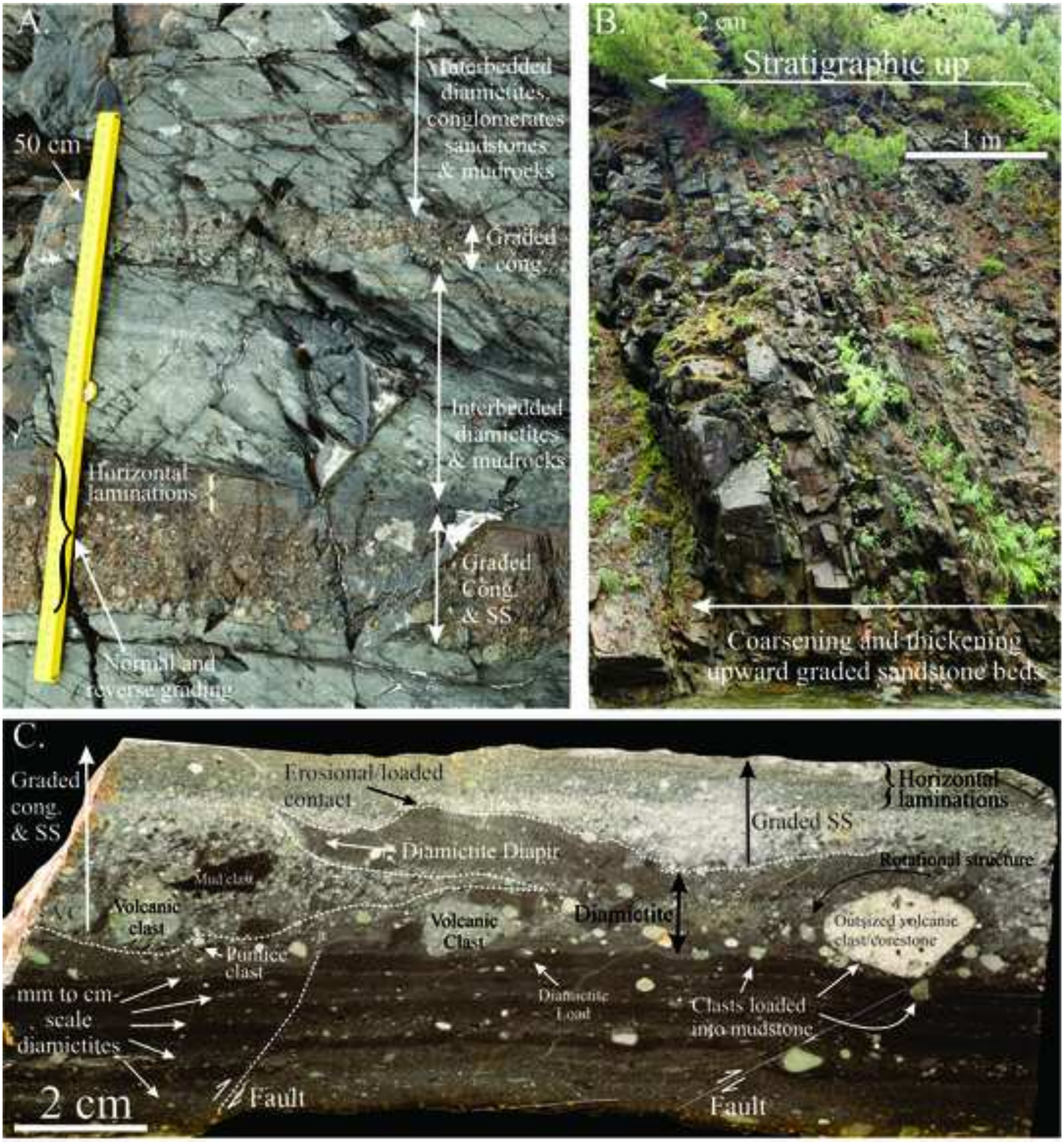

Figure 13. Isbell et al.
2 Column Image

Figure

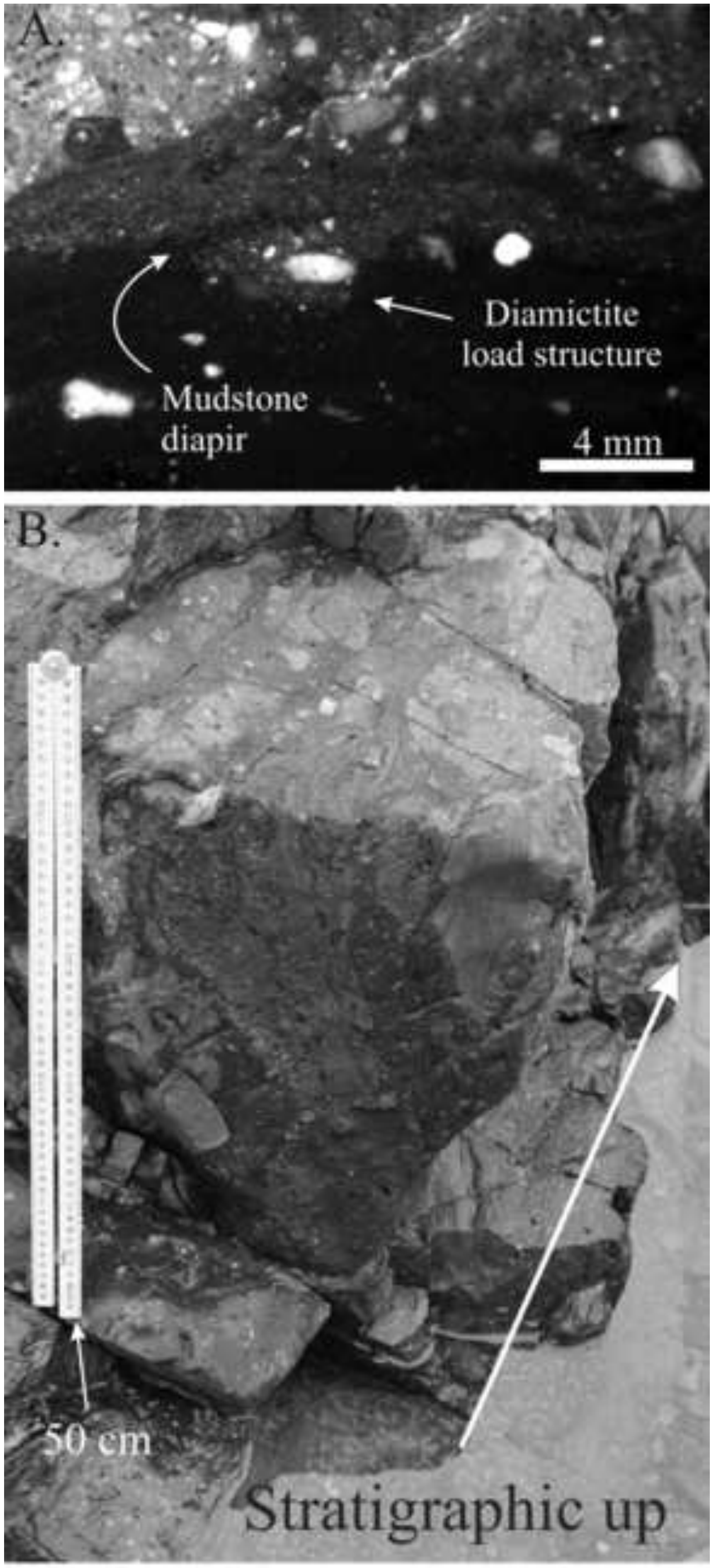

Figure 14. Isbell et al.
1 Column Image

Figure

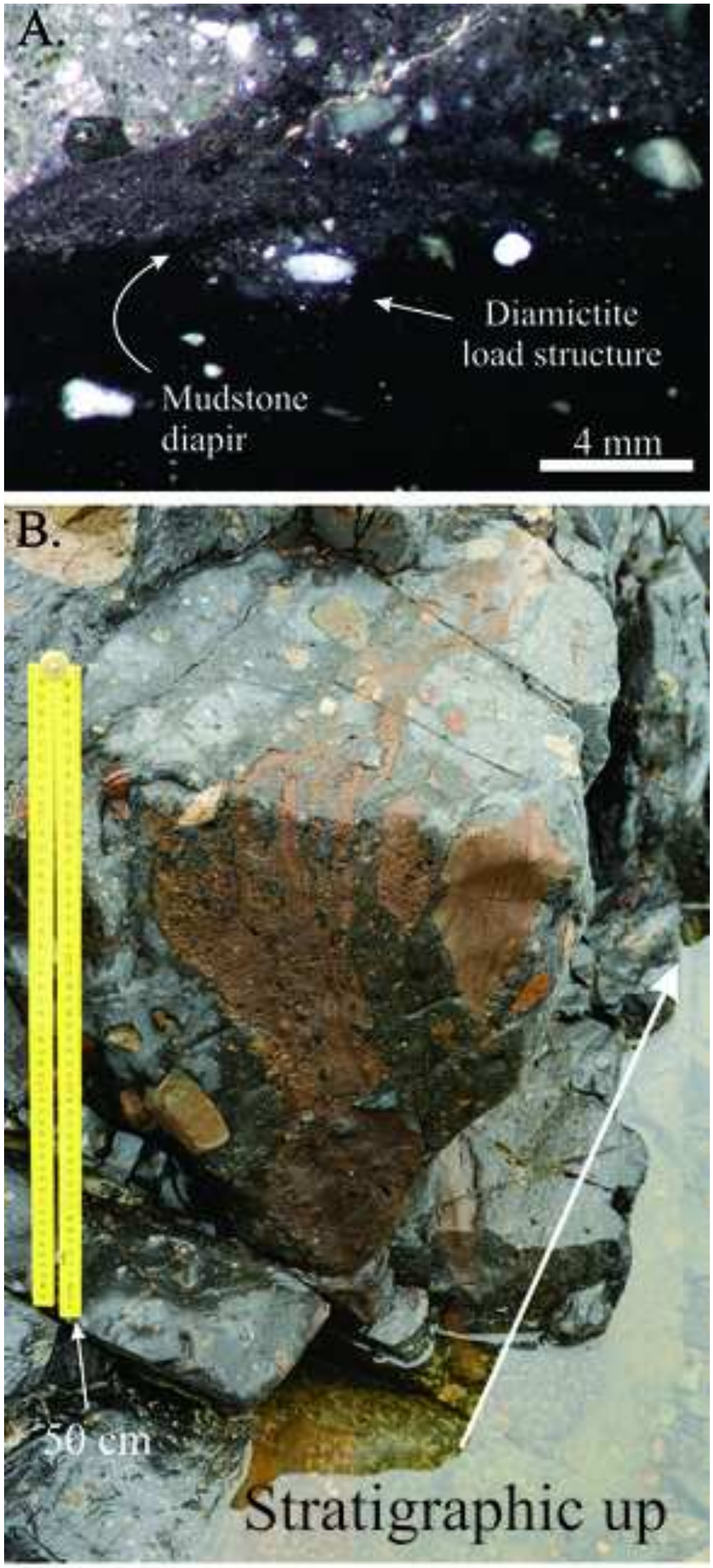

Figure 14. Isbell et al.
1 Column Image

Figure

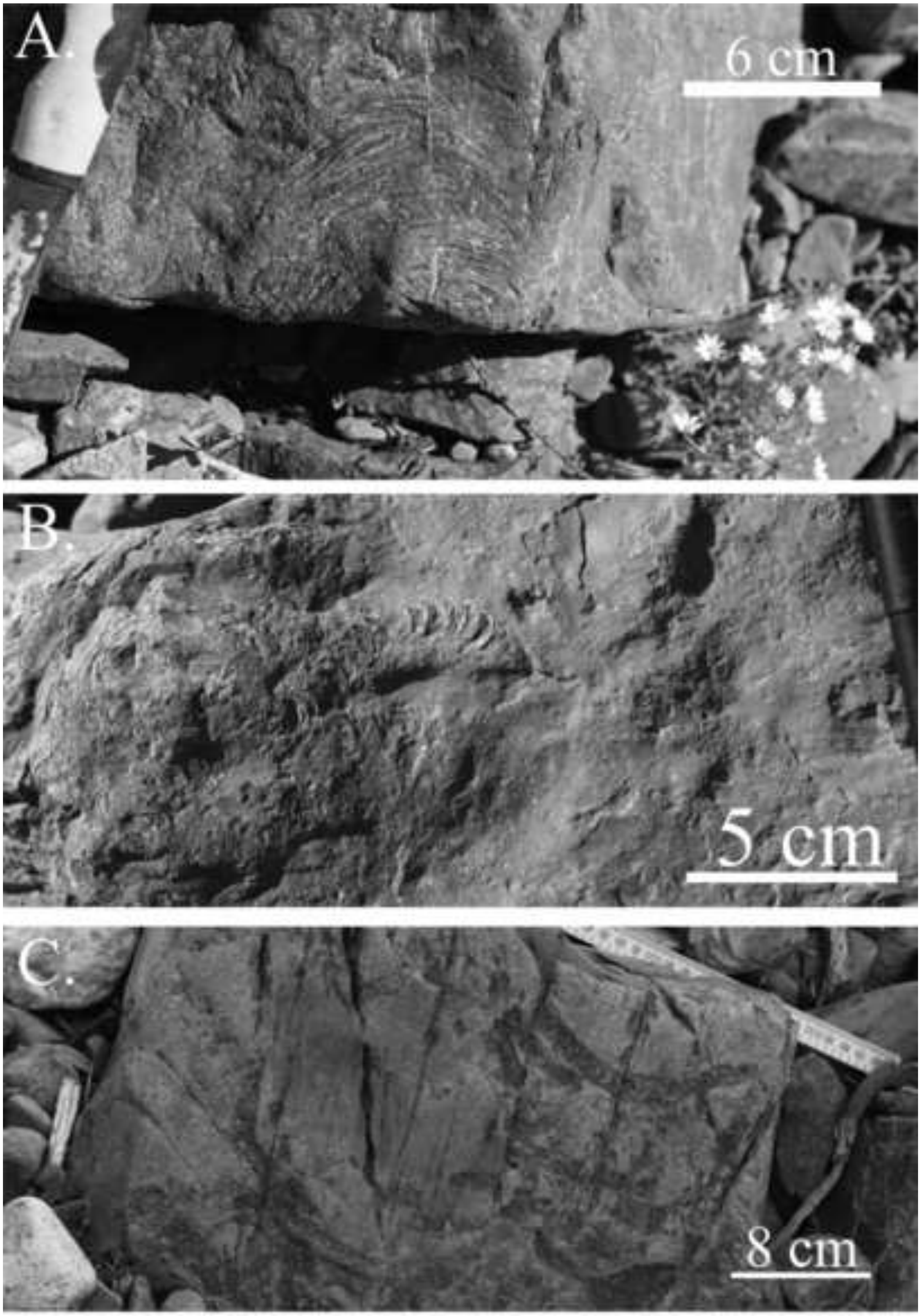

Figure 15. Isbell et al.
1 Column Image

Figure

Figure 15. Isbell et al.
1 Column Image

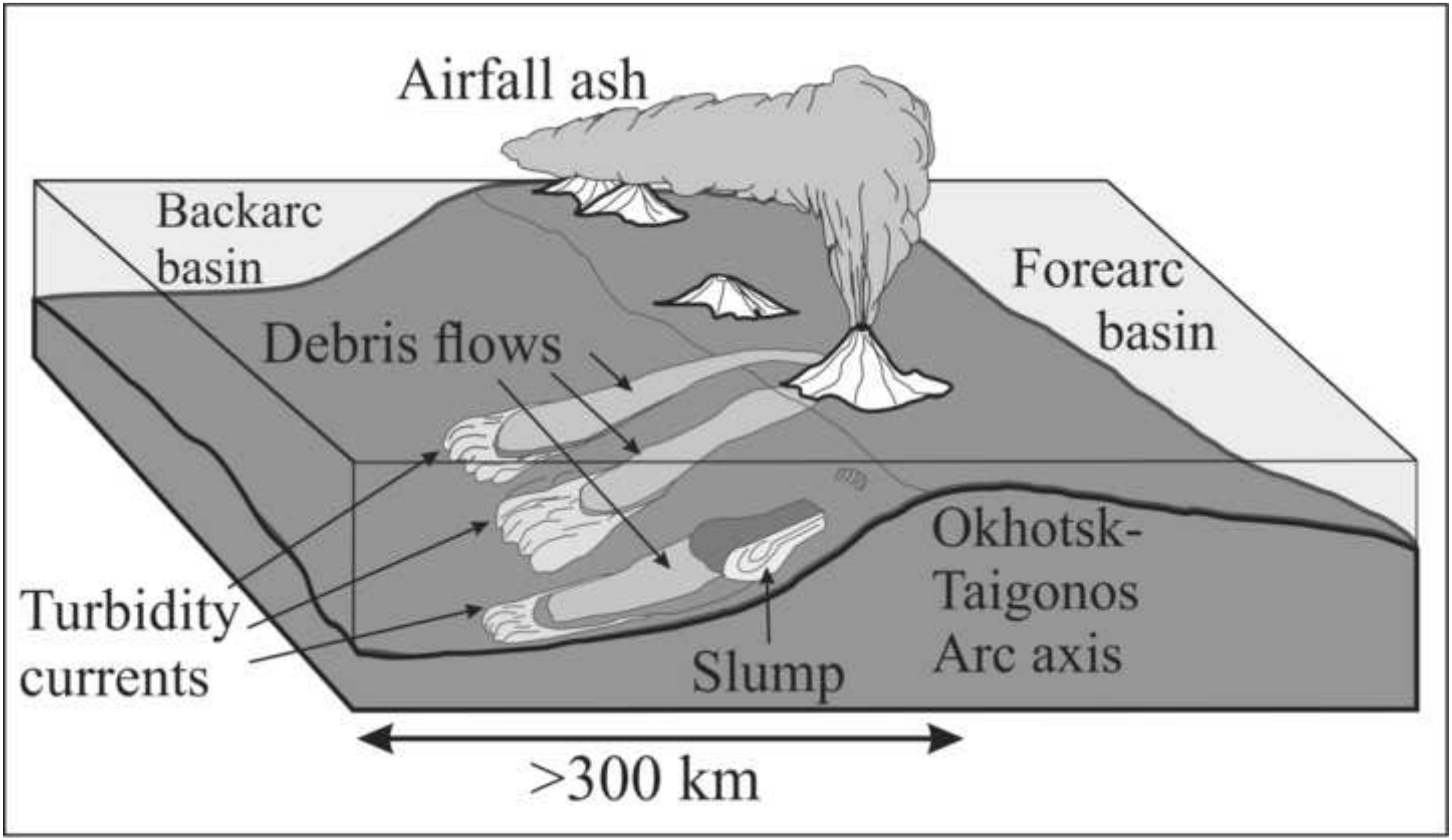

Figure 16. Isbell et al.
2 Column Image

Figure

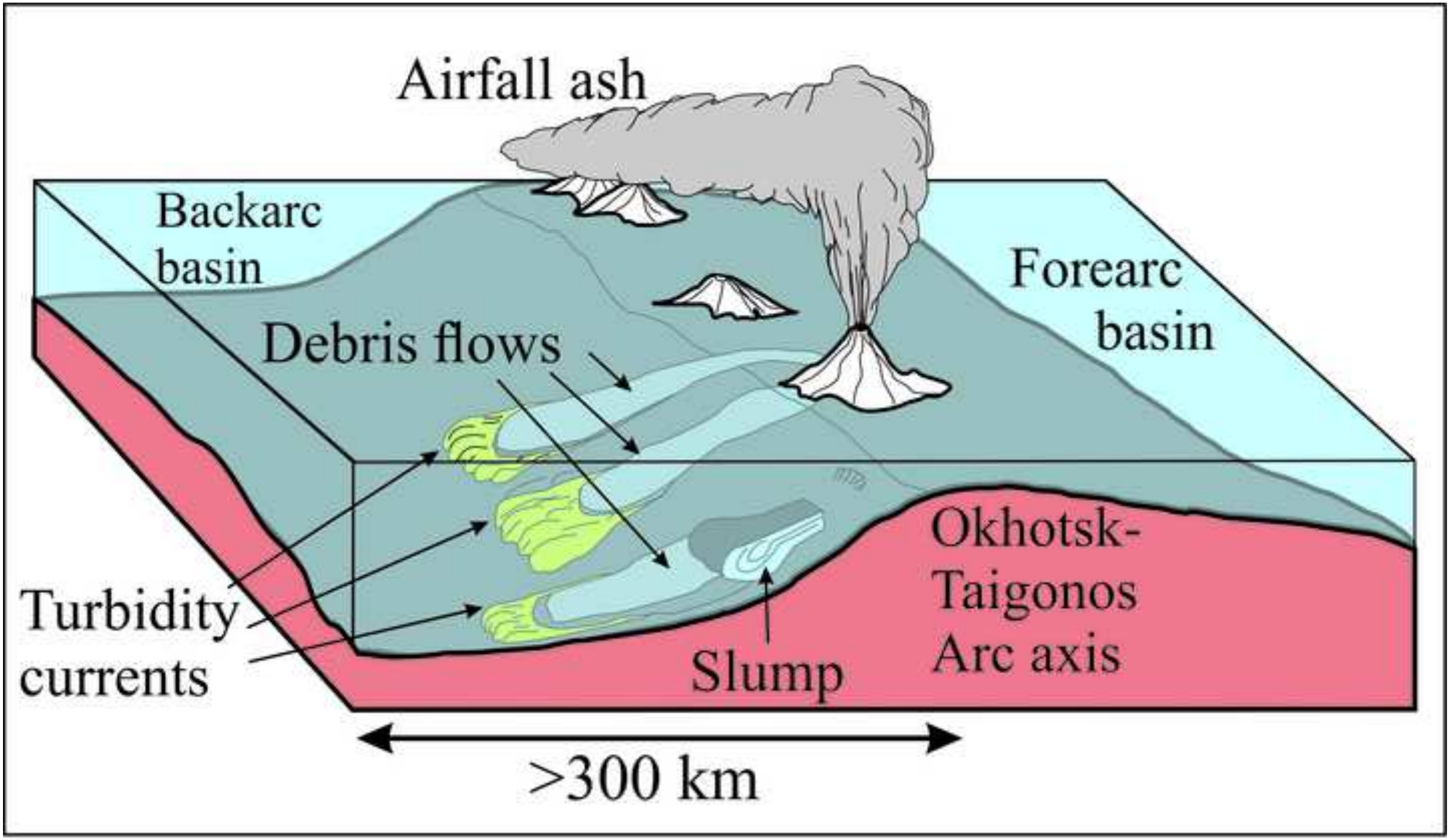

Figure 16. Isbell et al.
2 Column Image

Table

Table 1. Facies Associations of Capitanian Strata in North East Russia				
Facies Assemblage	Lithology and Bed Thickness	Sedimentary Features	Clast Shape and Composition	Interpretation
Bedded Diamictites	Cm- to m-scale thick beds of matrix-supported, clast-rich and clast-poor diamictites. Facies also contains chaotic bodies (up to 10 m thick) of folded diamictite, sandstone and mudstone. Rare tuff beds also occur	Diamictites occur as massive beds with sharp, non-erosive basal and sharp to gradational upper contacts. Units occur in thickening upward overlain by thinning upward successions. Downlapping diamictite beds also occur. Micromorphology of the diamictites are characterized by clast rotational structures, necking of matrix between grains, multiple diamictite domains, water escape structures, and an absence of oriented plasma fabric.	Diamictites contains very angular to rounded volcanic clasts up to boulder scale in diameter (average clasts are granule to pebble sized) with.71% occurring as subangular to very angular clasts. Clast with irregular shapes displaying protrusion and embayments are common. Clasts are composed of dacite, andesite, pumice/altered glass, and rhyolite. Some clast display columnar-like jointing while the matrix surrounding some clasts display alteration halos.	Subaqueous, deep-water volcanic debris flows with slump deposits and thin volcanic ash beds.
Interstratified diamictites, conglomerates, sandstones and mudrocks	Interstratified clast-rich diamictite, conglomerate, sandstone, and/or mudrock occur as coarse- and fine-grained couplets and triplets. Coarse members are mm to m scale in thickness and alternate with approximately equal thicknesses of mudrock, or in some cases, clast-poor diamictite.	Diamictite and conglomerates rest on sharp to erosional basal contacts and have erosional, sharp, and gradational upper contacts. Diamictites are massive with rare normal and inverse grading. Conglomerates are both normal and inversely graded. Sandstones are normally graded. Rotational structures, loading and water escape structures occur in the diamictites. Deep water trace fossils also occur.	Clast shapes and compositions are the same as clasts in the Bedded Diamictite Facies Assemblage. Individual clasts in the diamictites may have diameters larger than the thickness of individual units	Linked, co-genetic debris flows and turbidity currents.
Fossil-bearing mudrocks	Mudrocks are cm to several tens of m in thickness. Thin mudrocks are interstratified with graded sandstone, graded conglomerate, and diamictites. Thicker mudrocks are interstratified with thick diamictites successions.	Mudrocks occur as massive and thin bedded deposits. Thick successions are highly cleaved and poorly exposed.	Marine invertebrate fossils are common. Some mudstone contained dispersed clasts (<1%)	Deposited by settling from suspension of hemipelagic material, mudflows, and low-density turbidity currents

Table 2. Micromorphology of Atkan Diamictites								
Sample	**Rotational Structures**	**Grain Coatings**	**Necking Structures**	**Tile Structures**	**Multiple Plasma Domains**	**Water Escape Structures**	**Crushed Grains**	**Lineations including Stacked Grains**
DC1-2	+		+					
DC1-153				+	+	+		
DC1-169	+	+	+		+			
DC1-206	+		+		+	+		
DC1-242	+		+		+			
DC1-269	+				+			
DC-6	+				+			

Table 3. Glacioeustatic Changes Resulting from Volcanic Island Arc Glaciers			
Modern Volcanic Arcs	**Total Exposed Land Area**	**Sea Level Equivalent with Isostasy**	
		Assuming area is a Single Land Mass and a single glacier completely covers the land mass	**Calculation for multiple glaciers completely covering an area that was equally divided among the islands**
Scotia Arc (South Sandwich Islands)	310.3 km^2 (11 islands)	0.00012 m	0.000069 m
Lesser Antilles	4665 km^2 (19 islands)	0.0034 m	0.0017 m
Aleutian Islands	17,666 km^2 (69 islands)	0.0173 m	0.0065
Aleutian Islands and Alaskan Peninsula	~84,416 km^2 (69 islands + peninsula)	0.118 m	0.0951 m*
***** Total area for the Aleutian Islands was split equally between the 69 islands. The total sea level equivalency with isostasy (SLEI) for these islands was then added to the SLEI for a single glacier completely covering the Alaskan Peninsula.			